Mixed-integer optimization approaches to resource allocation problems with applications in healthcare asset management and epidemics

Item Type	Dissertation
Authors	Des Bordes, Emmanuel
Publisher	Wichita State University
Rights	Copyright 2015 Emmanuel Des Bordes
Download date	2026-02-07 05:39:52
Link to Item	http://hdl.handle.net/10057/12122

MIXED-INTEGER OPTIMIZATION APPROACHES TO RESOURCE ALLOCATION PROBLEMS WITH APPLICATIONS IN HEALTHCARE ASSET MANAGEMENT AND EPIDEMICS

A Dissertation by

Emmanuel des-Bordes

Master of Science, New Mexico State University, 2011

Master of Science, The University of Akron, 2008

Master of Science, Georgia State University, 2004

Bachelor of Science, Kwame Nkrumah University of Science and Technology, Ghana, 2000

Submitted to the Department of Industrial and Manufacturing Engineering
and the faculty of the Graduate School of
Wichita State University
in partial fulfillment of
the requirements for the degree of
Doctor of Philosophy

December 2015

MIXED-INTEGER OPTIMIZATION APPROACHES TO RESOURCE ALLOCATION PROBLEMS WITH APPLICATIONS IN HEALTHCARE ASSET MANAGEMENT AND EPIDEMICS

The following faculty members have examined the final copy of this dissertation for form and content, and recommend that it be accepted in partial fulfillment of the requirement for the degree of Doctor of Philosophy with a major in Industrial and Manufacturing Engineering.

İ. Esra Büyüktahtakın, Committee Chair

Krishna Krishnan, Committee Member

Don Malzahn, Committee Member

Ramazan Asmatulu, Committee Member

Laila Cure, Committee Member

Accepted for the College of Engineering

Royce Bowden, Dean

Accepted for the Graduate School

Kerry Wilks, Interim Dean

DEDICATION

To my grandparents, my parents, my wife, and my children

If you cannot explain it simply, you do not know it well enough.

ACKNOWLEDGEMENTS

Praise be to the Almighty God for giving me this opportunity to complete my dissertation. I would like to express my sincere appreciation to my academic advisor, Dr. Esra Büyüktahtakın, for her many years of thoughtful, patient guidance and support in putting this dissertation together. I would also like to acknowledge the financial support of the KEEP program at Wichita State University (WSU) through the Workforce Center, especially the constant advice from Diann Gregg and Sherry Gegen. I am also grateful to Dr. Krishna Krishnan, Dr. Don Malzahn, Dr. Ramazan Asmatulu, and Dr. Laila Cure for their time, valuable contribution, and willingness to serve as my dissertation committee members. Thanks are also due to professors of the College of Engineering at WSU from whom I have studied and gained so much knowledge.

I would also like to extend my gratitude to my friends and office mates at the System Optimization and Analytic Laboratory in the Department of Industrial and Manufacturing Engineering at WSU for making a significant impact and contribution to research work during my graduate work at WSU. I also want to thank all of my family friends, especially Mr. and Mrs. Mark Tetteh, Mr. and Mrs. Tetteh-Wayo Ablorh Odjidja, Mr. and Mrs. Benjamin Ablorh-Odjidja, Mr. and Mrs. Papa Kwame Opoku-Ansah, and Mr. and Dr. Davis Payne, who supported me with their enormous help in diverse ways while studying at WSU.

Finally, I thank my grandparents, Mr. Francis Duah Sr. (deceased) and Auntie Efua Ackon; my parents Mr. Joseph des-Bordes and Mrs. Agnes Duah-Mensah; my extended family, Francis Duah Jr., Frederick Duah, Christy Duah, Federick Oppong; and my in-laws, Mr. and Dr. Joseph Ablorh Odjidja for their unconditional love, support, and encouragement. I appreciate their consistent support, love, and guidance. My biggest thank you goes to my wife, Mrs. Maa Dede des-Bordes, and my children, Lennox Oppong Panyin des-Bordes and Lesleigh Oppong Kakra des-Bordes, who have always been my ultimate source of happiness, motivation, and success.

ABSTRACT

In this dissertation, we study mixed-integer programming (MIP) approaches to solve resource allocation problems with applications in healthcare asset management and epidemics. In particular, we study (*i*) valid inequalities for solving large-scale one-dimensional zero-one (0–1) knapsack problems (KPs), (*ii*) healthcare asset-replacement problems that involve several styles and types of magnetic resonance imaging (MRI) machines, and (*iii*) epidemics involving the Ebola virus disease (EVD) under resource constraints.

Using recursive solutions of the dynamic programming (DP), we present valid inequalities that can be added to the original 0–1 KP as cutting planes (CP) to tighten and improve the model formulation for facilitating solution methods. Extensive computational experiments show that our inequalities yield competitive results.

Operating assets generally suffer from deterioration, which results in high operation and maintenance (O&M) cost and decreased salvage value, while technologies allow newer machines to operate more efficiently at a lower cost. Therefore, we study the multiple style and type parallel asset-replacement problem (MST-PRES), which determines an optimal policy for keeping or replacing a group of assets that operate in parallel under a limited budget. Results show that the proposed MIP model provides valuable insights and strategies for decision-makers and government entities on the capital asset management.

Epidemic diseases, which are occurring more frequently, are a major health and economic problem for mankind. This section begins with a review of epidemiological disease models that have been used to study transmission dynamics of Ebola and their estimated key parameters from existing data set in order to explain important patterns by which it spreads to make significant public healthcare decisions. Following the review of Ebola, we develop a mixed-integer optimization of epidemic model to address the efficient allocation of epidemic resources and to assess the impact of traveling within Guinea, Liberia, and Sierra Leone for control of the 2014 Ebola outbreak. We conclude by presenting effective combinations of future intervention strategies and policy recommendation for controlling the EVD epidemics.

TABLE OF CONTENTS

Chapter Page

1 INTRODUCTION . . . 1

1.1 Background and Motivation . . . 1
1.2 The One-Dimensional Knapsack Problem: A Resource Allocation Problem . . . 2
1.2.1 Dynamic Programming Approaches to the 0–1 KP . . . 3
1.2.2 Generation of Valid Inequalities . . . 4
1.3 Parallel Replacement Analysis . . . 4
1.4 Epidemiological Models, Data Analyses, and Resource Allocation for Ebola Epidemics . . . 5
1.5 Contributions and Overview . . . 7

2 VALID INEQUALITIES FOR ONE-DIMENSIONAL KANPSACK FORMULATIONS THROUGH DYNAMIC PROGRAMMING . . . 10

2.1 Introduction . . . 10
2.2 Dynamic Programming Formulation . . . 13
2.3 Valid Inequality Derivation . . . 16
2.3.1 Flat and Ordered Inequalities . . . 16
2.3.2 Envelope Inequalities . . . 18
2.4 Lifting . . . 21
2.5 Computational Experiments . . . 23
2.5.1 Generation of Hard Instances . . . 23
2.5.2 Implementation and Experimental Design . . . 23
2.6 Summary of Results . . . 24

3 OPTIMIZING NEW TECHNOLOGY INVESTMENTS UNDER DETERIORATION: A CASE STUDY ON MAGNETIC RESONANCE IMAGING MACHINE REPLACEMENT . . . 31

3.1 Introduction . . . 31
3.2 Multiple Asset-Replacement Model Definition . . . 35
3.2.1 Model Notations . . . 36
3.2.2 Assumptions . . . 38
3.2.3 MST-PRES Model Formulation . . . 38
3.2.4 Defining δ Values . . . 41
3.3 Case Study Baseline Data and Computational Experiments . . . 42
3.3.1 Data Collection . . . 43
3.3.2 Experimental Design . . . 47
3.4 Performance of Model and Summary of Numerical Results . . . 48
3.4.1 Number of Assets in Operation and Inventory . . . 49
3.4.2 Replacement Periods, Ages, and Costs . . . 51

Chapter Page

3.4.3 Computational Analysis for Changing δ-Values 52
3.5 Sensitivity Analysis 57
3.5.1 Pareto Optimal Front 57
3.5.2 Budget Required for Zero Penalty 58
3.5.3 Single-Parameter Sensitivity Analysis 59
3.5.4 Two-Parameter (Budget and Demand) Sensitivity Analysis 62
3.5.5 Impact of Budget on Total Cost 63
3.5.6 Percentages of Cost Components 65

4 MATHEMATICAL MODELING AND DATA ANALYSES OF EBOLA EPIDEMICS: A REVIEW 67

4.1 Introduction 67
4.2 Methods for Article Inclusion and Exclusion 70
4.2.1 Sources of Data, Literature Searches, and Selections 71
4.2.2 Specific Criteria for Included Articles 71
4.2.3 Results of the Review 72
4.3 Ebola Compartmental Epidemic Models and Analyses 73
4.4 Epidemiological and Economic Data Analysis 79
4.4.1 Economic Cost and Implications of Ebola to West African Countries . 83
4.4.2 Biological Data Analysis for Compartmental Epidemic Models 86
4.5 Policy Recommendations 91

5 A MIXED-INTEGER OPTIMIZATION APPROACH FOR ALLOCATION OF RESOURCES AND CONTROL OF THE DYNAMICS AND SPREAD OF THE 2014 EBOLA EPIDEMIC IN GUINEA, LIBERIA, AND SIERRA LEONE 94

5.1 Introduction 94
5.1.1 Contributions 96
5.2 Mixed-Integer Optimization Model Definition 98
5.2.1 SITR-FB Compartmental Epidemic Model 98
5.2.2 Model Notations 100
5.2.3 Model Assumptions 102
5.2.4 Mixed-Integer Optimization Approach and Epidemic Model Formulation 103
5.2.5 Linearizing Conditional Function 106
5.3 Case Study Data and Parameter Estimation of 2014 Ebola Epidemic 108
5.3.1 Assessment Study of Treatment Cost of 2014 Ebola Epidemic 108
5.3.2 Geographic and Demographic Data From Guinea, Liberia, and Sierra Leone 111
5.3.3 Epidemiological Attributes of 2014 Ebola Epidemic 113
5.3.4 SITR-FB Epidemic Model Implementation and Experimental Design 116

TABLE OF CONTENTS (continued)

Chapter Page

5.4 Numerical Results and Analysis of SITR-FB Epidemic Model 117
  5.4.1 Examining Impact of Non-Control Intervention on 2014 Ebola Epidemic 117
  5.4.2 Analyzing Spatial Distribution of 2014 Ebola in Guinea, Liberia, and Sierra Leone: August 25, 2014, to August 15, 2015 120
  5.4.3 Examining Effect of Control and Non-Control Intervention on 2014 Ebola Epidemic 121
  5.4.4 Assessing Impact of Control Intervention on 2014 Ebola Epidemic . . 125
  5.4.5 Understanding Treatment Cost Components of 2014 Ebola Epidemic 127
  5.4.6 Studying Optimal Allocation of Treatment Facilities to Model Regions 129
  5.4.7 Examining Optimal Allocation of Treatment Facilities to Model Regions Without Migration 130
  5.4.8 Examining Impact of Control Intervention on Spatial Distribution of the 2014 Ebola Epidemic 131
  5.4.9 Analyzing Effect of Non-Control and Control Intervention on 2014 Ebola Transition Parameters: Sensitivity Analysis 1 and 2 133

6 CONCLUSIONS AND FUTURE STUDY 137

6.1 Valid Inequalities for 0–1 Knapsack Formulation 137
6.2 Optimizing New Technology Investments Under Deterioration 137
6.3 A Review of Mathematical Modeling and Data Analyses of Ebola Epidemics 141
6.4 A Mixed-Integer Optimization Approach for Controlling Spread and Dynamics of the 2014 Ebola Epidemic 143

REFERENCES 147

LIST OF TABLES

Table Page

2.1 Summary of Experiments with CPLEX Cuts for $n = 500; \alpha = 0.20, 0.22$, and 0.25 25

2.2 Summary of Experiments with CPLEX Cuts for $n = 1000; \alpha = 0.20, 0.22$, and 0.25 28

3.1 δ Values for Technological Change, Deterioration, Both, and Neither 42

3.2 Full-Body MRI (1.5 T) Data for Model Illustration 44

3.3 Full-Body MRI (0.5 T) Data for Model Illustration 44

3.4 eMRI (1.5 T) Data for Model Illustration 45

3.5 eMRI (0.5 T) Data for Model Illustration 45

3.6 Summary of Replacement Period, Average Replacement Age, Average Inventory Age, Cost, and Penalty 53

3.7 Experiments for Two Styles of MRI and eMRI Units Each with Two or Three Types 54

3.8 Single-Parameter Sensitivity Analysis 60

3.9 Impact of Budget and Demand on Asset Replacement Policy 63

4.1 Selected Ebola Compartmental Epidemic Models, Analysis, and Problem Formulations 80

4.2 Summary of Estimated 2014 Ebola Treatment Cost Per Month (WHO, 2014b) . 85

5.1 Economic Impact and Cost of 2014 Ebola Epidemic (WHO, 2014b) 109

5.2 Geographic and Demographic Characteristics in Guinea, Liberia, and Sierra Leone 111

5.3 Summary of Model Parameters Obtained from Literature for 2014 Ebola Epidemic 113

5.4 Baseline Case Study Initiated on June 16, 2014 (Althaus, 2014; GeoHive, 2014) 117

5.5 Effect of Control and Non-Control Intervention on 2014 Ebola Epidemic 122

5.6 Parameter sensitivity analysis in absence of control intervention 134

5.7 Parameter sensitivity analysis in presence of control intervention 136

LIST OF FIGURES

Figure Page

2.1 Network representation of dynamic programming algorithm 15

2.2 Graphical representations of $F_s(\lambda_s)$ values and envelope inequalities 20

3.1 Representation of MST-PRES model as a tree diagram with flow representing initial inventory supply (n), purchase (B), utilization (X), inventory (I), salvage (S), unmet demand (Y) variables and technological change and deterioration parameter (δ) for an asset with style k and type r 35

3.2 Average number of MRI and eMRI scanning machines in operation and in inventory for all four cases ($\bar{\mathrm{X}}$ and $\bar{\mathrm{I}}$ represent average number of assets in operation and in inventory, respectively) 50

3.3 Cost and penalty with varying objective function weights (note that some of the (w_1, w_2) labels are omitted from the figure for clarity) 58

3.4 Budget required for different demand levels in order to have zero penalty . . . 59

3.5 Impact of budget on total undiscounted cost for case 1 (B), case 2 (D), case 3 (T), and case 4 (T&D) (US $ millions) 64

3.6 Cost analyses for case 1 (B), case 2 (D), case 3 (T), and case 4 (T&D) (US $ millions) 66

4.1 Cumulative number of cases and deaths in past Ebola outbreaks in Africa (Evans and Kaslow, 1997; Oswald, 2007) (as of August, 2015, the 2014 Ebola outbreak cumulative number of cases and deaths are $28,956$ and $11,298$, respectively (Goufo and Maritz, 2015; Klenk and Becker, 2015). We omit the 2014–2015 case and death numbers from the figure due to scalability issues) 68

4.2 Ebola literature review using PRISMA flow chart 73

4.3 Timeline representation of transmission dynamics of Ebola through SEIR model 77

5.1 Network representation of transmission dynamics of Ebola and SITR-FB epidemic model for each model region (k, l). (Here we determine the number of individuals in each model region (k, l) who are susceptible (S), infected (I), treated (T), recovered with lifelong immunity (R), funerals (Ebola-related dead but unburied) (F), and who are safely buried (B)) 99

5.2 Examining impacts of non-control intervention on actual data and SITR-FB epidemic model prediction for cumulative number of cases (I) and funerals (F) of 2014 Ebola outbreak in Guinea, Liberia, and Sierra Leone 118

LIST OF FIGURES (continued)

Figure Page

5.3 Analyzing size of Ebola outbreaks and spatial spread by model region at end of August 25, 2014 to end of August 15, 2015 in absence of control intervention (changes in cumulative number of cases represented by different shades of the color pink) . . . 120

5.4 Assessing actual outbreak data and model predictions for cumulative number of cases (I) and funerals (F), in presence of control intervention . . . 125

5.5 Understanding cost components for different starting dates of implementing control intervention . . . 127

5.6 Spatial allocation of ETC facilities (50- and 100-bed) by model region at end of first and second weeks (wks) when control intervention begins on June 30, July 30, and August 29, 2014 . . . 129

5.7 Spatial allocation of ETC facilities at end of first, second, and fifth weeks (wks) with an optimal budget of $38.7M when control intervention begins on June 30 131

5.8 Examining size of Ebola outbreaks and spatial spread by model region at end of July 30, 2014 to end of October 24, 2015, (changes in number of cases is represented by different shades of the color pink) . . . 132

CHAPTER 1

INTRODUCTION

1.1 Background and Motivation

Resource allocation is a central decision-making problem in every institution. Resource allocation problems require firms to seek the best ways to allocate their limited resources among competing activities. Examples of classical problems that involve the allocation of limited resources are the following: capital budgeting problem in finance (Seitz and Ellison, 1995), management of healthcare facilities with a minimum budget (Shohet and Lavy, 2004), transportation of cargo with a minimum fleet cost (Bennington and Lubore, 1970), distribution of medical resources among a set of control intervention activities during an infectious disease outbreak (Zaric and Brandeau, 2001), and allocation of resources for controlling invasive species and land for biofuels (Büyüktahtakin et al., 2014; Cobuloglu and Büyüktahtakın, 2015). All of these examples of resource allocation have a similar underlying goal, which is to obtain the most efficient and effective ways to allocate their capital resources in order to optimize an objective function while some physical constraints are maintained.

Resource allocation in terms of capital budgeting is the process whereby investment decisions are made in order to select subsets of projects that can be funded within the available amount of budget, thus minimizing overall costs. Resource allocation problems have been studied in operations research for many decades (see, e.g., Hillier, 1995; Taha, 1975). Several resource allocation problems in the past have been formulated using linear programming (LP) and MIP approaches. For example, in 2004, Brown et al. (2004) developed a capital investment problem as an LP model for the U.S. military with a budget of $300 billion over a finite planning horizon of 25 years for the acquisition and maintenance of military assets. A number of resource allocation problems and applications have been presented and discussed extensively in the study of Katoh and Ibaraki (1998).

In this dissertation, we study some important applications of resource allocation problems with capital budgeting in healthcare management as well as the optimization of control intervention strategies for Ebola epidemics. The objective of this dissertation is to study MIP methods and develop decision-making tools to provide optimal solutions to resource allocation problems in healthcare.

The remainder of this chapter is structured as follows: In Section 1.2, we introduce the 0–1 KP, a core resource-allocation problem that forms the basis of all combinatorial optimization problems. In Section 1.2.1, we review dynamic programming, an exact approach for solving many small-sized 0–1 KPs. In Section 1.2.2, we then discuss the derivation of valid inequalities for solving large instances of the 0–1 KP that cannot only be solved to optimality using dynamic programming. In Section 1.3, we present our study on parallel asset replacement in the healthcare settings including magnetic resonance imaging. In Section 1.4, we provide our study on the application of MIP to properly implement control intervention and to allocate medical resources during an epidemic outbreak.

1.2 The One-Dimensional Knapsack Problem: A Resource Allocation Problem

Knapsack problems have been studied and received much attention from researchers in the past decades (Martello and Toth, 1990). In this dissertation, we study the 0–1 KP as a resource allocation problem where a single scarce resource is allocated to a level of activities in order to maximize value for the resource (Martello and Toth, 1990; Salkin, 1975). The knapsack model is an analogy to a hiker's problem, where a subset of items must be selected to fill the knapsack, but it also applies to numerous practical applications (Martello and Toth, 1990; Salkin, 1975). The 0–1 KP is formulated as an integer programming (IP) problem. IP has been widely used in operations research (OR) (Wolsey and Nemhauser, 2014). The polyhedral structure of IP has also been studied by Dantzig (1957) and Jeroslow and Lowe (1984). The general IP problem can be represented as a KP with multiple constraints. It is essential to mention that solution methods to solve IP problems include the CP method and the DP formulation.

1.2.1 Dynamic Programming Approaches to the 0–1 KP

Dynamic programming is a general optimization approach developed by Bellman (1952) for IP problems with an optimal substructure. In fact, iterative solutions of DP formulations are less difficult to build for small-sized optimization problems than in other methods, and that makes it a powerful OR tool (Pferschy, 1999). It is worth pointing out that many researchers have contributed to this field by developing several algorithms (see, e.g., Bellman and Dreyfus, 1966; Howard, 1960; Nemhauser and Ullmann, 1969; Toth, 1980). In particular, the aim of a DP algorithm is to identify an optimal policy that maximizes the return of long-term performance. Developing a DP algorithm mainly involves a solution approach that is achieved by solving an initial subproblem and then relating it to the next subproblem, based on the previous solution in an iterative fashion, until the global problem is solved (Cooper and Cooper, 1981; Denardo, 1982). Alternatively, Weingartner and Ness (1967) present the dual DP approach, whereby the DP algorithm starts with an infeasible solution in which the knapsack is packed with all items, and the items are removed sequentially until the algorithm attains a feasible solution. The algorithm of Bellman (1952) begins with an empty knapsack. Bellman's approach is further developed by Nemhauser and Ullmann (1969).

By using DP formulation, many 0–1 KPs are solvable in pseudo-polynomial time (Cooper and Cooper, 1981; Denardo, 1982; Pferschy, 1999). In general, the application of the principle of optimality is clearly visible in Bellman's functional equation (refer to Cooper and Cooper, 1981; Nemhauser, 1966; Pferschy, 1999). On the other hand, DP algorithm becomes computationally inefficient when both the size and capacity of the 0–1 KP increases (Cooper and Cooper, 1981; Powell, 2007). However, as the model grows, it suffers from computational growth and storage space, and the DP formulation becomes ineffective and attains its worst-case pseudo-polynomial solution time, a major limitation of DP. For this issue, we attempt to develop inequalities for the purpose of strengthening the model's formulation, as mentioned earlier.

1.2.2 Generation of Valid Inequalities

Recently many successful applications of CP approaches, including valid inequalities, have been studied to solve IP problems. For a detailed discussion of the interesting relationship of DP, LP, and MIP we refer the reader to (Aksüt, 2011; Appleget, 1997; Beyer, 2011; Nemhauser, 1966; Sashi Bhusan et al., 2011). Because it is very difficult to obtain the convex hull formulation of a 0–1 KP, instead we strengthen the problem formulation by adding valid inequalities in each instance. A valid inequality is derived from the special structured knapsack formulation, aimed at determining an integral optimal solution at the corner points of the modified feasible region (for details, see Balas, 1975; Padberg, 1975; Wolsey, 1975). In all of these studies, the knowledge of lifting is introduced to strengthen existing inequalities and, therefore, can be used to enhance solution methods, as discussed in this dissertation. Here, we study valid inequalities for solving an IP formulation of the 0–1 KP. We generate inequalities from the end-of-stage optimal return function values from the DP formulation of the 0–1 KP.

1.3 Parallel Replacement Analysis

Replacement problems under OR can be categorized into two groups: serial replacement of a single machine and parallel replacement of economically independent machines (Vander Veen and Jordan, 1989). The economic independence may be caused by demand constraint, budget constraint, and fixed cost. In this dissertation, we focus on asset management, especially the healthcare asset management under technological change and deterioration. Healthcare asset-replacement is a constant challenge for decision-makers in healthcare settings.

Machines may become obsolete in time because technological advancements render the ability of newer machines to operate more efficiently with reduced operation and maintenance (O&M) costs and improved capacity. Therefore, technological change motivates the asset-replacement decision (Rogers and Hartman, 2005). Other studies also document how technological change could influence optimal replacement decisions using a continuous-time model (Yatsenko and Hritonenko, 2008). Technological change is a major advantage of a newer asset over older ones. However, including technological change increases the complexity of the problem. On the other hand, deterioration causes an asset to have a reduced capacity and, as a result, motivates new replacements (Derman, 1963).

According to Christer and Scarf (1994), many healthcare industries aim to implement the best asset-replacement policy under limited capital budgeting. However, these policies are typically emotional decisions without quantifying key replacement data. To properly address the issue of asset replacement and its implementation, we develop an optimization model that captures all relevant information and data related to the cost of operating, keeping, and replacing an asset. The parallel replacement problem determines the keep-or-replace schedule for a group of assets that are economically interdependent and operate in parallel at a minimum cost. During each time period, we make decisions to either keep-or-replace an asset with a newer one with an improved technological change. The parallel replacement problem under economies of scale (PRES), defined to include both fixed and variable asset-replacement costs has been proven to be $\mathscr{N}\mathscr{P}$-hard (Büyüktahtakın et al., 2014). A number of serial and parallel asset-replacement problems with different attributes have been addressed in the literature. These studies include papers analyzing salvage value (Bean et al., 1994), multiple assets (Büyüktahtakın et al., 2014; Hartman, 2004), budget constraint (Hartman, 2000; Karabakal et al., 1994), demand constraint (Hartman, 2000; Rajagopalan, 1998) and technological change (Büyüktahtakın and Hartman, 2015; Hopp and Nair, 1991; Yatsenko and Hritonenko, 2009).

1.4 Epidemiological Models, Data Analyses, and Resource Allocation for Ebola Epidemics

Infectious diseases such as Ebola, malaria, tuberculosis, and others are documented as the leading cause of death and a fundamental problem in developing countries (Lopez et al., 2006). For example, infectious diseases accounted for almost 26% of the deaths in 2001 throughout the world (Kindhauser, 2003). In a similar manner, it is estimated by the World Health Organization (WHO) that approximately 17 million individuals die annually from infectious diseases (WHO, 1996). Therefore, there is an urgent need to study their transmission dynamics and control. In this dissertation, we study the epidemiological models and data analysis of Ebola epidemics.

Epidemic diseases, which are occurring more frequently, are a major health and economic problem for mankind (Jones et al., 2008). The 2014 Ebola outbreak, which has spread widely across several West African countries–Guinea, Liberia, and Sierra Leone (Althaus, 2014; Klenk and Becker, 2015)–has allowed epidemiologists to develop several different investigative techniques, including mathematical models. Mathematical models have become valuable tools for studying the transmission dynamics of these diseases, estimating key parameters from existing epidemiological data, and making significant public healthcare decisions (Hethcote, 2000). The aim of Chapter 4 is to review several approaches for developing epidemiological disease models and their analysis as well as techniques to assess the effectiveness of control interventions, thus improving our understanding of the Ebola virus disease (EVD). We also investigate considerable biological data to explain transmission patterns in affected populations by which Ebola spreads and the economic impact of the disease on affected nations. Insights we gain from this review could be used for policy implementation to aid healthcare managers in determining effective combinations of future intervention strategies.

More importantly, the spread of the 2014 EVD epidemic in West Africa has been the cause of more than twenty-seven thousand infected people and the death of more than eleven thousand people as of August 2015 (Goufo and Maritz, 2015; Klenk and Becker, 2015). Therefore, an Ebola epidemic model that incorporates the spatial spread of the disease and intervention strategies is critical to the eradication of the disease.

To continue our studies on impact of the EVD on the West African continent and the combined effect of control intervention, we formulate an MIP model that captures the dynamic transmissions and spread of the deadly virus through a set population using an extended version of the epidemiological susceptible-infected-removed (SIR) disease model from the study of Kermack and McKendrick (1932). Specifically, we develop a susceptible-infected-treated-removed-funeral-buried (SITR-FB) epidemic model. We also study the movement of susceptible and infected individuals between regions of a given country thus accounting for the geographic spread of the disease.

We illustrate our optimization model on a case study using data from Guinea, Liberia, and Sierra Leone. Our model shows that Ebola epidemic could ultimately be out of control in the absence of control intervention, thus affecting all susceptible individuals in the population. Numerical results also suggest that this optimization model can be used as a decision-making tool in the allocation of Ebola treatment center (ETC) facilities for epidemic-control intervention. Policy implementation is discussed to determine effectiveness in order to aid healthcare managers and government policymakers. Therefore, an epidemiological compartment model for the spread of the disease in a set population and treatment cost associated with intervention strategies are critical to the disease's eradication. In this dissertation, we propose a general epidemic-logistic model that can be applied to any infectious diseases.

1.5 Contributions and Overview

In Chapter 2, we study valid inequalities for the 0–1 KP. We derive valid inequalities using iterative solutions of the end stage of dynamic programming formulations for the 0–1 KP. We present three forms of inequalities including flat, ordered and envelope inequalities. We then employ lifting, with the intention of tightening the inequality to increase the dimension of the face induced by the inequality.

In Chapter 3, we study the optimization of new technology capital investments and deterioration while considering a case study of replacing healthcare assets, which include the advanced imaging device. In particular, we explain the impact of technological change and deterioration on two styles and two types of machines–of MRI and extremity MRI (eMRI) machines. We also provide insights about the complexity of the problem. The multiple style and type asset-replacement model can also be applied to other asset-management problems.

In Chapter 4, we review the literature on mathematical models and analysis for infectious diseases, with an emphasis on infectious disease caused by the Ebola virus. Mathematical modeling of infectious diseases is a tool to understand and describe their spread, to predict future cumulative cases, and to plan control interventions. The objective of this chapter is to review and analyze mathematical models with primary focus on understanding the dynamics of the EVD and the development of effective intervention strategies in order to stop this deadly disease in a set population. This review also presents epidemiological and economic data that could be used in future mathematical models for controlling the Ebola outbreak. We also provide a brief discussion of the control intervention policies that have been effective in containing the spread of the EVD and finally present policy recommendations for healthcare policymakers.

In Chapter 5, we propose a mixed-integer optimization approach for controlling epidemics with emphasis on the 2014 Ebola outbreak in West Africa. In particular, we present an optimization-based epidemic approach that incorporates budget and capacity constraints to study the spatial spread of the Ebola virus and strategies for optimal allocation of ETC facilities. Our proposed formulation eliminates the rate of treatment from infection to hospitalization and establishes the idea that all infected individuals are hospitalized based on the availability of space in treatment centers. We illustrate our model using case study data from the three most affected nations: Guinea, Liberia, and Sierra Leone. We further demonstrate the use of our optimization model on the optimal allocation of treatment facilities and medical resources to the most affected areas of the 2014 Ebola outbreak. The proposed optimization model tests and demonstrates control-intervention strategies during outbreaks. While past Ebola outbreaks have been concentrated in rural areas, the recent outbreak is reported to have invaded every major city in the three most-affected West African nations. This is because a fraction of the infected individuals will travel to seek better treatment. For this reason, we study the movement patterns of susceptible and infected individuals between geographic regions of a given country in our MIP model as they contribute to the spread of Ebola.

Chapter 6 concludes the dissertation and identifies areas for future research.

CHAPTER 2

VALID INEQUALITIES FOR ONE-DIMENSIONAL KANPSACK FORMULATIONS THROUGH DYNAMIC PROGRAMMING

2.1 Introduction

The 0–1 KP, a resource allocation problem with a single constraint is defined as follows: assume a set of items, each with a weight and a value attached to it, determine the items to be included in the knapsack so that the total value of the selected items is maximized while the total weight does not exceed a given fixed knapsack limit. The 0–1 KP, which is known to be $\mathscr{NP}$-hard, has been one of the broadly studied areas of IP and DP. In addition to its theoretical importance, it can be used to model real-life practical problems and can be extended to study other models such as capital budgeting (Lorie and Savage, 1955), cargo loading (Shih, 1979), resource allocation (Coffman et al., 1978), and production planning (Chen et al., 2011).

The standard 0–1 KP consists of a set $N = \{1, \cdots, n\}$ of discrete items, with each alternative item $j \in N$ having an integer value v_j and an integer weight w_j assigned to it. The goal is then to select a subset of items in such a way that their total value is maximized, while their total weight satisfies some capacity constraint W of the knapsack. More formally, a maximization instance of the 0–1 KP can be modeled as the following 0–1 MIP formulation:

$$F_n(W) = \max \sum_{j=1}^{n} v_j \cdot x_j \tag{2.1}$$

subject to :

$$\sum_{j=1}^{n} w_j \cdot x_j \leq W \tag{2.2}$$

$$x_j \in \{0, 1\},\ j \in N = \{1, \cdots, n\} \tag{2.3}$$

The objective function (2.1) of the model formulation maximizes the total value of the selected items packed into the knapsack, while constraint (2.2) ensures that the total weight of the included items in the sack does not exceed the fixed weight capacity of the knapsack. The

0–1 decision variable x_j in (2.3) determines which items are selected to be packed into the knapsack. That is,

$$x_j = \begin{bmatrix} 1 \text{ if item } j \text{ is selected into the knapsack and;} \\ 0 \text{ otherwise} \end{bmatrix.$$

For this well-stated 0–1 KP model formulation, we assume the following:

Item selection The model allows not more than one unit of any item,

Non-negative integer $w_j, v_j > 0$ for each $j \in N$, and

Weight limitation $w_j \leq W$ for each $j \in N$ and $W < \sum_{j=1}^{n} w_j$.

In this chapter, the capacity W of the knapsack is computed as $W = \lfloor \alpha * \sum_{j=1}^{n} w_j \rfloor$, where α represents the tightness ratio. The value of α impacts the computational difficulty of the proposed 0–1 knapsack model (see also Gavish and Pirkul, 1985).

This model formulation and its variants have received considerable attention, including several good algorithmic methods to solve it (Balev et al., 2008; Boyer et al., 2010). Many solution approaches have been developed to deal with the 0–1 KP including valid inequalities and facets for the underlying knapsack polyhedron, dating back to the work of Balas (1997, 1975); Oguz (2010); Wolsey (1975). For example, Hooker and Osorio (1999) propose facet defining inequalities for the 0–1 KP using special structural properties of the model.

Numerous additional studies are available to solve variants of the 0–1 KP using DP algorithms. For example, Boyer et al. (2010) provide an efficient algorithm based on DP and branch-and-bound (B&B) approaches for solving multi-dimensional knapsack problems (MKPs), with results competitive to other techniques. Similarly, Balev et al. (2008) also present an extensive DP-based reduction technique for the large 0–1 MKP. Moreover, Dyer et al. (1995) combine both DP and the B&B approach to implement a hybrid approach to solve the multiple-choice knapsack problem (MCKP). Results show that their approach is very competitive compared to other techniques. Likewise, Pisinger (2001) proposes a DP-based algorithm for MCKP using a significantly large number of generated instances to optimality. Furthermore, Gilmore and Gomory (1966) present a DP-based method for solving the KP after closely studying the one-dimensional stock-cutting problem. Later, Pisinger (1995b) illustrates a new DP approach to effectively solve large instances of the 0–1 KP to improve the work of Balas and Zemel (1980). Recently, Kellerer and Pferschy (2004) present an improved DP algorithmic method for solving large instances of the KP. Various approximation algorithms have been presented to solve the KP. In particular, Sahni (1975) develops one of the early polynomial approximation techniques for solving the KP, while Ibarra and Kim (1975) suggest a modified version, called the fully polynomial approximation algorithm for 0–1 KP, n items and accuracy $\epsilon > 0$ with complexity $O(n \cdot 1/\epsilon^2)$ and space complexity $O(n + 1/\epsilon^3)$ based on DP. The algorithmic approach of Ibarra and Kim (1975) was later improved by Lawler (1979).

Moreover, Horowitz and Sahni (1974) implement both divide-and-conquer and DP approaches to present an $O(2^{n/2})$ algorithm for the 0–1 KP. Martello and Toth (1977, 1990) develop a refined upper bound on the 0–1 KP, which is an improvement over the Dantzig (1957) bound. Their approach has been found to be effective in the B&B algorithm with good computational results (Pisinger, 1995a). Kolesar (1967) also present an efficient depth-first-search B&B algorithm for solving the 0–1 KP by branching on each decision variable where the binary variables are orderly fixed for both primal and dual bounding procedures.

This chapter makes contributions to the 0–1 KP problem literature by studying its polyhedron and identifying valid inequalities that are acquired from end-of-stage iterative solutions to a DP formulation of the 0–1 KP. Furthermore, for the valid inequality derivation, we combine both end-of-stage return value function of a truncated DP and the method of lifting (Balas, 1975; Sashi Bhusan et al., 2010; Wolsey, 1975). The lifting procedure is developed and applied to strengthen the proposed DP structural inequalities in an effort to obtain facet-defining inequalities. In this chapter, we used a similar approach implemented in the study of Hartman et al. (2010) for deriving DP-based inequalities for capacitated lot-sizing formulation. To the best of our knowledge, this is the first time such DP-based inequalities have been used to strengthen 0–1 KP formulations. Our numerical results show that proposed DP-based inequalities are promising in solving 0–1 KP instances with $(n = 500; 1,000)$ variables.

The remainder of this paper is structured as follows: In Section 2.2, we begin with the framework of the DP formulation and its network representation for the 0–1 KP. This section follows with a numerical example that illustrates the DP algorithm. Based on the DP, we develop three forms of valid inequalities and demonstrate them with a numerical example in Section 2.3. Section 2.4 is devoted to techniques for lifting and tightening valid inequalities derived in the previous section. This is followed, in Section 2.5, by a presentation of their performance using randomly generated high-dimensional 0-1 KP instances using computational experiments.

2.2 Dynamic Programming Formulation

Our DP approach is similar to the algorithm presented in Bellman (1952) where the state of the system for a 0–1 KP is defined as the weight limitation of the knapsack. In order to reformulate the 0–1 KP in equations (2.1) to (2.3) as a DP formulation, we define a family of subproblems by considering the first s stages where $1 \leq s \leq n$. The set of possible integral values of a decision variable is defined as $0 \leq x_s \leq \min\left\{1, \lfloor \frac{\lambda_s}{w_s} \rfloor\right\}$, where λ_s $(0 \leq \lambda_s \leq W)$ represents the total occupied capacity in stage s and is defined as a function of λ_{s-1} and x_s (Salkin et al., 1989). The function $F_s(\lambda_s)$ represents the total objective value of the subproblem that can be achieved with capacity λ_s $(\lambda_s = 0, 1, 2, \cdots, W)$. For a given value of x_s, The forward recursive function $F_s(\lambda_s)$ can be formulated as

$$F_s(\lambda_s) = v_s x_s + \max \sum_{j=1}^{s-1} v_j x_j \tag{2.4}$$

subject to :

$$\sum_{j=1}^{s-1} w_j x_j \leq \lambda_s - w_s x_s \tag{2.5}$$

$$x_j \in \{0, 1\},\ j = \{1, \cdots, s-1\} \tag{2.6}$$

However the maximization objective in equation (2.4) with respect to constraints (2.5) and (2.6) is precisely $F_{s-1}(\lambda_s - w_s x_s)$, which is calculated in stage $s-1$. Therefore, the general forward DP recursive function can be written as

$$F_s(\lambda_s) = \begin{bmatrix} F_{s-1}(\lambda_s), & \text{if} \quad \lambda_s < w_s \\ \max\{F_{s-1}(\lambda_s), [v_s + F_{s-1}(\lambda_s - w_s)]\}, & \text{otherwise} \end{bmatrix. \tag{2.7}$$

For each $s = 2, \cdots, n$, the DP equation (2.7) can be used to compute $F_s(\lambda_s)$ for $\lambda_s = 0, 1, \cdots, W$. The computations are initiated by calculating $F_1(\lambda_1)$ as

$$F_1(\lambda_1) = \max_{0 \le x_1 \le \lfloor \frac{\lambda_1}{w_1} \rfloor} v_1 \cdot x_1 \tag{2.8}$$

Note that by defining $F_0(\lambda_s) = F_s(0) = 0$, for each $s = 0, 1, \cdots, n$ and $\lambda_s = 0, 1, \cdots, W$, the DP equation (2.7) can be also used to compute the value function for $s = 1$.

The optimal solution x_s^* consists of recursive computations of $F_s(\lambda_s)$. The subproblem practically defines the values of x_s as

$$x_s = \begin{bmatrix} 1 & \text{if } F_s(\lambda_s) = v_s + F_s(\lambda_s - w_s) > F_{s-1}(\lambda_s) \\ 0 & \text{otherwise} \end{bmatrix. \tag{2.9}$$

Since the problem is to determine the optimal value of the objective function $F_n^*(\lambda_n)$, we repeat equation (2.7) until all items have been considered.

This 0–1 KP formulation can be modeled as a longest path problem (LPP) on a directed acyclic graph, as shown in Figure 2.1. Let G represent the directed, acyclic graph with nodes denoted as (s, λ_s) and arcs of the form $(\lambda_{s-1}, w_j + \lambda_{s-1})$, where $w_j + \lambda_{s-1} \le W$ with arc length v_j. The time complexity of the DP algorithm is given by $O(nW)$ and a state complexity of $O(n + W)$ from the computation of the optimal return function $F_s(\lambda_s)$ (Frieze, 1976; Kellerer et al., 2004; Salkin et al., 1989). The complexity of the problem is exponential in the size of the input. The underlying logic of the DP formulation is illustrated next as an example instance.

Example 2.1. *Numerical illustration of DP algorithm*

This problem will be used throughout this chapter to illustrate the initial research results, and its DP formulation is shown as a tree diagram in Figure 2.1. We consider an instance of the 0–1 KP with $n = 4$, $v_j = (1, 1, 3, 2)$, $w_j = (2, 1, 4, 3)$, $W = \lfloor 0.5 * \sum_{j=1}^{n} w_j \rfloor = 5$, and $0 \leq \lambda_s \leq W$ for $s = 1, 2, 3$, and 4.

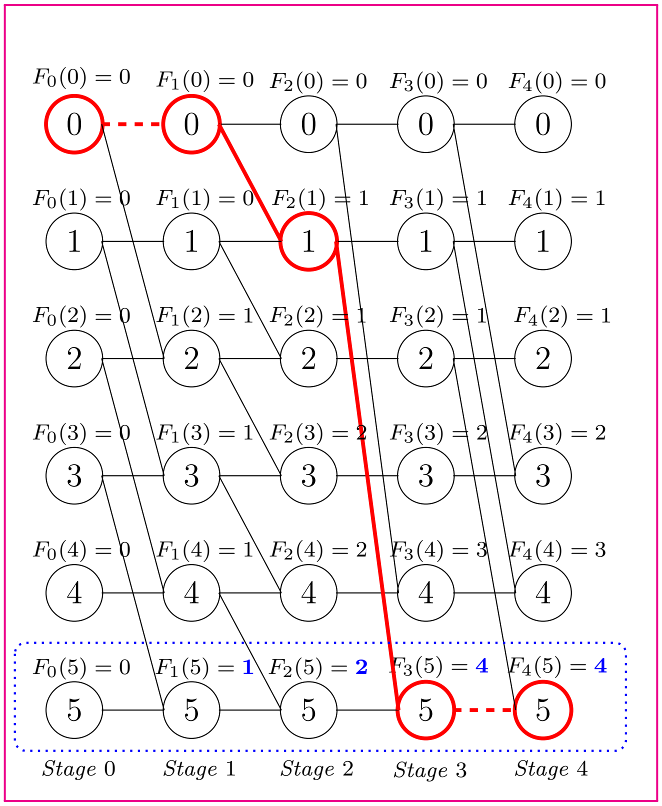

Figure 2.1: Network representation of dynamic programming algorithm

In the network presented in Figure 2.1, each stage and feasible state combination are represented as a node embedded in a two-dimensional coordinate system. Each arc defines a feasible decision for each state, and each arc length represents the value of the associated item selected to be packed into the knapsack. Furthermore, it can be seen from Figure 2.1 that no arc leaves the final node $(4, 5)$ or comes into the initial node $(0, 0)$. In the diagram, $F_s(\lambda_s)$ represents the length of each path with ending state λ_s in stage s. Thus, the optimal value is the length of the longest path, $F_4(5)$, from the source node $(0, 0)$ to the destination node $(4, 5)$, with the optimal solution given by $x^* = \{0, 1, 1, 0\}$ with its corresponding end-of-stage optimal return function values given as $F_s^* = \{0, 1, 4, 4\}$. However, maximal possible values are $\tilde{F}_s = \{1, 2, 4, 4\}$. The optimal return function values are shown above the nodes, and the optimal solution is the path drawn in red boldface.

2.3 Valid Inequality Derivation

The 0–1 KP has been used to formulate many combinatorial optimization problems (Chen et al., 2011). However, 0–1 KP, still remains a challenge, irrespective of modern algorithms and solution methods. This is because exact solutions mostly requires enormous computing time and storage space. This need has led to the development of several effective algorithms for solving them. Valid inequalities form an essential part of this developing area of operations research (OR), since they can be added to the original model as cutting planes to tighten and improve the model formulation for facilitating solution methods.

The DP algorithm presented in equations (2.7) and (2.8) is computationally efficient only when the problem size n is small (Cooper and Cooper, 1981; Powell, 2007). However, as the model grows, it suffers from computational difficulty, i.e., curse of dimensionality (Powell, 2007), and the DP formulation becomes ineffective and approaches its worst-case pseudo-polynomial solution time. Therefore, we generate valid inequalities from a limited number of stages of the DP algorithm in order to strengthen the 0–1 knapsack model formulation.

2.3.1 Flat and Ordered Inequalities

Our inequality generation procedure is similar to DP-based inequalities of Hartman et al. (2010). The authors propose inequalities for an MIP formulation of the capacitated lot-sizing problem using the end-of-stage solutions of its DP formulation. Unlike Hartman et al. (2010), in this paper, we focus on the 0–1 KP and its dynamic programming formulation. Furthermore, we represent envelope inequalities that depend on the range of the capacity parameter as opposed to defining it as a function of a variable as in Hartman et al. (2010). All proposed inequalities are valid for the original 0–1 KP presented in equations (2.1) to (2.3). First, we formulate the following flat inequality for all $s = 1, \cdots, n$:

$$\sum_{j=1}^{s} v_j \cdot x_j \leq F_s(W) \tag{2.10}$$

The inequality (2.10) is valid because $F_s(\lambda_1) \leq F_s(\lambda_2)$ for $0 \leq \lambda_1 \leq \lambda_2 \leq W$, where $F_s(W)$ represents the maximum optimal return of all feasible decisions through stage s. For flat and ordered inequalities, the set of valid inequalities is derived in a linear time; $O(s)$, where s is the number of stages in the subproblem s in addition to the computational time of constructing associated stages of the DP formulation.

Example 2.2. *Flat inequalities*

We demonstrate the technique for generating flat inequalities using the 0–1 KP instance presented in Example 2.1. Solving DP recursion, this procedure generates a set of four valid inequalities (2.11) that do not eliminate any feasible integer solutions to equations (2.2) to (2.3) as follows:

$$\mathit{Flat} := \begin{cases} x_1 \leq 1 \\ x_1 + x_2 \leq 2 \\ x_1 + x_2 + 3x_3 \leq 4 \\ x_1 + x_2 + 3x_3 + 2x_4 \leq 4 \end{cases} \tag{2.11}$$

The set of inequalities from equation (2.11) has the potential to cutoff the initial LP relaxation solution of the MIP formulation of the 0–1 KP. Next, we will provide an example of ordered inequalities, which are the same as flat inequalities in terms of the process for generating them with slight differences. We assume that the ordered inequalities could improve the model formulation compared to the flat inequalities. This is because the ordered inequalities are generated from an ordered 0–1 KP and so the Cplex solver speeds up the solution time. To illustrate the procedure for generating the ordered inequalities we perform the following process. The procedure involves re-ordering of the variables in the original 0–1 KP in decreasing order according to their ratio of value in the objective function and weight in the weight constraint in order to form a new 0–1 KP such that:

$$\frac{v_1}{w_1} \geq \frac{v_2}{w_2} \geq \cdots \geq \frac{v_n}{w_n}$$

With the ordered original 0–1 knapsack formulation, we follow the same approach for generating flat inequalities to obtain the ordered inequalities. Lastly, we solve the ordered 0–1 KP by adding the generated ordered inequalities to it. This approach is then illustrated in Example 2.3.

Example 2.3. *Ordered inequalities*

In order to generate the ordered inequalities, we reorder the variables of the example 2.2 instance from the highest ratio of value-to-weight to the lowest as explained in the literature. The problem data is now reorganized as follows: $n = 4$, $v_j = (1, 3, 2, 1)$, $w_j = (1, 4, 3, 2)$, and $W = 5$. Using DP, this data yields an optimal solution and end-of-stage optimal return function values as $x^* = (1, 1, 0, 0)$ and $\tilde{F}_s = (1, 4, 4, 4)$, respectively. Thus, the ordered inequalities obtained by this approach are given by

$$Ordered := \begin{cases} x_2 \leq 1 \\ x_2 + 3x_3 \leq 4 \\ x_2 + 3x_3 + 2x_4 \leq 4 \\ x_2 + 3x_3 + 2x_4 + x_1 \leq 4 \end{cases} \tag{2.12}$$

It can be easily seen that the fourth inequality presented above is tighter than the second and the third while the first and second inequalities do not dominate each other. The goal here is to strengthen these proposed valid inequalities at each stage s by taking into account the information from all available states. In the following section, we will describe the concave envelope inequalities that are generated using all state information.

2.3.2 Envelope Inequalities

As an alternative to flat and ordered inequalities, we can generate stronger inequalities by explicitly computing $F_s(\lambda_s)$ for all $\lambda_s = 0, \ldots, W$. Our aim is to strengthen the flat inequalities by taking into account all necessary state information contained in each stage of the DP process. Although $F_s(\lambda_s)$ is not necessarily concave, the inequalities that define the concave envelope of $F_s(\lambda_s)$ are valid for the 0–1 KP. The *envelope inequality* is defined as follows:

$$\sum_{j=1}^{s} v_j \cdot x_j \leq m_{s,q}\lambda_s + b_{s,q}; \quad 0 \leq \lambda_s \leq W \tag{2.13}$$

where parameters $m_{s,q}$ and $b_{s,q}$ are defined as the slope and intercept, respectively, for each stage s and defined line segment q. Envelope inequalities are valid because inequalities (2.13) form the concave envelope of $F_s(\lambda_s)$ (Hartman et al., 2010).

Algorithm 2.1. *Concave envelope algorithm*

In order to set up and calculate inequalities of the form in equation (2.13), given computed values $F_s(0), \cdots, F_s(W)$ for each stage s, we use a modified version of the algorithm of Chan (1996). This procedure has complexity $O(Wlog(W))$ for stage s. The algorithm that we use for generating concave inequalities is described as follows: In stage 1, the process begins with the leftmost state ($F_s(0)$). The slope for each segment is then successively derived with respect to all possible other states on its right, and an inequality with the maximum slope is constructed. The rightmost point of the inequality with the maximum slope represents the current state. Slopes from the current state are then computed with respect to the following states. An inequality with the maximum slope is again acquired. This process is repeated until the last rightmost point is included in an inequality. The envelope inequalities strengthen the original formulation, without excluding any feasible integer solution because all feasible functional values stay under the right-hand side of inequality (2.13). The set of inequalities derived from the model are shown in Figure 2.2.

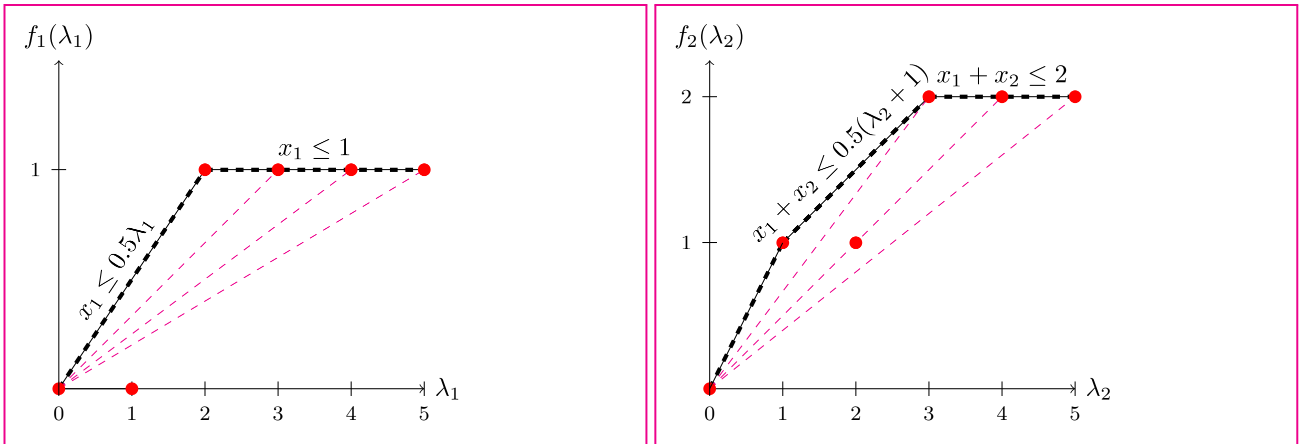

(a) $F_1(\lambda_1)$ values and envelope inequalities

(b) $F_2(\lambda_2)$ values and envelope inequalities

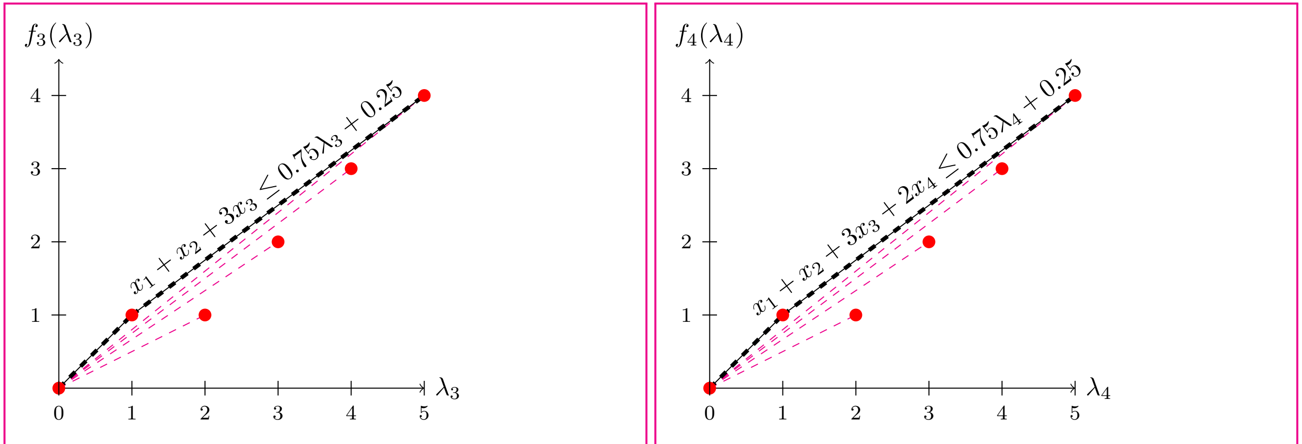

(c) $F_3(\lambda_3)$ values and envelope inequalities

(d) $F_4(\lambda_4)$ values and envelope inequalities

Figure 2.2: Graphical representations of $F_s(\lambda_s)$ values and envelope inequalities

The bold dashed lines represent the envelope inequalities. Next, we demonstrate the inequalities (2.13) in the following example.

Example 2.4. *Continuing example 1, we derive the following envelope inequalities* (2.13) *for stages* $s = 1, \ldots, 4$.

$$\textit{Envelope for stage 1} := \left[\begin{array}{ll} x_1 \le \frac{\lambda_1}{2}, & \textit{where } 0 \le \lambda_1 \le 2 \\ x_1 \le 1, & \textit{where } 2 \le \lambda_1 \le 5 \end{array}\right. \tag{2.14}$$

Immediately, it can be seen that the first inequality presented by equation (2.14) can be stronger than the flat inequality $x_1 \le 1$ when $0 \le \lambda_1 < 2$. The rest of the valid inequalities for stages 2, 3, and 4 of the reduced 0–1 model are presented as follows:

$$\textit{Envelope for stage 2} := \begin{cases} x_1 + x_2 \leq \lambda_2, & \textit{where } 0 \leq \lambda_2 \leq 1 \\ x_1 + x_2 \leq \frac{\lambda_2}{2} + \frac{1}{2}, & \textit{where } 1 \leq \lambda_2 \leq 3 \\ x_1 + x_2 \leq 2, & \textit{where } 3 \leq \lambda_2 \leq 5 \end{cases} \tag{2.15}$$

$$\textit{Envelope for stage 3} := \begin{cases} x_1 + x_2 + 3x_3 \leq \lambda_3, & \textit{where } 0 \leq \lambda_3 \leq 1 \\ x_1 + x_2 + 3x_3 \leq \frac{3\lambda_3}{4} + \frac{1}{4}, & \textit{where } 1 \leq \lambda_3 \leq 5 \end{cases} \tag{2.16}$$

$$\textit{Envelope for stage 4} := \begin{cases} x_1 + x_2 + 3x_3 + 2x_4 \leq \lambda_4 & \textit{where } 0 \leq \lambda_4 \leq 1 \\ x_1 + x_2 + 3x_3 + 2x_4 \leq \frac{3\lambda_4}{4} + \frac{1}{4}, & \textit{where } 1 \leq \lambda_4 \leq 5 \end{cases} \tag{2.17}$$

The concave envelope inequalities derived above are valid for the 0–1 KP. However they have not proven to be facet-defining for 0–1 KP. Therefore, further investigation is required to strengthen existing inequalities in order to approximate the convex hull of feasible solutions. This could be achieved by lifting the proposed valid inequalities into a higher dimensional space as discussed in the following section.

2.4 Lifting

Even with valid inequalities included in the problem formulation, certain instances still cannot be solved within few minutes, so for that reason, we employ an effective lift-and-tighten approach to build stronger valid inequalities for the 0–1 KP. For the lifting approach to work more efficiently, we use inequalities that are valid and have potential in the sense that they could define stronger valid inequalities. Next, a standard definition in the OR literature related to lifting and facets of KP is presented.

Definition 2.1. *The inequality* $\sum_{j=1}^{s} \beta_j x_j \leq \beta_0$*, which, when added to the 0–1 KP, does not cut any feasible integer solution to the 0–1 KP is a valid inequality for P, where P represents the polyhedron of the 0–1 KP.*

In order to strengthen the current valid inequality for the original problem, it is important that we lift with the intention of tightening the inequality to increase the dimension of the face induced by the inequality. Given an existing valid inequality as presented above, we can provide a lifted inequality $\sum_{\substack{j=1 \\ j \neq k}}^{s} \beta_j x_j + \beta_k x_k \leq \beta_0$, where the lifting coefficient β_k associated with variable x_k is computed from the IP problem given by:

$$\beta_k = \beta_0 - \max_{x \in P} \beta x \tag{2.18}$$

The main interest is to hopefully solve for a lifting coefficient that tends to be as large as possible, so as to keep the existing inequality valid for $P \cap \{x \in \{0,1\}^n | \, x_{k+1} = x_{k+2} = \cdots = x_n = 0\}$ (as seen in Wolsey, 1998). Moreover, if we wish to lift a second variable, then the lifting optimization problem must be updated by including k, and this can be done to the next variable by repeating the earlier algorithmic process until all variables are lifted (see, e.g., Balas, 1975; Wolsey, 1975; Zemel, 1978). Inequalities lifted to facet-defining inequalities for P have been seen as the best possible CPs to create and not be dominated by any other inequalities (see, e.g., Balas, 1975; Wolsey, 1975; Zemel, 1978). A numerical example to explore and understand sequential lifting is considered.

Example 2.5. *Lifted set of inequalities for the knapsack set in Example 2.1 with* $v_5 = 2$ *and* $w_5 = 2$.

The last inequality in equation (2.11) can be lifted into a higher dimensional space by adding the variable x_5 to the left-hand-side of the inequality. This becomes:

$$x_1 + x_2 + 3x_3 + 2x_4 + \beta_5 x_5 \leq 4 \tag{2.19}$$

By equation (2.18), the lifting coefficient for x_5 is given by

$$\beta_5 = 4 - \max_{x_5=1,\, x \in P} \{v \cdot x | 2x_1 + 1x_2 + 4x_3 + 3x_4 + 2x_5 \leq 5\} = 2 \tag{2.20}$$

where $v \cdot x = x_1 + x_2 + 3x_3 + 2x_4$

The resulting inequality is: $$x_1 + x_2 + 3x_3 + 2x_4 + 2x_5 \leq 4 \tag{2.21}$$

This newly generated inequality is stronger compared to inequality 2.10.

2.5 Computational Experiments

In this section, we perform several computational experiments that produce remarkable results from using the valid inequalities introduced earlier for solving different $0-1$ KP instances. In order to discuss the impact of the inequalities on the 0–1 KP, two distinct sets of experiments are performed. All experiments are performed using the default settings of CPLEX 12.6.

2.5.1 Generation of Hard Instances

This section tests the effectiveness of our inequalities on randomly generated instances. Gavish and Pirkul (1985) establish that the correlation between values and weights is crucial to the hardness of a data instance, and therefore it is reflected in our experimental data. Tightness ratio is defined as the parameter multiplied by the sum of the weight of each of the items considered to be selected into the knapsack to obtain the weight capacity for the 0–1 KP. Data shows that the closer the tightness ratio reaches zero, the more constrained the problem (Peker Cansizoglu, 2011). These problems have been generated with large weight and value coefficients to reflect properties that may influence solution times. In fact, problems that solve too quickly are eliminated, since they fail to show any effects of the inequalities. In particular, generators proposed by both Glover and Kochenberger (1996) to randomly generate 0–1 KP data instances with tightness ratios $\alpha \in \{0.20, 0.22, 0.25\}$ having strongly correlated data instances are used. Ten instances are generated for each combination of α value for $n = 500; 1,000$ and experiment for a total of 60 instances. Data is generated with the following parameter settings:

- $v_j = 51 * U(0, 10) + 50$ and
- $w_j = U(0, 10) + 0.1 * v_j(1 + U(0, 10))$

2.5.2 Implementation and Experimental Design

Performance of the valid inequalities with the following models are analyzed, and model solution times are compared. All experiments and algorithms are performed and written in $C{+}{+}$ using ILOG CPLEX (version 12.6) default settings. In particular, the derived inequalities are added to strengthen the 0–1 KP (2.1) to (2.3) are obtained using forward DP formulation. Results are shown in Tables 2.1 and 2.2 below to demonstrate comparison among efficiency of the generated inequalities from the several experiments performed. Due to space limitations, the following abbreviations are used in table headings.

Experimental design with corresponding table formats are adopted from the study in Hartman et al. (2010):

`base`: Formulations (2.1) to (2.3) without adding any user inequalities
`flat`: Flat inequalities (2.10) with base
`ordered`: Ordered inequalities (2.10) with base
`envel`: Envelope inequalities (2.13) with base
`flat+lift`: Lifting + flat inequalities (2.10) with base

2.6 Summary of Results

This section provides computational results to evaluate the valid inequalities for 0–1 KP. Tables 2.1 and 2.2 provide summaries of the initial results based on the experimental design with corresponding formulations. Tables 2.1 and 2.2 summarize the average results for 10 instances of each 0–1 KP, for each experiment for each of the three $\alpha \in \{0.20, 0.22, 0.25\}$ values for a 0–1 KP of 500 and 1000 variables for a totall of 60 instances. To demonstrate the impact of our inequalities on the model formulation, we perform experiments with and without our previously defined valid inequalities. In Tables 2.1 and 2.2, columns 1 and 2 give the number of variables in the original formulation and tightness ratios, respectively. Columns 3 and 4 define the experiments and number of stages used to generate DP inequalities, respectively. Columns 5 and 6 specify the initial gap defined as the percentage integrality gap of the 0–1 KP before the addition of cuts and the updated gap beyond the base, respectively. CPU times in seconds for deriving the cuts and solving the entire 0–1 KP are also shown. The computations used in obtaining initial gap and gap improvement in columns 5 and 6, respectively, is adopted from the study of Atamtürk and Muñoz (2004).

- The Initgap is defined as the percentage change between the initial upper bound and the objective function value of the 0–1 KP.
- The Gapimp is defined as the percentage change between the rootgap (the percentage gap after our cuts are added) and the initial gap of the 0–1 KP. Subsequently, the output for these columns are influenced as a result of these computations.

Columns 7, 8, 9, 10, and 11 present the number of valid inequalities added to the base formulation, the number of valid cuts generated by CPLEX, the number of nodes utilized in the tree search process, the average CPU time to derive valid inequalities, and the total average CPU time to solve the entire optimization problem, respectively.

Table 2.1: Summary of Experiments with CPLEX Cuts for $n = 500; \alpha = 0.20, 0.22,$ and 0.25

n	α	Exp	Stage	Initgap	Gapimp	DPineq	CPXineq	Nodes	Ineqtime	Time
500	0.20	base	–	0.01	–	0	3	2,975,269	0.00	122.50
		flat	50		86.99	50	3	2,975,269	0.14	124.59
		flat	100		87.29	100	3	2,975,269	0.22	125.28
		flat	150		89.37	150	6	1,369,436	0.34	67.55
		ordered	50		87.77	50	3	1,589,473	0.17	52.13
		ordered	100		88.65	100	5	1,724,317	0.24	53.02
		ordered	150		91.10	150	4	313,831	0.32	11.90
		flat+lift	50		91.68	51	4	1,888,203	0.16	131.64
		flat+lift	100		88.56	101	4	2,818,035	0.41	173.35
		flat+lift	150		95.05	151	4	259,565	1.51	14.94
		envel	50		89.30	1,044	4	1,035,187	7.63	43.18
		envel	100		86.69	3,600	3	936,051	24.07	56.00
		envel	150		87.45	7,073	3	933,408	45.72	78.30

Table 2.1 (continued)

n	α	Exp	Stage	Initgap	Gapimp	DPineq	CPXineq	Nodes	Itime	Time
500	0.22	base	—	0.01	–	0	3	4,189,234	0.00	198.74
		flat	50		83.97	50	3	4,189,234	0.14	197.78
		flat	100		83.97	100	3	4,189,234	0.23	198.40
		flat	150		84.04	150	2	3,392,826	0.32	186.30
		ordered	50		92.48	50	4	3,353,379	0.26	193.30
		ordered	100		91.34	100	3	1,348,666	0.25	93.98
		ordered	150		94.29	150	8	3,731,754	0.34	195.15
		flat+lift	50		93.97	51	3	4,189,234	0.14	199.51
		flat+lift	100		94.32	101	3	4,191,389	0.25	198.37
		flat+lift	150		93.18	151	3	3,547,026	2.25	175.24
		envel	50		93.99	1,044	3	4,189,354	8.36	221.10
		envel	100		94.51	3,600	3	3,774,349	29.91	56.15
		envel	150		95.00	7,130	3	792,794	31.99	83.41
500	0.25	base	—	0.01	–	0	5	8,898,283	0.00	402.22
		flat	50		94.57	50	5	8,894,056	0.17	378.30
		flat	100		94.57	100	5	8,898,283	0.25	409.52
		flat	150		94.57	150	5	8,577,855	0.33	390.98
		ordered	50		94.57	50	5	15,212,742	0.15	455.74
		ordered	100		94.17	100	8	6,260,430	0.23	256.15
		ordered	150		96.61	150	11	1,487,805	0.36	60.56
		flat+lift	50		94.57	51	5	8,897,760	0.17	477.73
		flat+lift	100		94.57	101	5	8,897,760	0.24	471.06
		flat+lift	150		94.62	151	5	7,895,959	1.21	371.14
		envel	50		94.31	1,044	5	5,884,788	9.57	378.19
		envel	100		94.77	3,537	5	8,463,808	30.59	406.49
		envel	150		96.45	7,191	5	2,054,611	59.59	139.24

First, we observe that model solution without any added inequalities is 402 seconds when experiment has $\alpha = 0.25$ (base experiment), approximately three times more than the base solution time with any of the α values as shown in Table 2.1. In each of our computations in Table 2.1, we derive user inequalities from solving up to 150 stages of the model formulation using partial DP in addition to CPLEX-generated cuts as mentioned. We can see from Table 2.1 that the 0–1 KP instances constructed with a tightness ratio of 0.25 are relatively difficult to solve compared to instances with tightness ratios of 0.22 followed by 0.20. Also, it is expected that the number of search nodes is seen to grow with the level of difficulty in the generated instances. We also notice that the initial gap remains constant within a value of 0.01, while gap improvement due to inequalities is seen to vary between 84% and 96%. The significant changes in gap improvement depend entirely on the tightness ratio of the 0–1 KP, number of stages used to derive DP-based inequalities and the type of experiment implemented. For example, 0–1 KP instances with tightness ratio of 0.25 are observed to have more than 90% gap improvement.

For these numerical results, we again observe that ordered inequalities demonstrate a 50% improvement in CPU times on average for $\alpha = 0.20$. We observe a significant improvement especially when the number of stages to derive DP inequalities are 100 or 150. In addition, we observe that under $\alpha = 0.20$ the ordered and envelope inequalities generated from 150 stages show significant improvement when compared to the results from the base and flat inequalities. This means that as the number of stages for the generation of the inequalities increase, some of the inequalities are seen to perform better than others. In particular, the envelope inequalities are considered to largely show some improvement in model solution time when the number of stages is to up to 150 for a 500 variable problem.

Table 2.2: Summary of Experiments with CPLEX Cuts for $n = 1000; \alpha = 0.20, 0.22$, and 0.25

n	α	Exp	Stage	Initgap	Gapimp	DPineq	CPXineq	nodes	Ineqtime	Time
1000	0.20	base	–	0.02	–	0	1	469	0.00	0.52
		flat	100		92.29	100	1	469	0.26	0.71
		flat	150		92.29	150	1	469	0.33	0.79
		flat	250		91.20	250	1	487	1.01	1.58
		ordered	100		92.82	100	1	511	0.31	0.76
		ordered	150		92.82	150	1	511	0.46	0.92
		ordered	250		91.81	250	1	431	0.92	1.36
		flat+lift	100		91.64	101	1	469	0.37	0.83
		flat+lift	150		93.55	151	1	397	0.56	1.00
		flat+lift	250		90.25	251	1	487	9.25	9.78
		envel*	25		90.26	330	1	434	4.77	5.40
		envel*	50		92.44	1,059	1	471	15.98	16.69
		envel*	75		91.01	2,190	1	494	33.05	33.95
1000	0.22	base	–	0.02	–	0	1	54,540	0.00	3.46
		flat	100		94.13	100	1	54,516	0.49	4.38
		flat	150		94.13	150	2	54,516	0.53	3.41
		flat	250		92.85	250	2	54,459	0.90	3.81
		ordered	100		94.06	100	2	561,212	0.28	25.88
		ordered	150		94.06	150	2	561,213	0.45	25.92
		ordered	250		94.14	250	1	561,171	0.86	26.56
		flat+lift	100		94.13	101	1	54,540	0.45	3.13
		flat+lift	150		94.46	151	1	54,523	0.55	3.46
		flat+lift	250		94.42	251	2	518,247	0.96	25.24
		envel*	25		94.48	296	1	54,505	5.10	8.23
		envel*	50		92.37	1,059	2	58,121	17.18	20.05
		envel*	75		93.63	2,190	2	55,195	39.10	42.08

* We observe that Cplex was out of memory when solving corresponding formulation, therefore specific Cplex codes were added in order to deal with memory problems.

Table 2.2 (continued)

`n`	α	`Exp`	`Stage`	`Initgap`	`Gapimp`	`DPineq`	`CPXineq`	`nodes`	`Ineqtime`	`Time`
1000	0.25	base	–	0.02	–	0	5	5, 098, 038	0.00	310.52
		flat	100		98.89	100	5	5, 098, 038	0.26	262.47
		flat	150		98.85	150	5	5, 079, 574	0.36	236.56
		flat	250		99.04	250	5	5, 079, 574	0.55	236.82
		ordered	100		98.99	100	5	4, 608, 150	0.34	197.14
		ordered	150		98.93	150	5	4, 608, 040	0.45	195.97
		ordered	250		98.85	250	5	4, 148, 903	0.86	177.80
		flat+lift	100		98.89	101	5	5, 464, 918	0.27	257.89
		flat+lift	150		98.82	151	5	4, 613, 871	0.64	225.67
		flat+lift	250		98.98	251	5	4, 760, 946	1.25	218.30
		envel *	25		98.78	296	5	1, 000, 003	5.83	68.31
		envel *	50		98.90	1, 059	5	1, 000, 002	19.63	78.63
		envel *	75		98.24	2, 190	5	1, 000, 003	39.48	88.19

* We observe that Cplex was out of memory when solving corresponding formulation, therefore specific Cplex codes were added in order to deal with memory problems.

Furthermore, Table 2.2 summarizes the average results for similar experiments for 0–1 KP with 1, 000 number of variables. Furthermore, the trend of the solution times and search tree nodes shown in Table 2.2 is similar to the results displayed in Table 2.1. Table 2.2 shows that our gap improvement varies within the range of 91% and 99% with changes in the α values, and thus the difficulty of the problem. In each of our computations, we derive user inequalities from solving 100, 150, and 250 stages of the model formulation using DP to obtain end-of-stage solution for generated inequalities. Envelope inequalities are only generated for 25, 50, and 75 stages due to Cplex memory problems.

In this experiment, we observe that the 0–1 model solution times for the base case for $\alpha = 0.25$ is 310.52 seconds while the addition of either flat or ordered inequalities improve the solution times by approximately a factor between 1 and 2 over the base case experiment. For example, the results obtained using the ordered inequalities for 150 number of stages shows a significant improvement of over 40% in its solution time when compared to the base case. Further, the CPU times achieved from using the ordered inequalities show approximately a 1.5 times improvement in the CPU time on average when compared to the flat set of inequalities. Therefore, the ordered variables in the 0–1 KP play a significant role in the improvement of the solution times. In addition, we observe that the envelope inequalities improve the solution times and tree nodes significantly by a factor of 2 and 4 when compared to the ordered inequalities and base case, respectively. This is due to the increased number of inequalities combined with less number of stages $\{25, 50, 75\}$. For the lifted inequality, we observe a slight gap performance compared to flat inequalities. On the other hand, the differences in solution times are largely noticed in experiments with values of α equal to or less than 0.25.

Overall, our valid inequalities have performed well and thus have shown significant improvement in solution times and search nodes. Out of the 60 0–1 KP instances solved for 500 and $1,000$ variables, it is seen that our computational analysis with ordered and lifted inequalities have shown improvements in solution times. Results in Table 2.1 shows that lifted flat inequalities do not improve CPU times when compared to non-lifted inequalities. However, lifted inequalities have larger gap improvements compared to the flat inequalities. This may be due to lifting only one variable to be added to our last inequality in the set of flat inequalities. Therefore lifting needs further investigation and is considered as a future research direction of this dissertation. Our valid inequalities could be added to larger size 0–1 KPs as CPs to strengthen their formulation. Other approaches could be incorporated into envelope inequalities to reduce the number of generated inequalities thus decreasing its inequality generation time and thereby improving CPU time.

CHAPTER 3

OPTIMIZING NEW TECHNOLOGY INVESTMENTS UNDER DETERIORATION: A CASE STUDY ON MAGNETIC RESONANCE IMAGING MACHINE REPLACEMENT

3.1 Introduction

The U.S. healthcare industry operates and manages large medical devices, such as MRI machines for the provision of health services, at a profit of \$110 billion in 2012, compared to \$75 billion in 2002 (Chatterji, 2009). The total number of MRI machines in use worldwide, including the full-body MRI unit and the smaller-extremity MRI unit, is $25,000$ (Duyn, 2012). Recognizing that MRI scanning machines are the most widely used advanced imaging machines, cost- and service-efficient utilization and replacement decisions are critical to the healthcare industry.

Healthcare machines are often utilized until the end of their operational life. The resulting high operation and maintenance (O&M) cost along with decreased salvage value impact the timing strategies for purchasing newer assets or keeping existing ones (Chen and Feldman, 1997). In addition, the acquisition of new technology makes it possible for the operation of newer machines more efficiently with higher capacity and lower initial O&M cost, and thus is a key driver for replacing assets with new ones (Büyüktahtakın et al., 2014). Asset-replacement decisions are also impacted by important replacement-related parameters, such as unit purchase cost, inventory holding cost, demand, replacement budget, and other factors. Furthermore, considering the fixed cost of purchase in each period gives rise to economies of scale in parallel replacement problems, and thus asset purchases are performed in bundles, if possible, in order to save on the fixed cost.

The complexity of healthcare asset replacement requires the development of an optimization model that captures all relevant information and data related to the cost of operating, maintaining, and replacing an asset in order to analyze efficient service delivery strategies with the minimum cost possible. In this Chapter, we propose a multi-objective

MIP (MOMIP) model for the multiple style and type parallel asset-replacement problem under economies of scale, which determines the decision-making schedule to either keep or replace a group of assets with different capacities and capabilities that operate in parallel and are economically interdependent under a limited budget and a fixed cost at a minimum cost.

The objective of this MIP model is to minimize total cost, including penalty cost (cost of not satisfying demand), fixed and variable purchasing costs, O&M cost, and inventory holding cost, while considering the impacts of technological change and deterioration over a finite planning horizon. The MST-PRES is difficult to optimize because the PRES, which embodies both fixed and variable costs related to machine replacements has been proven to be $\mathscr{NP}$-hard (Büyüktahtakın et al., 2014).

We demonstrate the use of the MST-PRES model on two different styles of healthcare assets: MRI and eMRI machines. The full-body MRI machine is considered ideal to image any part of the body, including the brain and spine, while the eMRI machine can only image peripheral joints of extremities. On the other hand, each style has two different types of assets: high field (1.5 Tesla [T]) and low field (0.5 T) units. The style and type of MRI scanning machines impact the quality of the image and cost of the asset (Cohen, 2006). The total service capacity available for the MST-PRES problem is the sum of the individual service capacities of the MRI and eMRI machines because each machine satisfies demand independently (Hartman, 2004). We assume that MRI machines can meet the demand for eMRI machines, while eMRI machines can only satisfy their own specific demand. Because demand needs to be met under a limited budget, how to allocate that budget over the finite planning horizon is a critical decision.

Existing approaches to solving the PRES include IP or MIP (Büyüktahtakın et al., 2014; Chen, 1998; Jones et al., 1991; Rajagopalan, 1998) and DP (Bellman, 1955; Wagner, 1969). Asset-replacement models involving multiple asset types are more difficult than the PRES models (Büyüktahtakın et al., 2014). Hartman (2004) considers the parallel asset-replacement analysis under variable utilization and stochastic demand for the case involving two assets. Using a case study, Keles and Hartman (2004) formulate and implement an IP model in a bus fleet replacement problem to study replacement decisions for multiple types of buses. Furthermore, Büyüktahtakın et al. (2014) examine a multiple type of asset-replacement problem under economies of scale where a fixed cost is incurred for each purchase made. They show that the PRES and the PRES with multiple asset types are $\mathscr{NP}$-hard, and then they provide CPs to strengthen the related problem formulations.

Technological change is a major advantage of a newer asset over older ones and thus motivates asset-replacement decisions (Büyüktahtakın and Hartman, 2015). Previous work considers serial replacement (Bean et al., 1994; Regnier et al., 2004) and parallel replacement (Büyüktahtakın and Hartman, 2015; Yatsenko and Hritonenko, 2009) in the presence of technological change. Büyüktahtakın and Hartman (2015) prove that the PRES under technological change is $\mathscr{NP}$-hard and provide optimal solution characteristics of the problem. Sobol (2012) shows how technological improvement increases the quality of images and provides faster scan times of MRI machines. Faster scanning machines can serve more customer demand in a unit time period. In this study, we interpret increased customer service acquired due to technological improvements as increased capacity, while deterioration reduces the capacity of an asset.

While PRES has been studied by many researchers under several cases, examining the modeling of technological change and deterioration using MIP approaches is needed. Büyüktahtakın and Hartman (2015) incorporate technological change in terms of capacity changes in a PRES MIP model. However, to our knowledge, none of the previous work simultaneously considers both different styles and types of assets as well as technological change and deterioration in an optimization model. Furthermore, little work explores asset-replacement in the healthcare industry. The proposed model closes this research gap by contributing to the asset-replacement and healthcare asset management literature in the following ways:

- To our knowledge, this study is the first to present a multi-objective MST-PRES MIP formulation to solve the healthcare asset-replacement problem. We develop an optimization model that is applicable to all kinds of machines, and we apply our model to study the replacement problem for two different styles of assets, the full-body MRI unit and the smaller eMRI unit, using both types (high field and low field) over a finite horizon under technological change and deterioration.
- We perform computational studies and detailed sensitivity analysis of the multi-objective MIP model and analyze the impact of key cost drivers of operation and replacement to provide insights into an optimal medical technology investment and replacement policy. We also analyze how optimal costs, replacement decisions, and problem difficulties change with various technological change and deterioration rate scenarios. In addition, we develop a weighted sum approach to determine the Pareto optimal front of the penalty and cost objectives by assigning uniform weights on each objective.
- Input data utilized in this paper is gathered by employing various sources such as the literature and the opinions of healthcare experts. Therefore, this paper also provides detailed cost and asset-replacement data for researchers and managers in healthcare MRI asset management.
- This chapter provides a useful reference for healthcare managers in MRI and eMRI asset-replacement decision-making and could also be utilized as a decision support tool for allocating a limited budget among various operations in order to minimize the total cost in asset-management while considering deterioration and technological advances.
- The proposed model is a general model, and could be applied to not only MRI asset replacement problems but also other replacement problems such as fleet and aircraft management.

The remainder of this chapter is structured as follows: Section 3.2 provides description of the MST-PRES and its MOMIP formulation. This section concludes with a description of four cases with respect to technological change and deterioration. Section 3.3 provides a case study related to two different styles and types of MRI and eMRI scanning machines, computational experiments, numerical results, and discussion. Section 3.4 describes performance of the MST-PRES model and numerical results using the baseline data including Pareto optimal front and analysis of replacement characteristics of assets (replacement periods, ages and costs). Section 3.5 presents sensitivity analysis to provide insights into the optimal replacement policy.

3.2 Multiple Asset-Replacement Model Definition

We develop a MOMIP model to determine the optimal replacement policy for the management of healthcare scanning machines. The proposed MST-PRES MIP model consists of formulating the total cost, including penalty cost, i.e., the cost of a lost opportunity for failing to satisfy a demand from both MRI and eMRI scanning machines, and the cost for operating and replacing both MRI and eMRI scanning machines. We represent the notation and model formulation with a network illustration, shown in Figure 3.1.

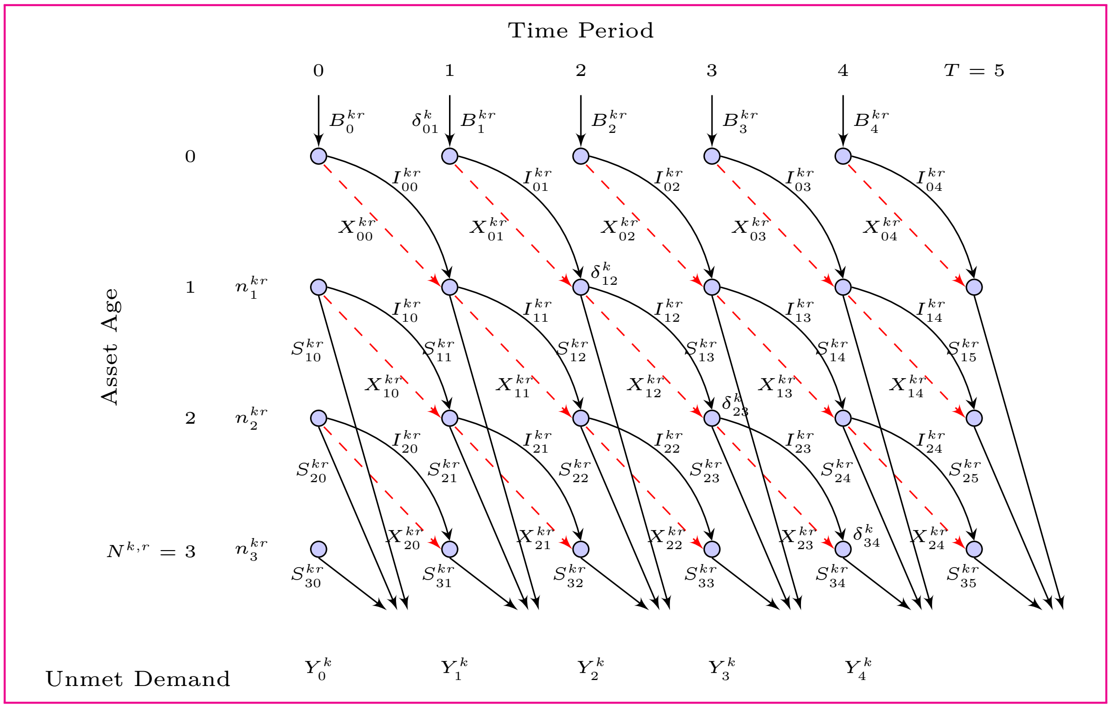

Figure 3.1: Representation of MST-PRES model as a tree diagram with flow representing initial inventory supply (n), purchase (B), utilization (X), inventory (I), salvage (S), unmet demand (Y) variables and technological change and deterioration parameter (δ) for an asset with style k and type r

For this model, an asset is identified by its age, $i = 0, \cdots, N^{k,r}$, as defined on the y-axis, while the time period, $j = 0, \cdots, T$, is represented on the x-axis. This network representation is drawn for a problem where $N^{k,r} = 3$ and $T = 5$ for an asset of style k and type r. Each asset cluster with age i at time j is represented as a node embedded in the two-dimensional coordinate system (i, j). The model is solved over T periods, with new purchases B_j^{kr} made at the end of periods $0, \cdots, T-1$. A newly purchased asset is shown as an incoming flow into each node $(0, j)$, which can be kept for a minimum of one period. As shown in Figure 3.1, an asset may be kept (in use or inventory) or salvaged after each period until it reaches its maximum age $N^{k,r}$, at which time all assets must be salvaged. The salvaged assets, S_{ij}^{kr}, are represented by bold arcs as outflows from any node (i, j).

On the other hand, assets in use, X_{ij}^{kr}, are represented by dashed arcs, while assets held in inventory, I_{ij}^{kr}, are represented by curved arcs as flows between (i, j) and $(i+1, j+1)$. Labels δ_{01}^k, δ_{12}^k, δ_{23}^k, and δ_{34}^k on top of each node from the coordinate $(0, 1)$ to $(3, 4)$ represent technological change and a deterioration parameter for an i-period-old asset at period j. We omit the δ-value labels from the remaining part of the figure for clarity issues. We represent the lost demand for asset style k in each period j by Y_j^k.

3.2.1 Model Notations

Notations for the mathematical model are given as follows:

Indices:

i	Index for age of asset, $i \in \{0, \cdots, N^{k,r}\}$
j	Index for period, $j \in \{0, \cdots, T\}$
k	Index for asset style, $k \in \tilde{K} \cup \bar{K}$
r	Index for asset type that belongs to style k, $r \in M_k$

Sets:

$\tilde{K}$	Set of category-one assets whose demand can only be met by their own style of assets
$\bar{K}$	Set of category-two assets whose demand can also be met by any of the category-one style of assets
M_k	Set of type r assets within style k

Parameters:

ρ_j	discount rate from end of time period j to end of time $j+1$
$N^{k,r}$	Maximum allowable age of a style k, type r asset
T	Number of periods in planning horizon
Ω	Total available budget
$\lambda^{k,r}$	Number of services provided by style k, type r assets
$n_i^{k,r}$	Number of style k, type r assets with age i in initial inventory (initial cluster size)
$H_{ij}^{k,r}$	Unit inventory holding cost of style k, type r assets with age i in inventory from end of time period j to end of time $j+1$
$R_{ij}^{k,r}$	Unit salvage value of style k, type r assets with age i at end of time period j
$P_j^{k,r}$	Unit purchase cost of style k, type r assets at end of time period j
$K_j^{k,r}$	Fixed purchasing cost (transportation and handling) of style k, type r assets at end of time period j
$C_{ij}^{k,r}$	Unit O&M cost to operate style k, type r assets with age i from end of time period j to end of time period $j+1$
d_j^k	Demand specific to style k assets from end of time period j to end of time period $j+1$
γ_j^k	Penalty cost of each lost demand for style k assets at end of time period j
$\delta_{ij}^{k,r}$	Capacity change parameter for style k, type r assets with age i from end of time period j to end of time period $j+1$
a_k	Minimum possible capacity of a style k asset in its lifetime
w_v	Non-negative weight parameter corresponding to objective function $v=1,2$

Decision variables:

$X_{ij}^{k,r}$	Number of style k, type r assets with age i in use from end of time period j to end of time period $j+1$
$I_{ij}^{k,r}$	Number of style k, type r assets with age i in inventory from end of time period j to end of time period $j+1$
$B_j^{k,r}$	Number of style k, type r assets purchased at end of time period j
$S_{ij}^{k,r}$	Number of style k, type r assets with age i sold at end of time period j
Y_j^k	Unmet demand specific to style k asset at end of time period j

$$Z_j^{k,r} \;=\; \left[\begin{array}{ll} 1, & \text{if a style } k\text{, type } r \text{ asset is purchased at end of time period } j; \\ 0, & \text{otherwise} \end{array}\right.$$

3.2.2 Assumptions

The primary assumptions for building our model are stated below:

- We divide the asset cluster into two: category-one assets whose demand cannot be met by any other style of assets, and category-two assets that can only meet their own specific demand and whose demand can be met by category-one assets. Two such examples for category-one and category-two assets are wide- and narrow-body aircraft and MRI and eMRI scanning machines.
- We make the demand specific to style, not type of asset. Therefore, within the same style, any type can satisfy that demand.
- The capacity change parameter is computed based on a combination of deterioration and technological change.
- We assume that O&M cost and salvage values are non-decreasing and non-increasing as a function of age, respectively (Büyüktahtakın et al., 2014).
- All assets are salvaged at the end of the planning horizon. This assumption is a natural consequence of considering a finite planning horizon problem (Keles and Hartman, 2004).

3.2.3 MST-PRES Model Formulation

The MST-PRES model determines the number of each style and type of assets to be purchased, utilized, held in inventory, or salvaged each period. With the variables and parameters defined above, the MST-PRES problem is represented as follows:

$$\begin{aligned} \min\ w_1 \cdot &\left[\sum_{k\in\tilde{K}\cup\bar{K}} \sum_{j=0}^{T-1} \rho_j \cdot \gamma_j^k \cdot Y_j^k\right] + w_2 \cdot \left[\sum_{k\in\tilde{K}\cup\bar{K}} \sum_{r\in M_k} \rho_j \left(\sum_{j=0}^{T-1} \cdot \left(P_j^{k,r} \cdot B_j^{k,r}\right.\right.\right. \\ &\left.\left.\left. + K_j^{k,r} \cdot Z_j^{k,r}\right) + \sum_{i=0}^{N^{k,r}-1} \sum_{j=0}^{T-1} \cdot \left(C_{ij}^{k,r} \cdot X_{ij}^{k,r} + H_{ij}^{k,r} \cdot I_{ij}^{k,r}\right) - \sum_{i=1}^{N^{k,r}} \sum_{j=0}^{T} R_{ij}^{k,r} \cdot S_{ij}^{k,r}\right)\right] \end{aligned} \tag{3.1}$$

subject to:

$$\begin{aligned}&\sum_{k\in\tilde{K}\cup\bar{K}}\sum_{r\in M_k}\left[\sum_{j=0}^{T-1}\left(P_j^{k,r}\cdot B_j^{k,r}+K_j^{k,r}\cdot Z_j^{k,r}\right)+\sum_{i=0}^{N^{k,r}-1}\sum_{j=0}^{T-1}\left(C_{ij}^{k,r}\cdot X_{ij}^{k,r}+H_{ij}^{k,r}\cdot I_{ij}^{k,r}\right)\right.\\&\left.-\sum_{i=1}^{N^{k,r}}\sum_{j=0}^{T}R_{ij}^{k,r}\cdot S_{ij}^{k,r}\right]\leq\Omega\end{aligned}\tag{3.2}$$

$$\sum_{k\in\tilde{K}\cup\bar{K}}\sum_{r\in M_k}\sum_{i=0}^{N^{k,r}}\lambda^{k,r}\cdot\delta_{ij}^{k,r}\cdot X_{ij}^{k,r}\geq\sum_{k\in\tilde{K}\cup\bar{K}}d_j^k-\sum_{k\in\tilde{K}\cup\bar{K}}Y_j^k\quad j=0,\cdots,T-1\tag{3.3}$$

$$\sum_{r\in M_k}\sum_{i=0}^{N^{k,r}}\lambda^{k,r}\cdot\delta_{ij}^{k,r}\cdot X_{ij}^{k,r}\geq d_j^k-Y_j^k\quad k\in\tilde{K},\ j=0,\cdots,T-1\tag{3.4}$$

$$\sum_{r\in M_k}\sum_{i=0}^{N^{k,r}}\lambda^{k,r}\cdot\delta_{ij}^{k,r}\cdot X_{ij}^{k,r}\leq d_j^k-Y_j^k\quad k\in\bar{K},\ j=0,\cdots,T-1\tag{3.5}$$

$$X_{i0}^{k,r}+I_{i0}^{k,r}+S_{i0}^{k,r}=n_i^{k,r}\quad k\in\tilde{K}\cup\bar{K},\ r\in M_k,\ i=1,\cdots,N^{k,r}-1\tag{3.6}$$

$$S_{i0}^{k,r}=n_i^{k,r}\quad k\in\tilde{K}\cup\bar{K},\ i=N^{k,r},\ r\in M_k\tag{3.7}$$

$$\begin{aligned}&X_{(i-1)(j-1)}^{k,r}+I_{(i-1)(j-1)}^{k,r}-X_{ij}^{k,r}-I_{ij}^{k,r}-S_{ij}^{k,r}=0\quad k\in\tilde{K}\cup\bar{K},\ r\in M_k,\\&i=1,\cdots,N^{k,r}-1,\ j=1,\cdots,T-1\end{aligned}\tag{3.8}$$

$$\begin{aligned}&X_{(i-1)(j-1)}^{k,r}+I_{(i-1)(j-1)}^{k,r}-S_{ij}^{k,r}=0\quad k\in\tilde{K}\cup\bar{K},\ r\in M_k,\ i=N^{k,r}\\&\&j=1,\cdots,T,\quad i=1,\cdots N^{k,r}\&\,j=T\end{aligned}\tag{3.9}$$

$$B_j^{k,r}=X_{0j}^{k,r}+I_{0j}^{k,r}\quad k\in\tilde{K}\cup\bar{K},\ r\in M_k,\ j=0,\cdots,T-1\tag{3.10}$$

$$B_j^{k,r}\leq\left\lceil\frac{\sum\limits_{\nu=j}^{T-1}\left(\sum\limits_{l\in\bar{K}}d_\nu^l+d_\nu^k\right)}{a_k^r}\right\rceil\cdot\left(\frac{1}{\lambda^{k,r}}\right)\cdot Z_j^{k,r}\quad k\in\tilde{K},\ r\in M_k,\ j=0,\cdots,T-1\tag{3.11}$$

$$B_j^{k,r}\leq\left\lceil\frac{\sum\limits_{\nu=j}^{T-1}d_\nu^k}{a_k^r}\right\rceil\cdot\left(\frac{1}{\lambda^{k,r}}\right)\cdot Z_j^{k,r}\quad k\in\bar{K},\ r\in M_k,\ j=0,\cdots,T-1\tag{3.12}$$

$$(X_{ij}^{k,r},I_{ij}^{k,r})\geq0\quad k\in\tilde{K}\cup\bar{K},\ r\in M_k,\ i=0\cdots N^{k,r},\ j=0,\cdots T\tag{3.13}$$

$$S_{ij}^{k,r} \in \{0, 1, 2, \cdots\} \quad k \in \tilde{K},\ r \in M_k,\ i = 1, \cdots, N^{k,r},\ j = 0, \cdots, T \tag{3.14}$$

$$(B_j^{k,r}, Y_j^k) \in \{0, 1, 2, \cdots\} \quad k \in \tilde{K},\ r \in M_k,\ j = 0, \cdots, T-1 \tag{3.15}$$

$$Z_j^{k,r} \in \{0, 1\} \quad k \in \tilde{K} \cup \bar{K},\ r \in M_k,\ j = 1, \cdots, T \tag{3.16}$$

$$\textit{where} \quad a_k^r = \delta^{k,r}_{N^{k,r}, \min\{j+N^{k,r}, T\}} \quad k \in \tilde{K} \cup \bar{K},\ r \in M_k,\ j = 0, \cdots, T-1$$

The objective function (3.1) minimizes the weighted sum of the discounted penalty for not satisfying the demand and total discounted cost, including unit purchase cost, fixed purchasing cost, O&M cost, and unit inventory holding cost minus salvage value, which are incurred throughout the planning horizon. We note that all cost and salvage values are multiplied by a discount factor, $\rho_j > 0$, in the objective function (3.1) in order to reflect the impact of discounting on the replacement decisions and to compute the net present value of the total costs incurred. Constraint (3.2) imposes a budget limitation on the sum of unit purchase cost, fixed cost, O&M cost, and unit inventory holding cost less salvage value over all periods. Constraint (3.3) ensures that demand for all styles of assets at each period j is met while allowing some of the demand to be lost. Constraint (3.4) ensures that there is enough capacity to satisfy demand specific to category-one assets while allowing unmet demand, whereas constraint (3.5) provides an upper bound on the capacity allotted for category-two assets. Constraint (3.6) ensures that the number of style k and type r assets utilized, in inventory and salvaged at the end of period zero, is equal to the number of style k and type r assets in the initial period. Constraint (3.7) ensures that all assets in the initial period are salvaged if they are at their maximum age.

Constraint (3.8) maintains the flow of assets from one period to the next, unless they are salvaged, for each style k and type r assets. Constraint (3.9) requires that assets are sold when their age limit or final time period is reached. Constraint (3.10) allows new asset purchases at the end of period j to be either utilized or put in inventory. Constraints (3.11) and (3.12) determine a bound on the number of assets that should be bought to satisfy the demand, while considering the decrease (increase) in capacity due to deterioration (technological change). Constraint (3.11) gives an upper bound on the purchased category-one assets, while constraint (3.12) bounds the total assets purchased for the category-two assets.

In the model formulation, a_k^r gives the minimum possible capacity in a lifetime of an asset with style k type r assets, respectively. We equate the maximum number of assets that could be bought in a period j to $\left\lceil \frac{\sum_{\nu=j}^{T-1}\left(\sum_{l\in\bar{K}} d_\nu^l + d_\nu^k\right)}{a_k^r} \right\rceil$ and $\left\lceil \frac{\sum_{\nu=j}^{T-1} d_\nu^k}{a_k^r} \right\rceil$ for category-one and -two assets, respectively, as we consider the future total demand to be satisfied by the new assets purchased. Constraint (3.13) ensures non-negativity of the utilized and inventory assets without imposing integrality. A fractional solution regarding the X- and I-variables can be interpreted as the percent of time that assets are utilized or kept in inventory, respectively. The set of constraints (3.14) and (3.15), and (3.16) impose the integrality and binary requirements, respectively.

3.2.4 Defining δ Values

Similar to the analysis of Büyüktahtakın and Hartman (2015) on technological change, we define $\delta_{ij}^{k,r}$ as a capacity parameter defining the level of technological change and deterioration in the model.This decision is based on one of four possibilities defined in Table 3.1 for each case with further explanations presented in example 3.1.

Table 3.1: δ Values for Technological Change, Deterioration, Both, and Neither

Case	Description	δ–Value
Case 1 (Baseline)	No technological change and no deterioration (B)	$\delta_{ij}^{k,r} = 1 \,\forall\, i,j$ except $j = 0 \,\&\, i > 0$
Case 2	Deterioration (D)	δ_{i0}^{k} is non-increasing in age i
		$\delta_{ij}^{k,r} \leq \delta_{(i-1),(j-1)}^{k} \,\forall\, i,j$ s.t. $i,j \neq 0$
Case 3	Technological change (T)	δ_{0j}^{k} is non-decreasing in time period j
		δ_{i0}^{k} is non-increasing in age i
		$\delta_{ij}^{k,r} = \delta_{(i-1),(j-1)}^{k} \,\forall\, i,j$ s.t. $i,j \neq 0$
Case 4	Technological change and deterioration (T & D)	δ_{0j}^{k} is non-decreasing in time period j
		δ_{i0}^{k} is non-increasing in age i
		$\delta_{ij}^{k,r} \leq \delta_{(i-1),(j-1)}^{k} \,\forall\, i,j$ s.t. $i,j \neq 0$

Example 3.1. *Numerical illustration of the concept of δ value*

- Given that an initial δ_{00}^{k} is equal to 1, after one year, the value of δ_{11}^{k} will correspond to 0.9, if we assume a degradation value of 10% each year. Multiplying this by X_{ij}^{kr} would make the asset 90% as efficient as its initial condition.
- Additionally, as each year j passes, technological improvement takes place, and thus efficiency is improved. For the same instance, if $\delta_{ij}^{k,r}$ values increase by 10% each year due to technological advances, then the capacity of new assets will increase to 110% of older assets purchased in the previous period. The 110% efficiency of the newly purchased assets will be reduced in time due to deterioration.

Therefore, in our model, $\delta_{ij}^{k,r}$ is defined as a function of both age of the asset and period in which the asset is utilized. For this study, as a base case scenario, we use a degradation value of 10% and technological change of 10% per increase in i and j, respectively, while we also analyze the impact of different $\delta_{ij}^{k,r}$ values on the replacement decisions.

3.3 Case Study Baseline Data and Computational Experiments

To illustrate how the proposed MIP model could help healthcare managers make optimal replacement policies, we consider a case study with two styles of assets serving different demands, as discussed earlier: a smaller eMRI and a large full-body MRI scanning machine. Each style of asset has two types of scanning machines: 1.5 T and 0.5 T. The MST-PRES determines when and how to replace such existing medical imaging devices.

Our study particularly focuses on a doctor's office of nine physicians who provide services to a major city of $400,000$ residents in the state of Kansas. They perform diagnostic imaging services to patients with various types of conditions. According to reviews of manufacturers' product declaration documents, the life span for both eMRI and full-body MRI scanning machines is estimated to be between seven and ten years (Hodge, 2011). Therefore, in this study, we set the maximum age to seven, and estimate the planning horizon to be fifteen years, approximately twice the maximum age of the asset (see, e.g., Christer and Scarf, 1994).

In this scetion, we present operations and a cost data set, which is used as input for the MST-PRES model. Additionally, we provide experimental design, numerical analysis, and discussion of the base case results.

3.3.1 Data Collection

The data set collected for this chapter is based on a variety of information gathered from sources such as journal publications and opinions of healthcare system experts. We interview two radiology technicians (manager and subordinate) from one of the imaging centers in Wichita, KS. We asked questions ranging from O&M costs for their current MRI machine, number of years they have had their current MRI machine, and consequences for a patient who misses an appointmnet. From this data, we utilize the average data values to define the baseline scenario.

The data obtained for the analysis includes the following: initial number of assets, fixed cost (transportation, personnel, insurance, administration, and infrastructure), unit inventory holding cost, unit purchase price, unit O&M cost (parts, labor, and maintenance), unit salvage value, demand, penalty cost, and limited budget for both eMRI and MRI scanning machines. In this section, we study two different types of eMRI and MRI scanning machines and assume that the initial inventory includes only one machine for each type and style in order to provide a general picture of doctors' offices that operate at least a smaller eMRI and full-body MRI unit with two types of each (1.5 T and 0.5 T) (see, e.g., Armstrong, 2005; Iglehart, 2006). All data values are summarized in Tables 3.2 to 3.5. The periodic discount rate, ρ_j, is set also to 6%, based on the study of Fletcher et al. (1999).

Table 3.2: Full-Body MRI (1.5 T) Data for Model Illustration

Parameter	Symbol	Data*	Reference
Initial cluster size	$n_1^{1,1}$	1	Armstrong (2005)
Fixed cost	$K_j^{1,1}$	\$0.60 and increasing by 10% each time period j	Barry (2004); Cergnul (2013)
Unit purchase cost	$P_j^{1,1}$	\$3.0 and increasing by 1% each time period j	Yoakam et al. (2013)
Unit inventory holding cost	$H_{ij}^{1,1}$	\$0.30 and increasing by 10% each time period j	Estimate value
Unit O&M cost	$C_{ij}^{1,1}$	\$0.70 and increasing by 10% each time period j	Kara (2014)
Unit salvage value	$R_{ij}^{1,1}$	70% of $P_j^{1,1}$ and decreasing by 25% each time period j	Expert Opinion
Demand	d_j^1	$4,500$ and increasing by 5% each time period j	Lexa et al. (2005)
Capacity	$\lambda^{1,1}$	$4,050$	Hill (2011)
Penalty cost	γ_j^1	\$0.00195 and increasing by 5% each time period j	Valesquez et al. (2012)
Budget	Ω	\$45	Estimate value

* US \$ millions

Table 3.3: Full-Body MRI (0.5 T) Data for Model Illustration

Parameter	Symbol	Data*	Reference
Initial cluster size	$n_1^{1,2}$	1	Armstrong (2005)
Fixed cost	$K_j^{1,2}$	\$0.40 and increasing by 10% each time period j	Barry (2004); Cergnul (2013)
Unit purchase cost	$P_j^{1,2}$	\$1.0 and increasing by 1% each time period j	Barry (2004); Yoakam et al. (2013)
Unit inventory holding cost	$H_{ij}^{1,2}$	\$0.20 and increasing by 10% each time period	Estimate value
Unit O&M cost	$C_{ij}^{1,2}$	\$0.55 and increasing by 10% each time period j	Kara (2014)
Unit salvage value	$R_{ij}^{1,2}$	70% of $P_j^{1,2}$ and decreasing by 25% each time period j	Expert Opinion
Capacity	$\lambda^{1,2}$	$2,255$	Hill (2011)
Penalty cost	γ_j^1	\$0.00195 and increasing by 5% each time period j	Valesquez et al. (2012)

* US \$ millions

Table 3.4: eMRI (1.5 T) Data for Model Illustration

Parameter	Symbol	Data*	Reference
Initial cluster size	$n_1^{2,1}$	1	Armstrong (2005)
Fixed cost	$K_j^{2,1}$	\$0.18 and increasing by 10% each time period j	Kara (2014)
Unit purchase cost	$P_j^{2,1}$	\$0.50 and increasing by 1% each time period j	Cohen (2006); Kara (2014)
Unit inventory holding cost	$H_{ij}^{2,1}$	\$0.09 and increasing by 10% each time period j	Estimate value
Unit O&M cost	$C_{ij}^{2,1}$	\$0.12 and increasing by 10% each time period j	Kara (2014)
Unit salvage value	$R_{ij}^{2,1}$	70% of $P_j^{2,1}$ and decreasing by 25% each time period j	Expert Opinion
Demand	d_j^2	$3,600$ and increasing by 5% each time period j	Cohen (2006); Kara (2014)
Capacity	$\lambda^{2,1}$	$3,240$	Hill (2011)
Penalty cost	γ_j^2	\$0.000625 and increasing by 5% each time period j	Cohen (2006)

* US \$ millions

Table 3.5: eMRI (0.5 T) Data for Model Illustration

Parameter	Symbol	Data *	Reference
Initial cluster size	$n_1^{2,2}$	1	Armstrong (2005)
Fixed cost	$K_j^{2,2}$	\$0.18 and increasing by 10% each time period j	Kara (2014)
Unit purchase cost	$P_j^{2,2}$	\$0.35 and increasing by 1% each time period j	Cohen (2006); Kara (2014)
Unit inventory holding cost	$H_{ij}^{2,2}$	\$0.09 and increasing by 10% each time period j	Estimate value
Unit O&M cost	$C_{ij}^{2,2}$	\$0.09 and increasing by 10% each time period j	Kara (2014)
Unit salvage value	$R_{ij}^{2,2}$	70% of $P_j^{2,2}$ and decreasing by 25% each time period j	Expert Opinion
Capacity	$\lambda^{2,2}$	$1,880$	Hill (2011)
Penalty cost	γ_j^2	\$0.000625 and increasing by 5% each time period j	Cohen (2006)

* US \$ millions

The penalty cost associated with our MST-PRES model is the cost of a lost opportunity for failing to satisfy demand for a single procedure performed in a doctor's office or hospital. Currently, an eMRI scan for an individual costs between \$350 and \$900, whereas an MRI scan costs in the range of \$400 and \$3,500, based on the procedure. For example, on average, a brain scan can cost approximately \$2,550 (see, e.g. Cohen, 2006; Peh, 2013; Valesquez et al., 2012). We present the average penalty cost for both eMRI and MRI units in Tables 3.2 to 3.5.

MRI scanning machines are maintained according to standards based on manufacturers' recommendations and FDA guidelines. We assume that the O&M cost includes the price of helium, the salary of technicians, and the cost of other services needed to run the machine (e.g., electricity). In our research, the maintenance cost of MRI units is limited to the cost of internal maintenance staff, education, consumables, and maintenance service provided by the manufacturer. In most clinics in the U.S., the O&M cost for eMRI units ranges between $\$90,000$ and $\$120,000$, while the O&M cost for MRI units ranges between $\$622,200$ and $\$700,000$. There are a number of reasons for variations in O&M costs such as condition and utilization of assets. Furthermore, on average, O&M costs for advanced imaging devices increase approximately 5% to 10% yearly (see, e.g. Barry, 2004; Cohen, 1997; Kara, 2014) because of the machine's deterioration over time. In our estimate, we assume the O&M cost to increase by 10% each period.

The current purchase price for eMRI units considered in this study is between $\$145,000$ and $\$270,000$ for a low-field unit and between $\$450,000$ and $\$500,000$ for a high-field unit (Cohen, 2006). We use $\$360,000$ and $\$500,000$ as purchase prices for the 0.5 T and 1.5 T eMRI units, respectively (Kara, 2014). On the other hand, the purchase price for MRI units is also between \$1M and \$3M. Therefore, we assume the extreme values of \$1M and \$3M as purchase prices for the 0.5 T and 1.5 T MRI units, respectively, with an increase of 1% each period (see, e.g. Yoakam et al., 2013).

In our analysis, we assume that salvage value declines with age. By interviewing healthcare experts, we estimate that in the first period, the salvage value of an MRI or eMRI unit is set at 70% of the purchase price and then declines at a rate of 25% in subsequent periods.

We define the fixed cost of purchasing an asset as the cost that remains constant irrespective of the number of assets purchased. For the 1.5 T MRI unit, fixed cost includes the cost of initial installation and room to house the machine. The fixed cost for a 1.5 T MRI unit is given as approximately $\$600,000$ in (Cergnul, 2013). We develop several estimates for eMRI units based on the fixed cost figures given in (Barry, 2004). Furthermore, the cost of assets that are kept in inventory include the cost of housing and maintenance. Therefore, we assume that the inventory holding cost is half of the incurred fixed cost, where both fixed and inventory holding cost increase at a rate of 10% each period.

Each style of asset has its own demand, based on the procedure to be done, either for full body or extremities. Specifically, we assume that different styles of assets (MRI and eMRI) serve different demands, while different types of assets (0.5 T or 1.5 T) within the same style can meet the same demand. For example, about $4,500$ procedures can be performed annually using the 1.5 T MRI unit (see, e.g. Lexa et al., 2005; Yoakam et al., 2013). An article by Peh (2013) states that, out of $8,100$ procedures performed for MRI scans during a 16-month period, $1,800$ of them are for extremities that did not require full-body imaging. This implies that more than 22% of all MRI tests are specifically for extremities. Therefore, we assume that MRI machines can serve the demand for eMRI machines, while eMRI machines can only serve for their own demand of $3,600$ procedures, as given in Table 3.4. Additionally, eMRI and MRI unit service capacity (e.g., maximum number of procedures per unit administered in a year) is assumed to be in the range of 50% and 90%, given their demand level (Hill, 2011). Finally, the value of the overall budget is generated based on the considered planning horizon of fifteen years.

3.3.2 Experimental Design

In this section, we present an optimal replacement policy for assets with different types and styles under different cases by solving the proposed model. We perform all computational experiments on a personal computer equipped with Windows 7, 1.50 GHz CPU and 4 GB memory. We model the problem using AMPL (Gay and Kernighan, 2002) as a front-end interface to CPLEX ILOG (2014), which is used for solving the multi-objective MIP model over a fifteen-period (year) horizon.

3.4 Performance of Model and Summary of Numerical Results

This section provides computational results and data analysis to evaluate the performance of the model formulation using the baseline data from Tables 3.2 to 3.5. For all experiments in this paper, except the Pareto optimal front analysis, w_1 and w_2 are set to one each. The baseline case includes no technological change and no deterioration with $\delta_{ij}^{k,r} = 1$ for all i, j, k, and r, except period 0, where the capacity of initial inventory assets is non-increasing in age.

We first explain the optimal replacement policy for the baseline scenario considering no technological change and no deterioration (case 1). In the optimal solution for the 1.5 T MRI, we observe that the single asset of the initial inventory is used until age six, at the end of which time it is salvaged. Then, at the end of period six, two new assets are purchased to satisfy the growing demand. Of these, 1.88 units of asset are utilized from the end of period six to seven, while 0.12 units of assets are held in inventory. Assets are kept or replaced until all 1.5 T MRI assets are salvaged at the end of period thirteen. We also observe that two 0.5 T MRI units and four 1.5 T MRI units are purchased, while three 1.5 T eMRI and zero 0.5 T eMRI units are purchased over the planning horizon. In this case, the total discounted cost is \$28.11M, including the penalty incurred (\$0.34M), and the solution time is 202.30 CPU seconds. In addition, the optimal replacement decision leads to a total revenue of \$404.59M.

Next, we analyze the optimal replacement policy for the baseline scenario with 10% deterioration and no technological change (case 2). Here, the total discounted cost is \$46.03M, including a penalty of \$16.27M, with a total revenue of \$374.36M. The solution time for the case 2 instance is 48.44 CPU seconds. We observe that the introduction of deterioration in case 2 results in reduced capacity, which requires new assets to be purchased. However, due to the limited budget, deterioration increases both cost and penalty incurred as compared to solving the same problem in case 1 with no deterioration. On the other hand, the optimal replacement policy for the baseline scenario with 10% technological change (case 3) is obtained in 17.55 CPU seconds. In this case, the total discounted cost is \$18.17M, including a penalty of \$0.03M, while generating a total revenue of \$405.34M. Finally, in the optimal replacement policy for the baseline scenario with 10% technological change and 10% deterioration (case 4), the total cost is \$20.82M, with a penalty of \$0.01M, and the solution time is 34.62 CPU seconds. This scenario generates a total revenue of \$405.32M.

In this experiment, first, we observe that some of purchased assets are utilized in operation, while the remaining assets are placed in inventory. The assets in use and in inventory can be fractional, but assets in inventory are strictly less than one under technological change (Büyüktahtakın and Hartman, 2015) and could be greater than one under deterioration. Second, under a similar cost structure, we observe that more 0.5 T MRI units are purchased than 1.5 T MRI units over the planning horizon, due to the high purchase and O&M cost of 1.5T MRI scanning machines.

These results imply that the introduction of technological change in case 3 reduces both the total cost and penalty incurred because O&M cost is reduced and the capacity of the assets is increased. However, the additional introduction of deterioration in case 4 increases the cost when compared to case 3. Furthermore, the solution time is increased in the presence of deterioration in case 4, as compared to the solution with only technological change in case 3.

3.4.1 Number of Assets in Operation and Inventory

In Figure 3.2, we provide the average number of MRI and eMRI scanning machines in operation and in inventory for all four cases of $\delta_{ij}^{k,r}$. In particular, we define the average number of assets in operation (inventory) per period as the ratio of the total number of assets utilized (stored) over all periods to the total number of periods over the planning horizon considered, respectively.

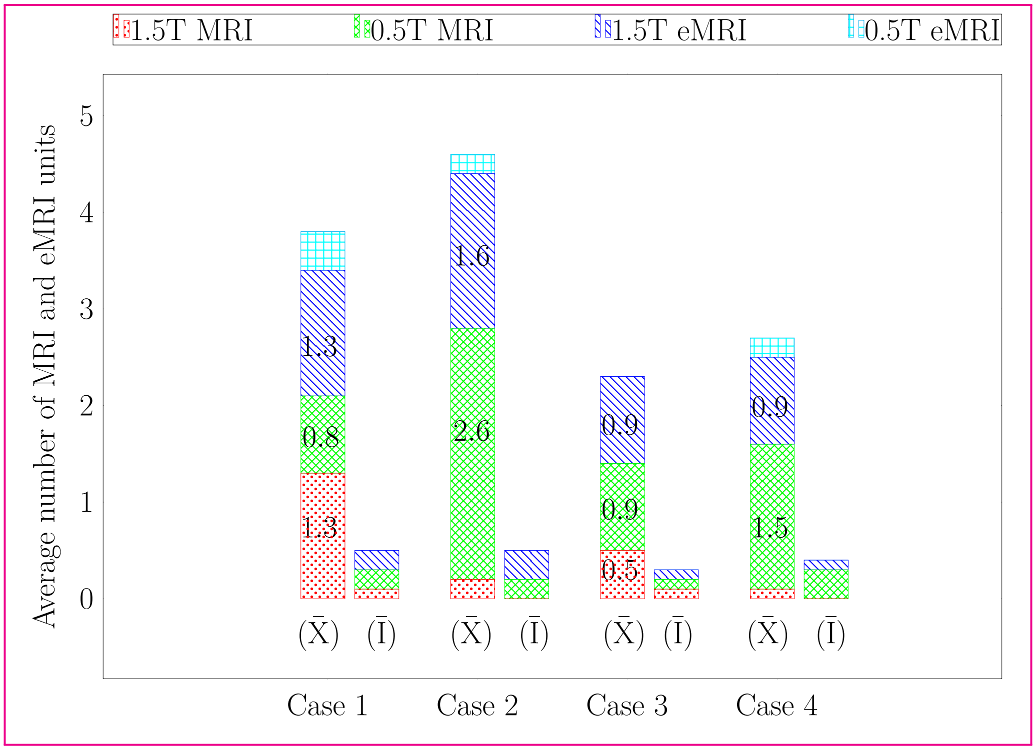

Figure 3.2: Average number of MRI and eMRI scanning machines in operation and in inventory for all four cases (X̄ and Ī represent average number of assets in operation and in inventory, respectively)

For example, in case 1, we notice that the average number of 1.5 T MRIs and 1.5 T eMRIs in operation is 1.3 units each, while the average number of 0.5 T MRIs and 0.5T eMRIs is 0.8 units and 0.4 units, respectively. On the other hand, the average number of units placed in inventory is seen to be less than or equal to 0.3 units in all four cases. For the sake of clarity in Figure 3.2, we omit the average number of inventory for all four cases as well as the numbers that are less than 0.4.

The results of this experiment imply that technological change reduces the average number of assets in operation while deterioration increases it. This is because increased capacity from technological change allows fewer assets to meet the same demand, while reduced capacity due to deterioration requires frequent purchases of new assets to meet future demand. Furthermore, the average number of assets in inventory decreases under the case of technological change.

3.4.2 Replacement Periods, Ages, and Costs

Table 3.6 shows a summary of results of the MIP model including all replacement periods, average replacement age, average inventory age, cost, and penalty regarding the optimal replacement decisions for a number of assets. We define the average age of an asset in use as the average replacement age, which is computed by dividing the total number of assets in use multiplied by their corresponding age to the total number of assets in use throughout the horizon. Similarly, the average inventory age is also defined as the ratio of the total number of assets in inventory multiplied by their corresponding age to the total number of assets in inventory throughout the planning horizon. For example, under case 1, the average replacement ages for the 1.5 T MRI and 0.5 T MRI units are 3.2 and 1.6 years, respectively. This result implies that the 0.5T MRI units require more frequent purchase of new assets than the 1.5T MRI units. We also observe that the average inventory ages for the 1.5T MRI and 0.5T MRI units are 2.7 and 2.6 years, respectively. We note that an asset is only salvaged (not replaced with a new asset) if the replacement period is represented by (–). In addition, the average replacement age of 0 implies that the asset in consideration is immediately salvaged at time zero (if initial inventory exists) and has not been utilized during the planning horizon.

The results of this experiment can be summarized as follows. First, including technological change results in more replacement periods and, thus, a shorter average replacement age than in the base case without technological advances. For example, a comparison of cases 1 and 2 as well as cases 3 and 4 shows that assets are more frequently replaced with technological change in order to take advantage of the new technology with increased capacity, as also declared in the study of Büyüktahtakın and Hartman (2015). Second, the average inventory age under technological change is higher than the inventory age under the case of deterioration. This is because an expensive asset with deterioration cannot be kept in inventory for long because more assets are utilized to satisfy the same demand due to reduced capacity. Third, the presence of new technology far decreases the penalty and cost incurred for failing to meet demand, while deterioration increases the penalty and cost considerably.

3.4.3 Computational Analysis for Changing δ-Values

Table 3.7 presents a number of experimental results to illustrate the impact of the number of asset types (2 and 3) within each style and δ-values on the difficulty of the MST-PRES instances. Here, we set a time limit of $1,200$ CPU seconds for all instances due to their computational difficulty. As shown in Table 3.7, we increase δ-values from 0% to 20% and 0% to 50% for the deterioration (case 2) and technological change (case 3) cases, respectively, to observe the difficulty of the problem for both type-two and type-three type instances. In this table, we report results including the *initgap* (*finalgap*) that represents the first (final) optimality gap reported by CPLEX. We also present the number of CPLEX *cuts* added and the number of *nodes* utilized in the branch-and-bound tree, the *objective* function value, and the elapsed CPU *time* for solving the problem.

Table 3.6: Summary of Replacement Period, Average Replacement Age, Average Inventory Age, Cost, and Penalty

	Replacement period				Average replacement age				Average inventory age				Cost *		Penalty *	
Case	1.5 T MRI	0.5 T MRI	1. eMRI	0.5 T eMRI	1.5 T MRI	0.5 T MRI	1.5 T eMRI	0.5T eMRI	1.5 T MRI	0.5 T MRI	1.5 T eMRI	0.5 T eMRI	MRI	eMRI	MRI	eMRI
Case 1 (B)	(6)	(13)	(3, 8)	–	3.2	1.6	2.8	3.5	2.7	2.6	1.3	0	\$36.35	\$5.89	\$0.00	\$0.74
Case 2 (D)	–	(3, 6, 9, 12)	(3, 7, 11)	–	2	1.1	1.7	2	0	0.7	0.7	0	\$37.88	\$7.09	\$24.62	\$6.36
Case 3 (T)	(9)	(2, 5)	(2, 4, 8)	–	2.3	1.3	2.1	0	1.7	1.1	1.4	0	\$22.11	\$3.68	\$0.03	\$0.00
Case 4 (T&D)	–	(2, 3, 4, 6, 8, 11)	(3, 5, 8, 11)	–	1.5	1	1.3	2	0	0.7	0.8	0	\$25.23	\$4.74	\$0.00	\$0.02

* undiscounted cost and penalty values in US $ millions, dashed line represents no purchases of new assets through the horizon.

Table 3.7: Experiments for Two Styles of MRI and eMRI Units Each with Two or Three Types

Type[a]	δ(%)	Case	Inigap(%)[b]	Fingap(%)[c]	Cuts[d]	Nodes[e]	Objective[f]	Time[g]
2	0	Base case	92.74	0.01	543	252, 484	28.11	202.30
2	2	Deterioration	92.39	0.01	444	249, 885	29.61	218.09
	4		92.07	0.01	597	144, 515	33.38	183.30
	6		91.80	0.01	600	56, 908	37.46	68.81
	8		91.64	0.01	518	70, 384	41.90	82.87
	10		91.55	0.01	506	43, 097	46.03	48.44
	12		91.50	0.01	441	42, 206	49.60	41.78
	20		91.47	0.01	316	5, 054	59.97	6.52
2	2	Tech. change	93.49	3.40	529	345, 983	26.27	1, 200
	4		94.13	4.86	504	268, 583	24.48	1, 200
	6		94.70	4.89	433	307, 983	22.38	1, 200
	8		95.22	0.01	5536	31, 028	19.41	39.44
	10		95.70	0.01	544	6, 861	18.70	17.55
	12		95.22	0.01	558	8, 044	17.17	20.61
	20		97.31	0.01	544	849	13.37	2.70
	30		98.11	0.01	531	347	11.20	2.87
	50		98.7	0.01	263	745	9.03	1.69
3	0	Base case	27.36	4.59	627	169, 646	26.32	1, 200
3	2	Deterioration	38.51	7.31	535	182, 182	28.46	1, 200
	4		37.83	8.50	523	174, 892	30.21	1, 200
	6		56.24	11.51	310	132, 593	33.28	1, 200
	8		39.87	6.43	591	143, 580	36.50	1, 200
	10		91.51	0.01	659	569, 726	39.97	680.29
	12		91.26	0.01	618	239, 345	43.33	299.23
	20		90.60	0.01	477	30, 959	53.58	36.77

Table 3.7 (continued)

Type[a]	δ(%)	Case	Inigap(%)[b]	Fingap(%)[c]	Cuts[d]	Nodes[e]	Objective[f]	Time[g]
3	2	Tech. change	23.72	4.63	602	254,082	24.03	1,200
	4		27.11	6.54	524	204,622	22.00	1,200
	6		31.55	8.28	418	231,964	20.44	1,200
	8		95.75	0.01	646	204,056	17.52	218.88
	10		96.23	0.01	719	89,669	16.19	298
	12		96.64	0.01	503	5,886	14.87	27.58
	20		97.84	0.01	634	5,101	11.59	38.27
	30		98.65	0.01	582	4,280	9.21	9.42
	50		99.24	0.01	313	3,614	7.13	3.68

[a] number of types associated with each style units in experiment, [b] first percentage integrality gap of optimization problem reported by CPLEX, [c] final percentage integrality gap of optimization problem reported by CPLEX, [d] number of valid cuts generated by CPLEX, [e] number of nodes utilized in tree search process, [f] objective function value (discounted total costs) in US $ million, [g] total CPU time to solve entire optimization problem.

For the type-two instances, under the base case where δ-values are set to 0%, we observe that the problem is easier to solve with shorter CPU time compared to the technological change case with δ-values up to 6%. Type-two instances with δ-values of 2% to 6% could not be solved to optimality for technological change. However, as the δ-value changes from 8% to 50%, the type-two instances could be solved to optimality with the default final integrality gap of 0.01%, while the number of nodes as well as the solution time are significantly reduced. As we increase the δ-values from 8% to 50%, the type-two instances become easier to solve because constraints (3.11) and (3.12) are tightened with larger δ-values, thus reducing the feasible solution space.

Type-three instances are more difficult to solve than type-two instances under all cases. Our results show that incorporating either deterioration or technological change as well as increasing the number of types for each style of assets increases the complexity and thus the solution time of the MST-PRES instances, while the most difficult instances are those with three types and deterioration.

For both type-two and type-three instances, we observe that as we increase δ-values, the objective function value decreases (increases) under technological change (deterioration) due to the increased (decreased) capacity. The optimal solution also implies that the number of new asset purchases shows a decreasing (increasing) trend under technological change (deterioration) as the δ-values increase. We also observe that more 0.5 T eMRI units are purchased and more frequently replaced than 1.5 T eMRI units on average under technological change. It is also noticeable that more 1.5 T MRI units are purchased than 1.5 T eMRI units due to their larger capacity. Interestingly, only new 0.5 T MRI and 1.5 T eMRI units are purchased under deterioration with a δ-value of 8% and above. While both 1.5T and 0.5T eMRI units are replaced for technological change up to a δ-value of 30%, the optimal solution structure changes to purchasing only 0.5T eMRI units when the δ-value is increased to 50% and beyond. This is because the increased capacity of 0.5 T eMRI units allow for meeting demand with lower cost than the 1.5 T eMRI units when technological advances are large enough.

The average replacement age under technological change for all considered δ-values is smaller than the base case, implying that technological advances motivates more frequent replacements. We also observe that the replacement age shows a decreasing trend as we increase the deterioration parameter. On the other hand, under technological change, average replacement and inventory ages fluctuate until the δ-value increases up to 18% and then begins to decline as the δ-value increases. This result shows that optimal replacement frequency is specific to the δ-value and the case considered, and cannot be generalized due to the high complexity of the problem.

3.5 Sensitivity Analysis

In this section, we provide a sensitivity analysis in order to determine the impact of various parameters on the optimal solution presented in Section 3.4. Specifically, we investigate how the optimal replacement polices and total cost are affected as we adjust budget, demand, salvage value, fixed cost, O&M cost, and inventory holding cost. We also illustrate a graphical analysis in terms of budget, demand, and percentage of cost components for operating and replacing the MRI and eMRI scanning machines.

Additionally, a Pareto optimal front is constructed by using a weighted sum approach for determining optimal asset-replacement strategies for the baseline case by adjusting the weights of the two objectives: minimizing penalty and minimizing cost simultaneously. This study helps healthcare managers to not only determine the optimal replacement policy for MRI and eMRI assets but also perform the numerical analysis under various cases by adjusting the weights corresponding to penalty and cost.

3.5.1 Pareto Optimal Front

In this section, to illustrate the nature of trade-offs between penalty and costs, we perform a weighted-sum approach. This procedure attempts to find Pareto optimal solutions one after the other, by orderly changing the weights of the objective function presented in equation (3.1). Therefore, we generate a Pareto optimal front by varying the weight parameters $(w_1, w_2) \in [0, 1]$ allocated uniformly such that $w_1 + w_2 = 1$ and $(w_1, w_2) \geq 0$. As an illustration, we consider different combinations of w_1 and w_2, where we set $\{(w_1, w_2)\}$ to $\{(0, 1), (0.1, 0.9), \cdots, (1, 0)\}$. Given these weights as the relative importance for each objective function, equation (3.1) is solved with the same constraints (3.2) to (3.16), in order to obtain the Pareto optimal front illustrated in Figure 3.3 for a set of eleven different values of the weight parameter.

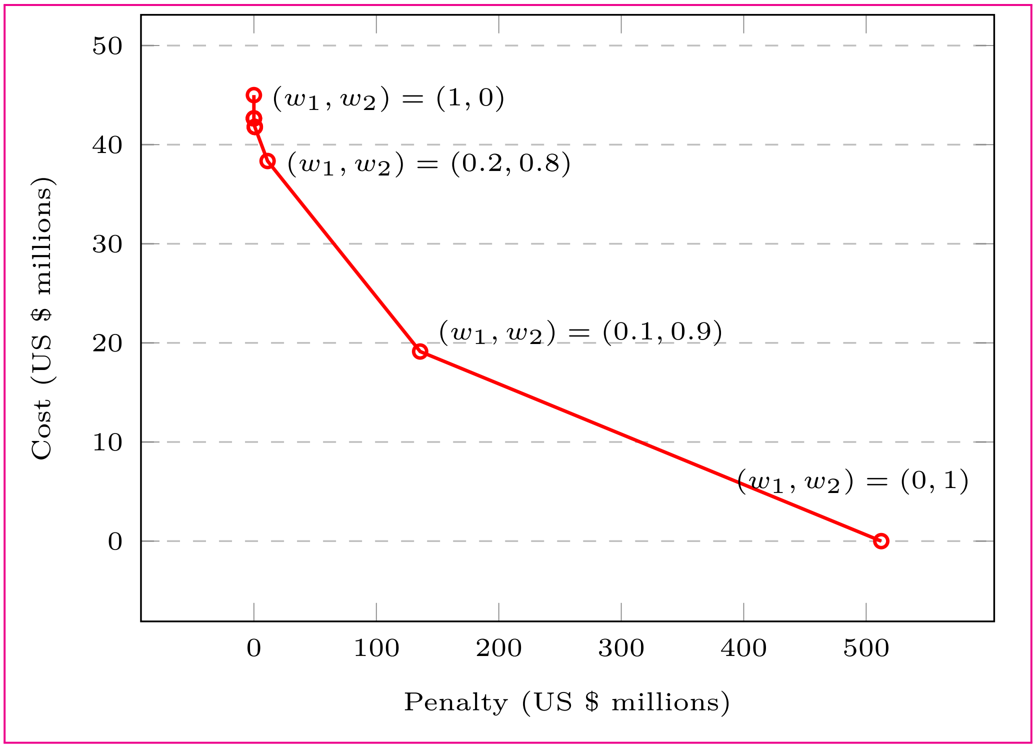

Figure 3.3: Cost and penalty with varying objective function weights (note that some of the (w_1, w_2) labels are omitted from the figure for clarity)

Figure 3.3 provides important information for decision-makers. First, the area with the undefined slope indicates that w_1 (penalty weight) is greater than 0.5, implying that changes in cost yield little or no changes in penalty. On the other hand, the area with a steep slope indicates that when w_1 is less than or equal to 0.5, small changes in cost yield large changes in penalty. Second, this result suggests that in order to achieve a zero penalty, the weight allocated to the penalty must be greater than the weight allocated to the cost. This analysis will assist decision-makers and managers in identifying the best values for the weight parameter, based on their interest in penalty and cost.

3.5.2 Budget Required for Zero Penalty

In Figure 3.4, we provide a detailed analysis of the minimum amount of budget for a given demand level in order to achieve a zero penalty. Setting $w_1 = 1$ and $w_2 = 0$, the objective function (3.1) is solved subject to constraints (3.2) to (3.16) under all four cases of $\delta_{ij}^{k,r}$ values.

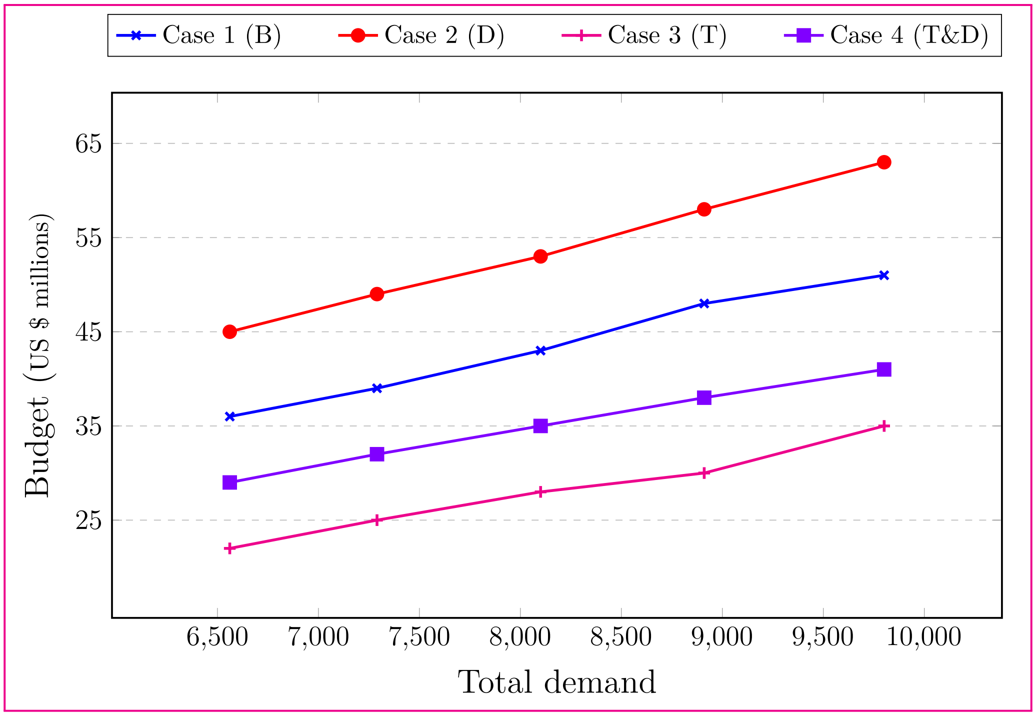

Figure 3.4: Budget required for different demand levels in order to have zero penalty

Figure 3.4 illustrates combinations of budget and demand levels related to four cases of $\delta_{ij}^{k,r}$ values where a zero penalty is incurred. Results show that when demand is increased from $6,500$ to $10,000$, there is a significant increase in the total budget required. Case 3 requires the least amount of budget for a given demand level in order to achieve a zero penalty, because fewer assets are needed in the technological change case due to the increased amount of capacity. However, this result is followed by cases 4, 1, and 2, with case 2 requiring the highest budget for a given demand level to reach a penalty of zero. This is because under deterioration (case 2), more assets are needed to meet demand levels. This analysis can assist decision-makers in evaluating the combinations of budget and demand levels in order to satisfy all demands with zero penalty.

3.5.3 Single-Parameter Sensitivity Analysis

To assess the effect of key parameters on the optimal solution and the objective function value, an additional numerical analysis is performed. In Table 3.8 showing the results of single-parameter sensitivity analysis, the columns represent the model parameters, their symbols, corresponding data values, objective function values, and CPU time in seconds.

Table 3.8: Single-Parameter Sensitivity Analysis

Parameter	Symbol	Data		Objective *	Time †
Budget %Δ10	Ω	$36.45		$39.86	14.94
		$40.50		$29.65	89.25
		$45.00		$28.11	202.3
		$49.50		$28.11	200
		$54.45		$28.11	160.18
Unit salvage value† 70% of $P_0^{k,r}$	$R_{11}^{k,r}$	%Δ − 15		$26.9	260.57
		%Δ − 20		$27.58	318.09
		%Δ − 25		$28.11	202.3
		%Δ − 30		$28.51	99.19
		%Δ − 35		$28.8	135.89
Demand %Δ10	d_0^1 & d_0^2	3645	2916	$23.26	503.81
		4050	3240	$25.73	314.3
		4500	3600	$28.11	202.3
		4950	3960	$32.91	95
		5445	4356	$46.33	13.12
Penalty %Δ10	γ_0^1 & γ_0^2	$0.0016	$0.00051	$28.04	174.57
		$0.0018	$0.00057	$28.07	136.55
		$0.0020	$0.00063	$28.11	202.3
		$0.0021	$0.00069	$28.13	198.85
		$0.0024	$0.00076	$28.13	381.13

* discounted total cost in US $ millions, Δ represents changes in baseline data values by amount next to it, underlined data values are initial values used for baseline case, † total CPU time in seconds.

Table 3.8 (continued)

Parameter	Symbol	Data				Objective*	Time†
Fixed cost %Δ10	K_0^{11}, K_0^{12}, K_0^{21} & K_0^{22}	\$0.49	\$0.32	\$0.15	\$0.15	\$27.83	600
		\$0.54	\$0.36	\$0.16	\$0.16	\$27.94	435.21
		\$0.60	\$0.40	\$0.18	\$0.18	\$28.11	202.3
		\$0.66	\$0.44	\$0.20	\$0.20	\$28.32	268.7
		\$0.73	\$0.48	\$0.22	\$0.22	\$28.53	98
Unit inventory holding cost %Δ10	H_0^{11}, H_0^{12}, H_0^{21} & H_0^{22}	\$0.24	\$0.16	\$0.07	\$0.07	\$27.87	103.93
		\$0.27	\$0.18	\$0.08	\$0.08	\$28.00	270.4
		\$0.30	\$0.20	\$0.09	\$0.09	\$28.11	202.3
		\$0.33	\$0.22	\$0.10	\$0.10	\$28.26	179.79
		\$0.36	\$0.24	\$0.11	\$0.11	\$28.41	541.63
Unit purchase cost %Δ10	P_0^{11}, P_0^{12}, P_0^{21} & P_0^{22}	\$2.43	\$0.81	\$0.41	\$0.28	\$26.58	600
		\$2.70	\$0.90	\$0.45	\$0.32	\$27.31	493.81
		\$3.00	\$1.00	\$0.50	\$0.35	\$28.11	202.3
		\$3.30	\$1.10	\$0.55	\$0.39	\$29.00	500
		\$3.63	\$1.21	\$0.61	\$0.42	\$31.02	430
Unit O&M cost %Δ10	C_0^{11}, C_0^{12}, C_0^{21} & C_0^{22}	\$0.57	\$0.45	\$0.10	\$0.07	\$24.48	170
		\$0.63	\$0.50	\$0.11	\$0.08	\$26.33	136.44
		\$0.70	\$0.55	\$0.12	\$0.09	\$28.11	202.3
		\$0.77	\$0.61	\$0.13	\$0.10	\$30.92	274.47
		\$0.85	\$0.67	\$0.15	\$0.11	\$37.92	99.19

* discounted total cost in US \$ millions, Δ represents changes in baseline data values by amount next to it, underlined data values are initial values used for baseline case, † total CPU time in seconds.

As shown in Table 3.8, only one model parameter corresponding to MRI and eMRI scans in the baseline case is varied in each experiment, while the others are held constant at their baseline data values. Table 3.8 presents results for a 10% increase or decrease in the baseline values, as considered by Christer and Scarf (1994). We first examine how changes in the data impact the objective function value for key parameters such as demand, O&M cost, and unit purchase cost, as well as salvage value, inventory holding cost, and fixed cost. We then provide further analysis for these key parameters in order to observe their impact on the replacement decision.

The analysis presented in Table 3.8 shows that changing the baseline demand and O&M data yields a percentage change in the range of 6% to 13% and 10% to 35% in the objective function, respectively. Furthermore, a change in the unit purchase price impacts the solution by up to 10%, On the other hand, a change in the inventory holding cost, fixed cost, and penalty cost results in about 1% change in the solution and thus has less impact on the replacement decision, as compared to parameters such as demand and O&M cost. Therefore, O&M, demand, and unit purchase costs form the major cost drivers, while fixed and inventory holding costs have a relatively lower impact on results in the healthcare imaging machine-replacement case.

Budget and demand parameters have a significant impact on the model's output. It is also essential to show the relationship between the two. Therefore, we provide a budget and demand sensitivity analysis to evaluate their impact on the average replacement age and objective function values.

3.5.4 Two-Parameter (Budget and Demand) Sensitivity Analysis

This section examines the effects of varying both the budget and demand on penalties, costs, and average replacement ages. As shown previously in Figure 3.4 and Table 3.8, there is a positive correlation between demand and budget. Table 3.9 shows a two-parameter sensitivity analysis, where both parameters are adjusted simultaneously while the remaining parameters are kept fixed at their baseline values. First we observe that the 1.5T scanning machines are replaced between 2.3 and 3.2 years, while the 0.5 T scanning machines are replaced between 1 and 3.5 years, for different budget levels. This result implies that the 1.5 T scanning machines are retained longer and thus are less frequently replaced than the 0.5T scanning machines on average. This is because the 1.5 T MRI scanning machines have more capacity and thus large utilization compared to the 0.5 T MRI scanning machines. Second, the 10% increase in budget leads to a decrease in penalty and total costs while increasing O&M costs. Third, when the budget is set to a constant value while the demand increases, we notice that the average replacement age shows a decreasing trend because the model aims to reduce O&M cost by more frequently replacing assets under high demand while paying an increased penalty. Here, we consider the baseline total budget ($45M) and demand (4,500 for MRI units, and 3,600 for eMRI units) and draw some conclusions. We consider $49.50M and $54.45M budget allocations over the horizon as an increase of 10% and 20% over the baseline budget ($45M), respectively.

Table 3.9: Impact of Budget and Demand on Asset Replacement Policy

		Demand			Objective		Average replacement age				
Average	Budget*	MRI	eMRI	%Δ	Penalty*	Cost*	1.5 T MRI	0.5 T MRI	1.5 T eMRI	0.5 T eMRI	Average
	$45.00	4500	3600	10%	$0.34	$27.77	3.18	1.61	2.80	3.50	2.77
		4950	3960		$2.43	$29.64	3.04	1.63	2.39	2.50	2.39
		5445	4356		$15.49	$30.45	2.49	2.10	2.45	2.50	2.39
		5990	4792		$31.70	$30.77	2.54	2.00	2.34	2.00	2.22
		6588	5271		$54.78	$30.71	2.71	1.00	2.73	1.00	1.86
Average		5494.60	4395.80		$20.95	$29.87	2.79	1.67	2.54	2.30	
	$49.50	4500	3600	10%	$0.34	$27.77	3.18	1.61	2.80	3.50	2.77
		4950	3960		$0.44	$30.18	3.04	1.71	2.73	3.50	2.75
		5445	4356		$1.42	$32.91	2.49	2.32	2.45	2.50	2.44
		5990	4792		$16.41	$32.26	2.94	1.60	2.78	1.50	2.21
		6588	5271		$37.10	$32.90	2.30	1.00	2.73	1.50	1.88
Average		5494.60	4395.80		$11.14	$31.20	2.79	1.65	2.70	2.50	
	$54.45	4500	3600	10%	$0.34	$27.77	3.18	1.61	2.80	3.50	2.77
		4950	3960		$0.44	$30.18	3.04	1.71	2.73	3.50	2.75
		5445	4356		$0.04	$33.65	2.49	1.45	2.38	2.50	2.21
		5990	4792		$0.77	$36.15	3.07	1.00	2.54	2.00	2.15
		6588	5271		$13.27	$36.33	2.85	1.50	2.73	1.00	2.02
Average		5494.60	4395.80		$2.97	$32.82	2.93	1.45	2.64	2.50	

* discounted values in US $ millions

3.5.5 Impact of Budget on Total Cost

In this section, we perform a sensitivity analysis to visualize relationships among critical parameters and how slight variations in input data affect numerical results. Figure 3.5 illustrates the impact of budget on total cost when the baseline budget is increased and decreased by 10% in all four cases of technological change and deterioration.

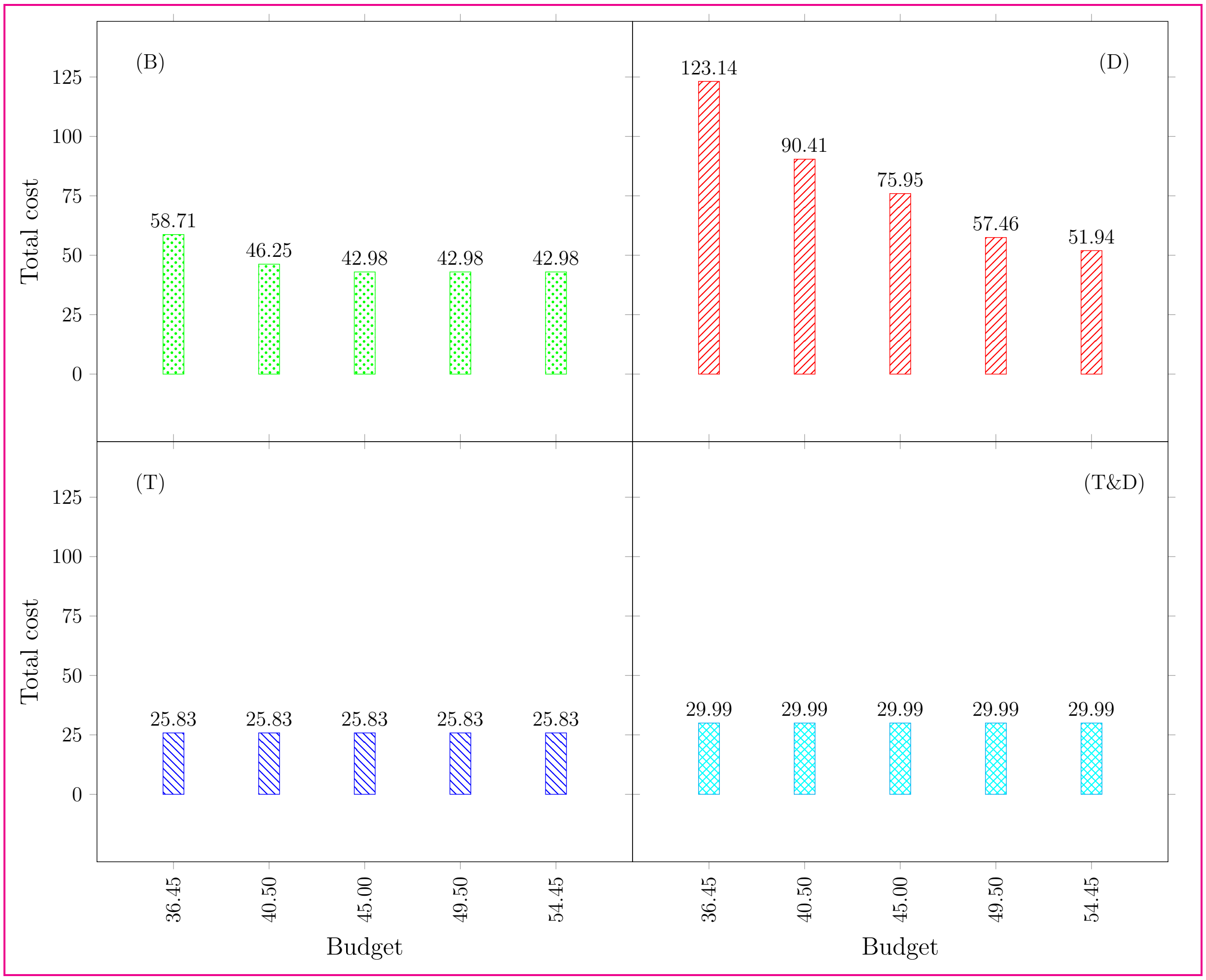

Figure 3.5: Impact of budget on total undiscounted cost for case 1 (B), case 2 (D), case 3 (T), and case 4 (T&D) (US $ millions)

First, we observe that as the budget increases in each period, the total cost in cases 1 and 2 decreases from $58.71M to $42.98M and $123.14M to $51.94M, respectively. Second, both cases 3 and 4 experience a constant total cost of $25.83M and $29.99M across the board, respectively. This result can be explained by the fact that incorporating technological change (case 3) in the model leads to increased capacity, less assets retained, and consequently less cost, while satisfying the demand with a smaller budget than the one required without technological change.

Furthermore, in cases 3 and 4, the model achieves an optimal minimum value for both penalties and costs by using budget levels of $25.83 and $29.99, respectively. In these cases, we notice that a further increase in the allocated budget does not reduce the total cost. On the other hand, deterioration (cases 2) results in decreased capacity, which requires more assets to be utilized, thus increasing the total cost. The behavior shown by Figure 3.5 reveals that technological change and deterioration are critical factors that impact optimal replacement cost.

3.5.6 Percentages of Cost Components

Figure 3.6 shows the percentages of each of the MRI and eMRI scanning machine cost components over the finite planning horizon. As shown the unit purchase cost and O&M cost account for a major percentage of the total cost and, consequently, are highly sensitive parameters defining replacement cost and impacting the optimal replacement policy results of the model. First, O&M cost accounts for more than 55% of the total cost for MRI units in case 1, while this is 40% in case 4. Similarly, in cases 3 and 2, the O&M cost accounts for more than 49% and 32% of the total cost for MRI units, respectively. For eMRI units, in cases 3 and 1, O&M cost accounts for approximately 7% and 8% of the total cost, respectively, while cases 4 and 2 make up 6% and 5% of the total cost, respectively. Cases 1 and 3 incur higher total O&M costs, compared to cases 2 and 4 because assets are retained longer, thus implying longer utilization and hence less-frequent replacement of assets under cases 1 and 3.

On the other hand, in the deterioration case without technological improvement (case 2) the highest penalty is incurred, compared to all other cases, implying that the optimal policy suggests paying a lower O&M cost by frequently replacing or salvaging deteriorating assets at the expense of lost demands.

Next, we notice that the unit purchase cost of MRI units accounts for 24% to 30% of the total cost, while the unit purchase cost of eMRI machines accounts for 3% to 6% of the total cost, in all four cases. This result is expected because more MRI scanning machines are acquired with higher purchasing cost compared to eMRI scanning machines. As mentioned earlier, the presence of technological change decreases the incurred penalty while deterioration increases it. In summary, these results show that the O&M cost is the most significant cost, followed by the unit purchase cost, and finally the fixed cost. Impact of the inventory holding cost is small compared to the other three types of cost. The penalty cost is only significant under deterioration.

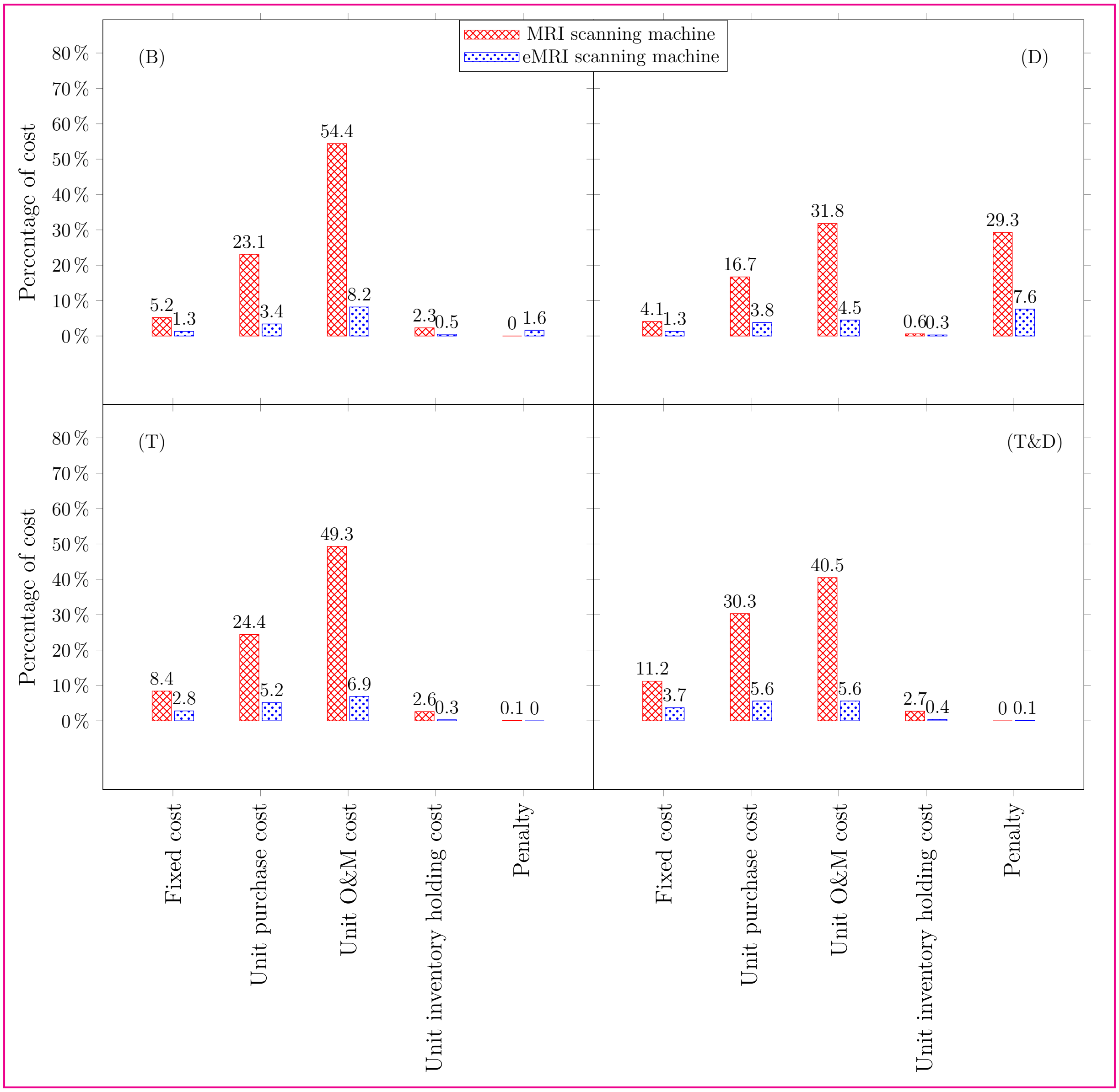

Figure 3.6: Cost analyses for case 1 (B), case 2 (D), case 3 (T), and case 4 (T&D) (US $ millions)

CHAPTER 4

MATHEMATICAL MODELING AND DATA ANALYSES OF EBOLA EPIDEMICS: A REVIEW

4.1 Introduction

Recently, several countries in West Africa have been hit hard by the EVD, which is considered one of the deadliest viruses ever known, with a case fatality rate (CFR) of up to 90% (Baize et al., 2014; Hoenen et al., 2006). The Ebola outbreak has quickly become a significant global public health challenge because of its persistent and exponential growth (WHO, 2014b). As of August 2015, spread of the virus has been the cause of more than twenty-seven thousand reported cumulative cases, and the death of more than eleven thousand individuals in the three at-risk countries—Guinea, Liberia, and Sierra Leone–including five hundred healthcare workers (Gostin, 2015; Klenk and Becker, 2015). The increasing number of cumulative cases and deaths ensures the establishment of several ETCs and additional healthcare workers in order to isolate and treat infected individuals, thereby properly managing the disease's spread (WHO, 2014b).

The cross-border outbreak began in Guinea, in December 2013, quickly spread to its neighboring country Sierra Leone by late May 2014, and then spread to Liberia in June 2014 (Althaus, 2014). In 2014, Ebola is reported to have also spread to other West African countries including Mali, Senegal, and Nigeria (Bogoch et al., 2015), the first-ever outbreak to occur in this part of West Africa (Fowler et al., 2014; Shuaib et al., 2014; Songwe, 2015).

Ten African countries have experienced 17 Ebola outbreaks intermittently over the last four decades (Bogoch et al., 2015; Evans and Kaslow, 1997; Oswald, 2007). Ebola was officially detected for the first time in the Sub-Saharan African country of the Democratic Republic of Congo (DRC), in a village near the Ebola river in August of 1976. Subsequent reports reveal that the outbreak simultaneously occurred in the villages of Yambuku in northern DRC and N'zara in southern Sudan (CDC, 2003; Feldmann and Geisbert, 2011; Okware et al., 2002).

The historical number of cases and deaths of the past Ebola outbreaks in Africa are presented in Figure 4.1.

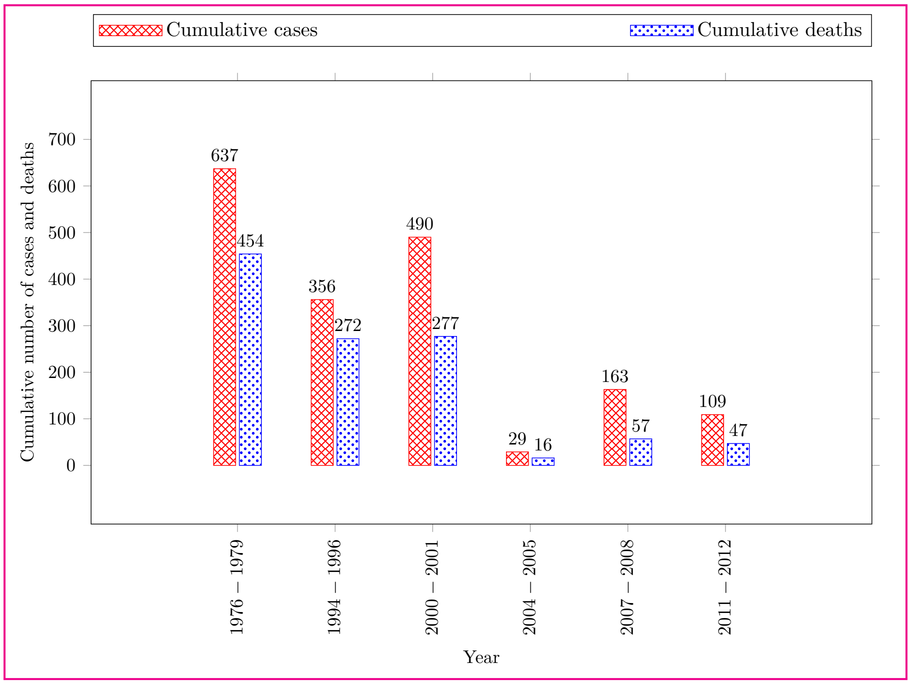

Figure 4.1: Cumulative number of cases and deaths in past Ebola outbreaks in Africa (Evans and Kaslow, 1997; Oswald, 2007) (as of August, 2015, the 2014 Ebola outbreak cumulative number of cases and deaths are $28,956$ and $11,298$, respectively (Goufo and Maritz, 2015; Klenk and Becker, 2015). We omit the 2014–2015 case and death numbers from the figure due to scalability issues)

According to Figure 4.1, in time period 1976–1979, more than 600 diagnosed cases are experienced while at least 71% of the infected individuals died. However, during the time period 1994–1996, the disease reemerged in Gabon, La Cote D'Ivoire, DRC, and South Africa, with a total of approximately 356 confirmed cases, nearly one-half during that time period 1976–1979. Moreover, during the time period 2000–2012, the disease reemerged intermittently and caused hundreds of cases and deaths. Then in December 2013, the highest Ebola outbreak occurred in West Africa, causing approximately $28,956$ cases and $11,298$ deaths by August 2015.

According to a report from the WHO and Yazdanpanah et al. (2015), new patients are infected with the EVD through direct contact with blood or body fluids (including but not limited to urine, saliva, sweat, feces, vomit, and breast milk) of an individual who is already infected with or has died from Ebola. Ten percent of the cases that occurred in the 2014 Ebola outbreak have been reported to be healthcare workers (WHO, 2014c) who have contacted the disease in treatment centers. Furthermore, it is estimated that approximately 60% of the total cases have been associated with traditional funerals of family members, where burial rituals involve touching the body of the deceased individual (Chan, 2014; Hewlett and Amola, 2003). A study by Hwang (2014) explains that 81% of healthcare workers and 23% of family members giving care to Ebola-infected individuals became infected with the virus in the 1976 Ebola outbreak in Sudan. Studies suggest that once the Ebola virus infects an individual, symptoms such as viral hemorrhagic fever and severe bleeding begin to show between two and twenty-one days (for the average person, this is between four and nine days), with death occurring within seven to sixteen days (see, e.g., Astacio et al., 1996; Hunt, 2014). Approximately 10% of the Ebola-infected individuals recover by the second week, on average, after their initial infection (Griggs, 2014). For a comprehensive review of past and current Ebola outbreaks in Africa and detailed information on the specifics of the EVD, we recommend the following list of references: Bogoch et al., 2015; CDC, 2003; Evans and Kaslow, 1997; Feldmann and Geisbert, 2011; Geisbert et al., 2003; Hewlett and Hewlett, 2007; Joffe and Haarhoff, 2002; Mishra et al., 2014; Muyembe-Tamfum et al., 2012; Oswald, 2007; WHO, 2014b; Wilson, 2014.

For about a century, mathematical models have been utilized as valuable tools for studying the transmission dynamics of infectious diseases, estimating key parameters from existing epidemiological data, and making significant public healthcare decisions (Waaler et al., 1962). For example, the 2014 Ebola epidemic in West Africa has motivated many researchers to develop several mathematical models and computer simulations such as curve fitting, compartmental, and statistical models (Anderson et al., 1992; Hethcote, 2000). Mathematical models also provide insight into the future prediction of the disease growth and spread, and thus the comparison of appropriate control interventions.

These epidemic disease models can also be used to estimate the cost and benefits of different control interventions. Therefore, appropriate Ebola epidemiological data as well as economic cost data are required to properly implement models, analyze the impact of various control alternatives, and perform sensitivity analysis on problem parameters (Chowell and Nishiura, 2014; Hethcote, 2000).

The objective of this study is to review and analyze mathematical models with the primary focus on understanding the dynamics of the EVD and the development of effective intervention strategies in order to stop this deadly disease. This review also presents epidemiological and economic data that could be used in future mathematical models for controlling the Ebola outbreak. We also provide a brief discussion of the control intervention policies that have been effective to contain spread of the EVD.

The remainder of this paper is organized as follows. In Section 4.2, we present methods for inclusion and exclusion of Ebola articles in our review and also describe a procedure for our literature search, selection, and review while we demonstrate the search process with the help of a PRISMA flowchart, as shown in Figure 4.2. In Section 4.3, we provide a concise background on infectious disease compartmental models and discuss key concepts in epidemiological models including the basic reproductive number. We then review various types of compartmental models describing the transmission dynamics of Ebola. In particular, we analyze the use of mathematical models to determine and evaluate control interventions such as hospitalization and safe burial in an effort to limit the impact of spread of Ebola in affected areas. We then present tables that categorize compartmental models on Ebola with respect to their analysis, problem formulation, objective of the study, and control intervention strategies. In Section 4.4, we present a key epidemiological data set as well as economic data collected from the literature on various Ebola outbreaks.

4.2 Methods for Article Inclusion and Exclusion

To aid our assessment of the selected literature, we apply the following summarized criteria for inclusion and exclusion in order to select studies related to Ebola compartmental models and the estimation of Ebola epidemiological parameters and data. We also describe the procedure for our literature search, selection, and review that focuses on the topic of interest. The PRISMA flowchart shown in Figure 4.2 explains the entire review process.

4.2.1 Sources of Data, Literature Searches, and Selections

To collect articles specific to our study, we perform an extensive literature search using the following databases: PubMed, PLOS ONE, and Google Scholar relative to mathematical modeling and data analyses of Ebola epidemics from the time the virus was discovered in 1976 until August 2015. The key terms used for the search include Guinea, Liberia, Sierra Leone, DRC, Uganda, Sudan, Ebola, infectious diseases, policy recommendation, fatality rate, control intervention, mathematical model, and combinations of some of these terms. We perform the reviews in two specific steps:

- To perform a general search for studies on Ebola.
- To ensure that any selected studies satisfy inclusion and exclusion criteria by narrowing the review to specific studies on Ebola related to the topic.

4.2.2 Specific Criteria for Included Articles

We present criteria used in the inclusion and exclusion of Ebola articles specific to our study.

Criteria for inclusion

- Ebola studies on compartmental models, problem formulation, and control intervention.
- Ebola studies on data analyses, including transition parameters, cost data, and economic implication of the 2014 EVD outbreak.

Criteria for exclusion

- No information regarding a compartmental model for the study of Ebola.
- No relevant data analysis and transition parameters concerning Ebola studies.

4.2.3 Results of the Review

Having established our key research terms, our initial literature search and reviews on studies related to Ebola generated $37,345$ papers from all of our sources of information. Since we are mostly interested in compartmental models and data analysis focused on Ebola studies, we perform further screening to eliminate duplicates and articles that do not meet our established review criteria. First, after duplicates have been removed from our first search, we eliminate a total of $22,994$ articles that have minimal or no information on Ebola epidemics. We perform further review and selection of articles on the remaining $1,806$ articles.

Second, based on our selection criteria for inclusion and exclusion with Ebola background information, we conduct an extensive literature review to finally gather 136 papers for a full literature review in addition to information from other sources such as the WHO and the Centers for Disease Control and Prevention (CDC). Next, we select 81 articles that focus on transmission dynamics of the EVD using specific compartmental models in their problem formulation as well as control intervention and data analysis. Then we identify 46 articles for final inclusion in our compartmental model selection criteria, as shown in Table 4.1.

For data analysis (35 articles), we explore the remaining searched articles in addition to the already-selected 46 papers as categorized and presented in section 4.4. To develop an in-depth understanding of the EVD, we include 81 articles that describe transmission dynamics and spread of Ebola. Out of our final selection articles on Ebola, 55 papers are used to provide background information including policy recommendation and transmission dynamics of the disease. We implement the PRISMA flow chart shown in Figure 4.2 to summarize the search-and-review process.

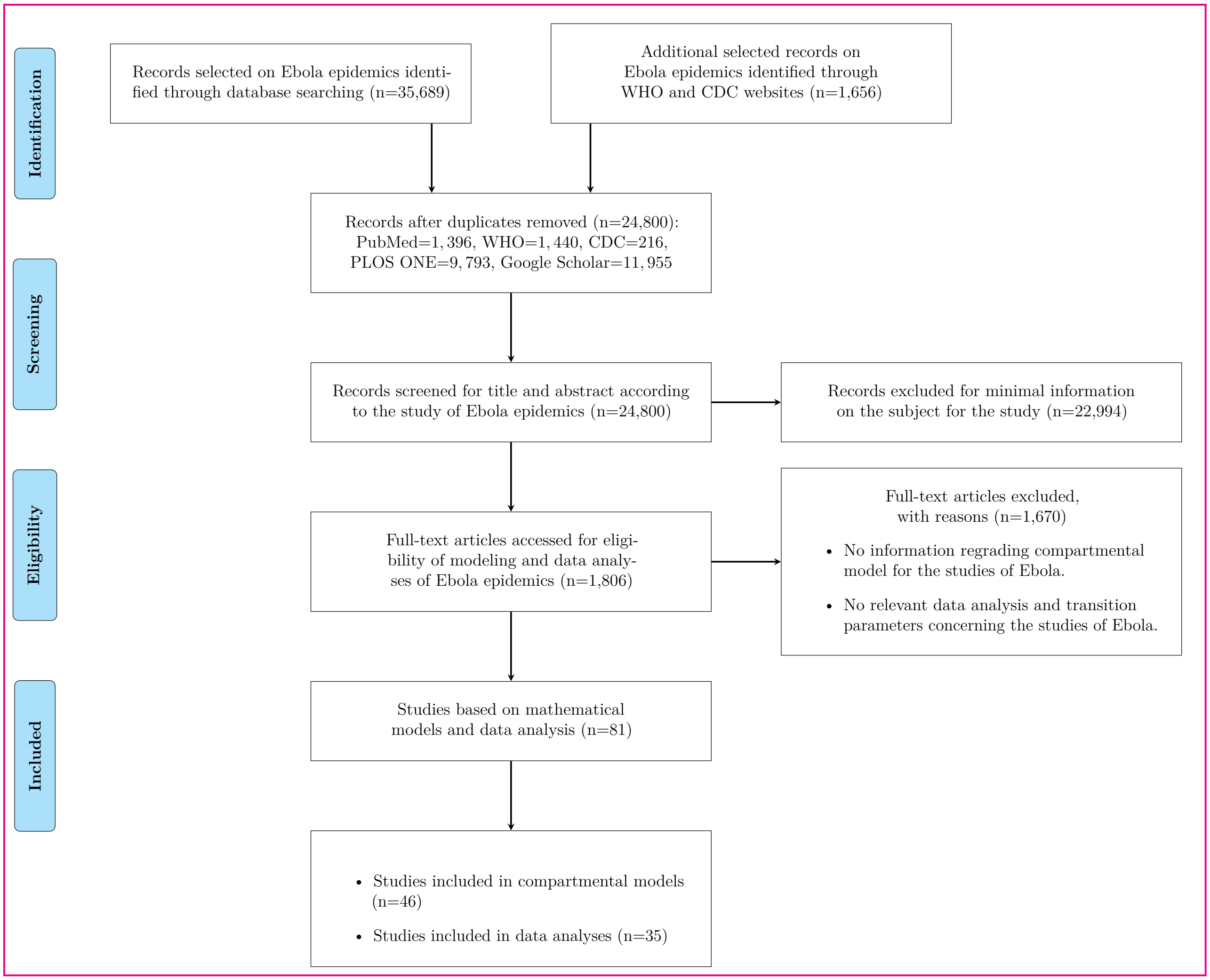

Figure 4.2: Ebola literature review using PRISMA flow chart

4.3 Ebola Compartmental Epidemic Models and Analyses

This section reviews some of the basic terminology and models previously used in the study of mathematical and statistical models of infectious diseases with a particular focus on compartmental classes for the Ebola virus disease. Our review emphasizes on Ebola epidemic models that provide key parameter estimates and incorporate control interventions such as hospitalization (treatment) and death (funeral).

The first mathematical model to study the transmission dynamics of infectious diseases was introduced in 1766 by Daniel Bernoulli, in order to make significant public healthcare decisions aimed at improving life expectancy for smallpox in England (Bernoulli, 1760). In

1906, William Hamer formulated a discrete-time mathematical model for the transmission of measles (Lancaster, 2012). Then in 1910, Ronald Ross developed a differential equation model for the spread of malaria (Ross, 1910). Following the work of Ross (1910), many mathematical models for epidemic diseases have been developed and implemented for specific diseases such as cholera, Ebola, gonorrhea, HIV, and SARS (see, e.g., Allen et al., 2008; Bailey et al., 1975; Hethcote, 2000).

Different types of mathematical models that have been employed in studying infectious diseases can be categorized as deterministic and stochastic models. In deterministic approaches, transition dynamics are based on known parameter values and initial conditions for the disease (Arreola et al., 1999; Chowell et al., 2004; Lekone and Finkenstädt, 2006; Ndanguza et al., 2013), while a stochastic model takes into account the random effects of disease transmission on a limited population (Arreola et al., 1999; Legrand et al., 2007; Meltzer et al., 2014; Rivers et al., 2014). Allen and Burgin (2000) review the difference between stochastic and deterministic disease models. Epidemic models can also be categorized as continuous-time or discrete-time. Many studies that consider continuous-time models are formulated on the basis of a set of differential equations (Arreola et al., 1999; Chowell et al., 2004), while discrete-time models are often formulated with a set of difference equations (Allen, 1994; Ndanguza et al., 2013). For example, numerous studies involving the Ebola epidemic outbreak have considered continuous-time models as either deterministic (Chowell et al., 2004), stochastic (Lekone and Finkenstädt, 2006; Webb et al., 2014), or both (Arreola et al., 1999; Rivers et al., 2014). Other mathematical modeling approaches include simulation-based models (Das and Savachkin, 2008; Germann et al., 2006), network models (Eubank, 2005; Keeling and Eames, 2005), and statistical-based approaches (Longini, 1986; Longini et al., 1989).

A central aspect of an epidemic model is the basic reproductive number ($\mathscr{R}_0$), which determines the severity of an outbreak. The $\mathscr{R}_0$ value can be defined as the expected number of secondary cases generated by an infectious individual in a completely susceptible population over the period of infection in the absence of intervention (Chowell et al., 2004). Mathematically, $\mathscr{R}_0$ can be expressed as the product of the risk of transmission, effective disease transmission rate, and average infectious period (Funk et al., 2009; Heffernan et al., 2005). Extensive epidemic modeling studies have been performed to compute $\mathscr{R}_0$ for many infectious diseases including Ebola (Althaus, 2014; Anderson et al., 1992; Chowell et al., 2004; Diekmann et al., 1991).

The $\mathscr{R}_0$ value is an important number used for public health decision-making because it indicates if an infectious disease can spread through a set human population. If $\mathscr{R}_0 \geq 1$, then the epidemic continues to grow, while $\mathscr{R}_0 < 1$ would indicate possible control of the epidemic (see, e.g., Fraser et al., 2004; Smith, 2010). For a review of methods to estimate basic and effective reproductive numbers from data for infectious diseases including Ebola, see, e.g., Bailey et al., 1975; Chowell et al., 2004; Diekmann et al., 2012; Rothman, 2012.

In most epidemiological models such as those for Ebola, the set population is typically divided into distinct compartments connected to each other by transition rates based on the status of the disease (Jacquez, 1972). Compartmental models have been used to simulate infectious diseases including the 1865 cholera outbreak in London (Alexanderian et al., 2011). A special case of compartmental epidemic models is the susceptible-infected-removed model, which was developed back in the 1920s (Kermack and McKendrick, 1932). In SIR models, it is assumed that once infected, a susceptible individual becomes infectious and immediately moves to the infectious compartment, where an individual may either recover with lifelong immunity, die, or be removed from the population set (Hethcote, 2000). Several studies involving Ebola and other infectious diseases have implemented the SIR model to explain spread of diseases and explore control interventions, such as with measles (Bjørnstad et al., 2002), swine influenza (H1N1) (Coburn et al., 2008), and malaria (Cox and Abeku, 2007). For a comprehensive discussion and review of the specific compartmental models for infectious diseases, we refer the reader to several studies (see, e.g., Anderson, 2013; Capasso and Serio, 1978;

Gani, 2010; Grenfell and Harwood, 1997; Iannelli and Pugliese, 2014; Isham and Medley, 1996; Riley et al., 2003; Ross, 1910). '

Using a stochastic simulation approach, Arreola et al. (1999) analyze the Ebola epidemic with a modified version of an SIR epidemic model formulation in which they include two infection stages and a quarantine compartment as a control intervention. Their simulation analysis examines several variations of quarantine rate. The authors conclude that a higher quarantine rate significantly reduces the number of infected individuals in compartment I_2, while exposed individuals in compartment I_1 spread the disease when they move to the infectious stage.

Moreover, to understand spread of Ebola in the 1995 DRC epidemic, Zaman et al. (2009) introduce a time-delayed SIR model and apply control-treatment strategies by varying control parameters, with the objective of maximizing the number of susceptible and recovered individuals. Their numerical results show that control (treatment) significantly reduces the total number of infected individuals to a low level after 30 days.

Furthermore, Rizkalla et al. (2007) present an SIR model to study the simultaneous effect of hunting and transition dynamics of the Ebola virus in western lowland gorillas and its subsequent effect on humans in the 2003 DRC Ebola epidemic that resulted in 114 deaths. Their findings propose the following control interventions: (*i*) develop an effective vaccine, and (*ii*) impose natural barriers (rivers) to potentially control the growing outbreak of the disease.

The majority of existing studies on Ebola epidemic models are based on modifying the basic SIR model to take into account the specifics of the transmission dynamics of the 2014 Ebola outbreak in West Africa (Althaus, 2014; Chowell et al., 2004; Lekone and Finkenstädt, 2006; Towers et al., 2014). Variants of the SIR compartmental model include the susceptible-exposed-infected-recovered (SEIR) model, where an infected individual remains latent in the exposed (E) compartment. However, exposed individuals who are incapable of spreading the disease may later progress to an active infected (I) class (Li and Muldowney, 1995).

The biological aspect of the SEIR epidemic model provides transmission dynamics of the virus in four disjoint compartmental stages in a set population (Jacquez, 1972), as illustrated in the timeline of the Ebola epidemic shown in Figure 4.3.

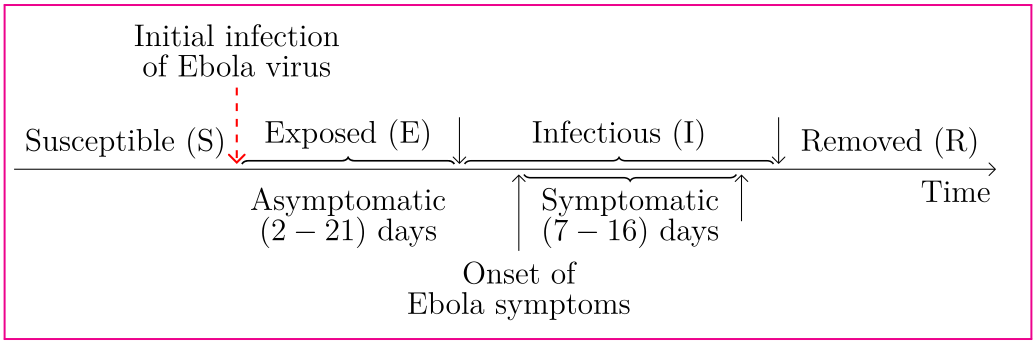

Figure 4.3: Timeline representation of transmission dynamics of Ebola through SEIR model

In his study, Chowell et al. (2004) formulate the deterministic SEIR mathematical model of Ebola as a continuous-time Markov chain. The authors estimate the $\mathscr{R}_0$ value and secondary cases of the EVD from the outbreak case data during the 1995 DRC and 2000 Uganda epidemics to be 1.83 and 1.34, respectively. Further, they perform an uncertainty analysis to show that early control measures in place minimize the final size of the epidemic by an approximate factor of 2 using a time-varying transmission rate. In another study, Althaus (2014) estimates the reproductive number of the transmission dynamics of the epidemic during the 2014 EVD outbreaks in West Africa using a similar model formulation as in the work of Chowell et al. (2004).

In a similar manner, Lekone and Finkenstädt (2006) consider a stochastic discrete-time SEIR dynamic model to study the transmission of EVD and to estimate epidemiology data parameters while considering a case study of the 1995 Ebola epidemic in the DRC. Their numerical results estimate a lower $\mathscr{R}_0$ value of 1.36 for DRC similar to the study of Chowell et al. (2004). Their studies show that the outbreak will last five times longer, with two-thirds of the population becoming infected if no intervention is put in place. More recently, the studies of Ndanguza et al. (2013) employed two sets of data from the same 1995 DRC Ebola epidemic.

Meltzer et al. (2014) investigate the 2014 Ebola outbreak by constructing an SEIR model to predict future cases for Liberia and Sierra Leone, where Ebola patients are categorized into three types of isolation including hospitalization, home or community setting, and home without effective isolation, according to the condition of their disease. Their analysis shows that if 70% of the infected individuals are placed in ETC facilities, then the epidemic eventually ends.

Similarly, Towers et al. (2014) utilize the SEIR model formulation to study temporal variations in basic reproductive number in the presence of intervention during the 2014 West Africa Ebola outbreak. Based on the assumptions of incubation and infectious periods of seven days, their analyses show an exponential growth in the cumulative cases, and they estimate $\mathscr{R}_0$ values in the ranges of 1.6–2.3, 1.5–2.1, and 1.2–1.3 in Guinea, Liberia, and Sierra Leone, respectively, between July 1 and September 8 in 2014. For further studies on other SEIR epidemic modeling of the Ebola outbreaks, we refer the reader to a number of references (see, e.g., Chowell et al., 2014; Haas, 2014; Hotta, 2010; Kiskowski, 2014; Ndanguza et al., 2013).

Other epidemic models on Ebola extend the basic SIR or SEIR model by including various compartments to specify control interventions. For example, hospitalized (H) or treated (T) are considered to identify individuals who are being provided with supportive medical care (Rivers et al., 2014). In addition, traditional funeral (F) or dead but unburied (D) compartments are included to analyze the impact of Ebola-related dead individuals and burial transmission rates during funeral ceremonies (Rivers et al., 2014).

Similarly, other models incorporate the burial (B) compartment (Camacho et al., 2014; Hu et al., 2015) to observe the cumulative number of safe burials and the quarantine (Q) compartment to define infected individuals who are isolated from the community as a control measure (Arreola et al., 1999). For example, Legrand et al. (2007) extend the infection compartment in the SEIR epidemic model of Chowell et al. (2004) to include hospitalized (H) and traditional funeral (F) to obtain an SEIHFR model. The authors explain the impact of control intervention using simulation where they group patients into three levels corresponding to the type of transmission: (*i*) in communities, (*ii*) at traditional burial funerals, and (*iii*) in hospitals. Recently, Camacho et al. (2014) reconsider the model in the work of Legrand et al. (2007) to study the 1976 DRC Ebola epidemic with an $\mathscr{R}_0$ estimate of 1.34. An exact compartmental model is then studied in Gomes et al. (2014) to make a three-month forecast of the geographic spread of Ebola in West Africa and the danger of international spread of the ongoing epidemic.

In addition to the already-mentioned control intervention, which involves hospitalization, numerous researchers have applied other control interventions for the containment of Ebola, thereby decreasing the total number of cases and strengthening coordination of the disease response. Studies of Chowell et al. (2004) suggest further control measures including a three-week quarantine period and education of healthcare personnel on patient management. The study of Haas (2014) indicates that increasing the quarantine period beyond 21 days for initially exposed individuals will reduce the risk of infection in the community by 0.2%–12%. Other studies have also estimated that the basic reproductive number will significantly decline to less than one if hospitalization of an infectious individual occurs within 60 hours and safe burial takes place within 34 hours of death (Hu et al., 2015).

To improve the understanding of the SIR model and its extensions that are studied to analyze the dynamics of Ebola spread and its control, we compile all compartmental models reported in 40 of the 129 publications on studies from the Ebola epidemic with various problem formulations, objective functions, and different types of control intervention strategies, as presented in Table 4.1.

4.4 Epidemiological and Economic Data Analysis

In this section, we provide Ebola epidemiological and treatment cost data, which could be utilized as input to the mathematical models for EVD. Epidemiologists have utilized specific models to assess key parameters from data sets, explain important trends and uncertainties in epidemiological data, and perform sensitivity analysis to parameter changes

Table 4.1: Selected Ebola Compartmental Epidemic Models, Analysis, and Problem Formulations

Epidemic model	Analysis	Problem formulation	Objective of the study	Control intervention	Reference
SIR	Simulation	Discrete	• Compute $\mathscr{R}_0$ for each country • Study transmission dynamics of EVD	Hospitalization	Evans and Mammadov (2014)
	Sensitivity	IDEA	• Evaluate growth patterns in 2014 EVD • Assess extent of outbreak control	Behavioral change	Fisman et al. (2014)
	Simulation	Differential	• Predict propagation of 2014 EVD • Study allocation of medical resources	Medical measures	Liu et al. (2015)
	Optimal control	Differential	• Explain effects of vaccines on 2014 EVD • Understand community mixing in Liberia	Mass vaccination	Rachah and Torres (2015)
	Simulation	Differential	• Study impacts of Ebola and hunting on gorillas	Control hunting	Rizkalla et al. (2007)
	Simulation	Differential	• Predict spread of 2014 Ebola using social media • Determine initial transmission parameters	Early diagnosis	Smailhodzic (2015)
	Simulation	Differential	• Analyze EVD model within a set population	Quarantine	Yarus (2012)
	Optimal control	Differential	• Minimize probability of infection spread • Maximize susceptible and recovered people	Treatment	Zaman et al. (2009)
$SIRD$	Simulation	Differential	• Study impact of EVD and migration on population resources	Education	Goufo and Maritz (2015)
$SI(Q)RD$	Simulation	Differential	• Determine effect of parameters on transmission dynamics of Ebola • Determine effect of quarantine on transmission dynamics of Ebola • Perform stability analysis of models	Quarantine	Amenaghawon et al. (2015)
SI_1I_2RQ	Simulation	Differential	• Reduce size of epidemic • Determine number of fatalities	Quarantine	Arreola et al. (1999)
$SEIR$	Curve fitting	Differential	• Understand spread of infection of the 2014 EVD • Estimate $\mathscr{R}_0$ and $\mathscr{R}_t$ for 2014 EVD	Social distancing	Althaus (2014)
		Differential	• Assess effectiveness of control intervention in China	Surveillance	Chen et al. (2014)
	Network	Differential	• Study spread of Ebola beyond Africa • Determine $\mathscr{R}_0$ for 2014 EVD	Education	Bashar et al. (2015)
	Fractional	Differential	• Study comparison between model and actual outbreak data • Estimate total number of cases for 700 days	Health measures	Area et al. (2015)
	Pontryagin	Differential	• Minimize weighted sum of latent and infected people • Study effect of control interventions on EVD	Education	Grigorieva and Khailov (2015b)
	Trade-off	Differential	• Re-evaluate 21-day quarantine period • Examine trade-offs between costs of quarantine and risk	Quarantine	Haas (2014)

D: death (funeral) class, IDEA: Incidence Decay with Exponential Adjustment, I_1: first stage of infectious class, I_2: second stage of infectious class, Q: quarantined class, $\mathscr{R}_t$: effective reproductive number.

Table 4.1 (continued)

Epidemic model	Analysis	Problem formulation	Objective of the study	Control intervention	Reference
$SEIR$	Markov chain	Differential	• Estimate cases in 1995 DRC and 2000 Uganda • Compute $\mathscr{R}_0$ for EVD outbreaks	Education	Chowell et al. (2004)
	Simulation	Network	• Determine impact of community mixing in Guinea & Liberia • Study effect of transmission dynamics in 2014 Ebola	Hand washing	Kiskowski (2014)
	Bayesian	Differential	• Estimate parameters in 1995 DRC and 2000 Uganda • Study effects of control intervention	Surveillance	Lekone and Finkenstädt (2006)
	Simulation	Differential	• Forecast number of infected and death cases • Estimate $\mathscr{R}_0$ for all three nations	Medical care	Mamo and Koya (2015)
	Simulation	Spreadsheet	• Predict cases for Liberia and SL • Study factors in disease growth	Medical intervention	Meltzer et al. (2014)
	Differential	Bayesian	• Determine exposed and infectious periods • Estimate $\mathscr{R}_0$ in SL	Treatment	Stadler et al. (2014)
	Curve fitting	Binomial	• Find rate of exponential rise in 2014 EVD • Determine effect of intervention on spread of outbreak	Quarantine	Towers et al. (2014)
SEI_+I_-R	Sensitivity	Differential	• Assess benefit and risk of CCC in SL	Monitoring	Kucharski et al. (2015)
$SEIT$	Sensitivity	Differential	• Evaluate various intervention strategies in Guinea • Determine model parameters by LSM	Vaccination	Li et al. (2015)
$SEIRD$	Sensitivity	Differential	• Evaluate control measures during 2014 EVD	Contact tracing	Freeman (2014)
	Simulation	Differential	• Analyze impact of early intervention in Nigeria • Assess $\mathscr{R}_0$ and $\mathscr{R}_t$ during outbreak	Contact tracing	Althaus et al. (2015)
	Simulation	Differential	• Use post-death transmission to predict Ebola spread • Predict exponential increase in cases	Safe burial	Weitz and Dushoff (2015)
$SEII_SRD$	Simulation	Differential	• Analyze sensitive parameter $\mathscr{R}_0$ • Explain two control parameters in the model	Isolation	Tri Juliansyah et al. (2015)
$SEICI_IR$	Simulation	Differential	• Assess several policies for control of Ebola	Isolation	Webb et al. (2014)
$SEID_bD_lR$	Simulation	Network	• Approximate EVD dynamics on a small world network • Examine effects of burial practices to disease transmission	Early diagnosis	Siettos et al. (2015)

C: contaminated deceased class, CCC: Ebola community care center, D: death (funeral) class, D_b: safely buried class, D_l: unburied class, F: Funeral class I_-: EVD-like symptoms class, I_+: infectious in the community class, I_I: isolated exposed and infectious class, LSM: least squares method, SL: Sierra Leone.

Table 4.1 (continued)

Epidemic model	Analysis	Problem formulation	Objective of the study	Control intervention	Reference
$SEIHP$	Simulation	Differential	• Study case fatality rate and transmission tree in Nigeria • Assess impact of control interventions on final epidemic size	Infection control	Fasina et al. (2014)
$SEIHFR$	Pontryagin	Differential	• Study effective control measures • Assess dynamics of EVD related population	Education	Grigorieva and Khailov (2015a)
	Simulation	Differential	• Assess impact of intervention in 1995 DRC and 2000 Uganda • Estimate disease transmissions in three settings	Contact tracing	Legrand et al. (2007)
	Simulation	Differential	• Predict spread of Ebola in Liberia and SL • Evaluate impact of control intervention on EVD	Medical care	Rivers et al. (2014)
	Simulation	Network	• Estimate key parameters in Ebola transmission • Forecast spread of EVD in West Africa and international	Travel restriction	Gomes et al. (2014)
SEI_1I_2HFR	Simulation	Differential	• Examine dynamics of ETC and intervention in 2014 EVD • Investigate three stages of disease progression	Treatment	Eisenberg et al. (2015)
SEI^AI^MHUR	Simulation	Differential	• Predict cases of EVD averted across 12 districts of SL • Policy for possible future outbreaks of EVD	Treatment beds	Kucharski et al. (2015)
S_LS_HEIHR	Simulation	Differential	• Estimate $\mathscr{R}_0$ for Ebola in Liberia and SL • Determine transmission parameters from previous studies	Social distancing	Khan et al. (2015)
$SEIHRDB$	Scenario	Differential	• Estimate previous outbreak parameters • Compare 1976 and 2014 EVD outbreaks	Isolation	Camacho et al. (2014)
	Simulation	Differential	• Predict probable evolution of Ebola for 30 days • Explain Be-CoDiS spatial temporal model	Surveillance	Ivorra et al. (2014)
	Simulation	Differential	• Evaluate intervention efforts • Reduce virus transmission	Hospitalization	Barbarossa et al. (2015)
	Sensitivity	Differential	• Determine effects of human behavior in 2014 EVD • Examine social interaction within countries	Behavioral change	Hu et al. (2015)
$SEIJFDR$	Simulation	Difference	• Develop measures to control 2014 EVD • Predict future cases in Ebola outbreak	Hygiene burial	Pandey et al. (2014)

D: death (funeral) class, I^A: ascertained infectious class, I^M: non-ascertained infectious class, S_L: low risk susceptible class, S_H: high risk susceptible class, P: death (funeral) class, Pontryagin: Pontryagin maximum principle, J: hospital infection class, SL: Sierra Leone, H: community care center, U: Ebola treatment units, Be-CoDiS: Between-Countries Disease Spread

(Hethcote, 2000). Instead of discussing how the related data is derived in these studies, we confine our discussion to provide parameter definitions, reported values and ranges, and the corresponding reference, in particular, for Guinea, Liberia, and Sierra Leone from various literature and data sources.

4.4.1 Economic Cost and Implications of Ebola to West African Countries

The immediate spread of the 2014 Ebola epidemic has had a significant effect on the economic and social sectors of the three countries that are highly affected. The economic cost of the 2014 Ebola includes two key cost components: direct and indirect (Bartsch et al., 2015). The direct cost involves resources such as medical costs used in the control intervention of the disease, while indirect cost covers lost productivity and income for patients (Farnham, 1994). The direct costs (e.g., the cost of establishing treatment centers and allocating resources for control intervention) could be useful to formulate an epidemic model, which provides trade-offs between the economic cost of intervention efforts and their impacts on reducing the disease progression.

The economic burden of the 2014 Ebola outbreak is notably substantial in Guinea, Liberia, and Sierra Leone. In its 2015 economic growth report, the World Bank Group (WBG) estimates that the 2014 economic growth across the three highly affected nations of Guinea, Liberia, and Sierra Leone is -2%, -2%, and 3% compared to 4.3%, 8.9%, and 6.8%, respectively, in the previous growth report of the WBG before the Ebola crisis (WBG, 2014). This implies that from 2014 to 2015, Guinea, Liberia, and Sierra Leone are expected to lose income of more than \$800 million, \$250 million, and approximately \$1.3 billion, respectively (WBG, 2014). These drastic losses in income are not only due to the disastrous EVD epidemic in West Africa which has taken many lives, but also lost productivity from work and community services. To have a better understanding of the economic impact that Ebola has caused in West African nations including Guinea, Liberia, and Sierra Loene, the following list of references are provided for further reading: Brown and Cropley, 2014; Frieden et al., 2014; Hodge Jr et al., 2014; Ippolito et al., 2015; Nyampong, 2015; Ryan, 2014.

Furthermore, the economic consequences of the Ebola outbreak are experienced by many sectors, including agriculture, mining in rural areas, and business in urban communities, which provide jobs for citizens, thus crippling the already-weak economy and healthcare (Fan and Glassman, 2014; Wilkinson and Leach, 2014). For instance, Wilkinson and Leach (2014) state that Sierra Leone lost several millions of dollars when a London-based mining company stopped working and canceled all operations in July of 2014 when the Ebola outbreak was officially announced in the country.

Moreover, the significant impact of the 2014 Ebola outbreak reveals the broken and poor healthcare system in the most affected nations (low-income countries). For example, Liberia had 0.1 physicians, 2.7 nurses, and 8 hospital beds per $10,000$ people, and Sierra Leone had 0.2 physicians and 1.7 nurses per $10,000$ people before the Ebola outbreak occurred (UN, 2014). This situation makes it difficult, especially for hospitalized individuals with Ebola, to get the proper medical care needed. Hence, the Ebola outbreak is due to delaying necessary treatment for Ebola-infected individuals (Fauci, 2014). This result implies that as the Ebola epidemic continues to spread exponentially, its long-term economic impact could be disastrous. Also, the 2014 Ebola epidemic has demonstrated how fast infectious diseases including Ebola can spread in absence of appropriate healthcare infrastructure.

The CDC documents that a significant portion of the Ebola treatment cost is attributed to the cost of establishing and operating ETC facilities and bringing healthcare professionals to provide care for patients. Therefore, the cost of Ebola diagnosis as well as treatment costs incurred by sick patients could amount to a major problem for developing countries, especially in rural areas. Estimates of the total cost of Ebola treatment for one patient ranges from as low as $\$37,500$ to as high as $\$145,000$ in the West African nations, which are currently receiving humanitarian aid and other support (WHO, 2014c). Other studies have estimated that the average cost of Ebola treatment for a single patient who recovers from the disease is between \$480 and \$912, while patients who end up dying from the disease incur costs between $\$5,929$ and $\$18,929$ (Bartsch et al., 2015). The economic impact of Ebola-related deaths is approximately twenty times that of infected individuals who recover (Bartsch et al., 2015) because of the additional cost of disinfection and safe burial for the deceased. However, the very high cost of healthcare in West Africa forces Ebola-infected individuals in villages to seek a more affordable treatment through traditional healing methods, which could further increase infections among the community (Breman and Johnson, 2014). Therefore, in the event of an outbreak of this magnitude, financial support is the best assistance to effectively ensure eradication of the disease (Leslie, 2000).

We next provide estimates for the cost of EVD treatment based on existing information from the work of the WHO (WHO, 2014b) and summarize each category in detail in Table 4.2.

Table 4.2: Summary of Estimated 2014 Ebola Treatment Cost Per Month (WHO, 2014b)

	Treatment cost component		
Description of treatment cost	Fixed cost[1]	Variable cost[2]	Burial cost[3]
Establishment of 50-bed Ebola treatment center	$386,000	$881,000[a]	
Establishment of isolation unit center (IUC)	$112,500	$181,250[b]	
Mobile laboratory diagnosis of infected individuals	$100,000	$129,600[c]	
Establishment of social mobilization		$79,800[d]	
Establishment of subnational Level technical and logistical coordination		$450,000[e]	
Contact tracing and surveillance		$225,450[f]	
Safe burial			$225,450[g]
Total	**$598,500**	**$1,947,100**	**$225,450**

[1] fixed cost for setting up a 50-bed ETC, IUC, and laboratory diagnosis [2] variable cost of various treatment operations, [3] cost of safe burial performed by trained burial teams, [a] cost of operating a 50-bed ETC per month, [b] cost of isolating 80 suspected cases per month, [c] cost of lab diagnosis for 600 samples per month. Each infected case requires 5 laboratory samples, [d] cost of 54 trained teams needed to coordinate mobilization in the affected community per month, [e] cost of 10 offices needed to coordinate activities such as infection control and case management per month, [f] cost of tracing 1,000 contacts of infected people by a team of 100 people per month, [g] cost of 100 safe burials performed per month.

Fixed cost of ETC facilities

We define fixed cost as a one-time set-up cost for establishing facilities such as ETC facilities, isolation unit centers for separating individuals suspected of having the disease, and laboratory diagnosis procedures for testing possibly infected individuals in isolation.

Variable cost of treatment and operating ETC facilities

We describe the variable cost of treatment as the operational cost for care provided to Ebola patients and the cost for other indirect services, such as daily operational activities of ETC facilities and isolation unit centers. Another relevant cost is the estimation of the subnational level technical portion of the operational cost that specifically deals with management of infection control, EVD investigation, and coordination of control intervention strategies.

Safe burial cost of deceased Ebola patients

Safe burial cost is the cost associated with prompt and safe burial of individuals who have died from Ebola. This is carried out by professional teams in order to stop close relatives from becoming infected through traditional burial.

4.4.2 Biological Data Analysis for Compartmental Epidemic Models

Throughout history, epidemic diseases have been known to follow a peculiar trend, spreading through a set population in a group of people. Spread of disease is determined by certain characteristics of the infectious agent including the length of infection, transmission rates, and severity (Anderson and May, 1979). In this subsection, we present transition parameters describing the transmission dynamics of the 2014 EVD in Guinea, Liberia, and Sierra Leone as well as past Ebola outbreaks from DRC and Sudan. We gather related data from literature and various sources and provide it in a compact form, which could be very useful for Ebola modelers and healthcare providers.

Non-hospitalized case fatality rate

Case fatality rate (CFR) is one of the important epidemiological characteristics of the Ebola virus disease. We note that the timing and conditions for the measurements for CFR has a significant impact on determining rates, and thus various ranges of values are defined in the literature for different countries and different time frames. The fatality rate of Ebola patients who are not hospitalized is the percentage of Ebola-related deaths among EVD cases who do not receive medical care from an ETC facility. This data has fluctuated among outbreaks, including those in the DRC and Sudan, with CFRs of around 88% and 66%, respectively (Arreola et al., 1999; CDC, 2003; Chowell et al., 2004; Okware et al., 2002). Similarly, the WHO reported that the CFR for past Ebola outbreaks is observed to be approximately between 25% and 90% (WHO, 2003). The recent 2014 Ebola outbreak in West Africa has an estimated CFR in the range of 50% to 90%, with specific CFRs for Guinea, Liberia, and Sierra Leone of 74%, 71%, and 48%, respectively (Althaus, 2014; Fowler et al., 2014).

Hospitalized case fatality rate

Similarly, the CFR for hospitalized Ebola patients describes the percentage of Ebola-related deaths among EVD cases who receive medical care from an ETC facility. According to the 2014 WHO Ebola response road-map report, the CFR for hospitalized individuals varies from 60% to 61% in Guinea, Liberia, and Sierra Leone. We note that the timing and conditions for the measurements for CFR has a significant impact on determining rates, and thus various ranges of values are defined in the literature for different countries and different time frames.

Latent or incubation period

Past studies of the EVD epidemics report the incubation period to be in the range of 6 to 10 days (Breman et al., 1978; Lekone and Finkenstädt, 2006) while the 2001 Ebola epidemic in Uganda is estimated in the studies by Okware et al. (2002) to range from 6.3 to 12 days. On the other hand, Rivers et al. (2014) estimate the mean incubation period during the 2014 Ebola outbreak in Liberia and Sierra Leone as 12 days and 10 days, respectively. Several estimates have also been reported in the following studies: Camacho et al., 2014; Chowell and Nishiura, 2014; Eichner et al., 2011; Ivorra et al., 2014.

Time from onset of Ebola symptoms to hospitalization

According to Camacho et al. (2014), the mean duration until Ebola patients are hospitalized after onset of the first-stage symptoms is estimated to range from 2.81 to

3.20 days. Moreover, studies from Rivers et al. (2014) indicate that Liberia and Sierra Leone have fitted corresponding values of 3.24 days and 4.12 days, respectively. The majority of Ebola publications, such as those of Gomes et al. (2014) and Pandey et al. (2014), also report a mean time of 5 days until hospitalization. Other study reports indicate that Guinea, Liberia, and Sierra Leone have related parameter values in the range of 5.3 ± 4.3 days, 4.9 ± 5.1 days, and 4.6 ± 5.1 days, respectively (Team, 2014).

Time from onset of Ebola symptoms to funeral

In their study, Camacho et al. (2014) estimates that the expected time from the onset of symptoms for individuals suspected of Ebola until death is between 7.30 and 7.69 days. On the other hand, Team (2014) assumes that it takes approximately 6.4 to 17 days from the beginning of the onset of symptoms for individuals infected with Ebola in Guinea, Liberia, and Sierra Leone to die.

Time from onset of Ebola symptoms to recovery

Here, the report applies to Ebola-related individuals who become hospitalized at the ETC facility. Several studies have shown that the 2014 Ebola outbreak has an expected recovery time (mean infection length) in the range of approximately 15 to 20 days, using fitted values for Liberia and Sierra Leone (Rivers et al., 2014). Time to recovery is also reported to vary from 9 to 10.19 days, as provided in other research papers (Camacho et al., 2014; Pandey et al., 2014). Many studies on Ebola estimate the daily rate of recovery in the community and hospital in the range of 0.05 and 0.18 (Althaus, 2014; Gomes et al., 2014; Legrand et al., 2007; Towers et al., 2014).

Time from hospitalization to funeral

Based on recent studies of Rivers et al. (2014), it is assumed that it takes approximately 10.38 days and 13.31 days for Ebola-infected individuals in Liberia and Sierra Leone, respectively, to die while hospitalized. Meanwhile, in Guinea, Team (2014) suggests that it takes approximately 2.5 ± 3.4 days for hospitalized individuals to die. The duration from hospitalization to funeral in Liberia has also been reported as 4.6 days

(Gomes et al., 2014). Studies also report that up to 72% hospitalized individuals die from complications of the disease between a day and eleven days (Team, 2014).

Time from hospitalization to recovery

The expected amount of time it takes an Ebola-infected individual to recover while receiving treatment is estimated to be 15.88 days in both Liberia and Sierra Leone (Rivers et al., 2014). However, other studies estimate this to be 11 ± 5.4 days for Guinea, 12.8 ± 8.1 days for Liberia, and 12.4 ± 5.8 days for Sierra Leone (Team, 2014). According to the WHO, infectious individuals in the hospital have a lower probability of 25% of infecting other individuals compared to community and funeral transmissions. Further, studies of Ivorra et al. (2014) show that the mean length stay in the hospital to be 4.5 days.

Time from funeral to safe burial

Rivers et al. (2014) indicate that the mean time from traditional funerals to safe burials by trained teams in Guinea, Liberia, and Sierra Leone varies between 2.01 days and 4.05 days. According to Eisenberg et al. (2015), the time from death until burial is estimated to be 1 to 3 days. Meanwhile, previous studies on past Ebola outbreaks in DRC and Sudan suggest that the time to safe burial is approximately 2 days (Gomes et al., 2014; Legrand et al., 2007; Pandey et al., 2014).

Transmission rate in the community

This is defined as the rate at which individuals become infected with the virus during socializing in the community. According to a study by Althaus (2014), transmission rates via person-to-person contact during community interaction are reported to be 0.27 in Guinea, 0.28 in Liberia, and 0.45 in Sierra Leone. Moreover, several estimates on transmission rates have been published in various studies on Ebola with reported values between 0.01 and 0.45 (Camacho et al., 2014; Hu et al., 2015; Pandey et al., 2014; Rivers et al., 2014). Other studies such as those of Chowell et al. (2004) estimate this rate during the 1995 DRC and 2000 Uganda Ebola outbreaks to be 0.33 and 0.38, respectively.

Transmission rate at traditional funerals

We define transmission rate at funerals as the rate at which susceptible individuals become infected with the virus during tradition funeral and burial practices. Transmission rates via person-to-person contact during traditional funerals is estimated to change within the interval 0.08–2.00 because cultural practices pertaining to burial might vary among African countries (Camacho et al., 2014). Others report the general transmission rate at traditional funerals during the 2014 Ebola outbreak as 0.65 (Hu et al., 2015), while some studies use 0.49 for Liberia and 0.11 for Sierra Leone (Rivers et al., 2014).

Hospital transmission rate

Recent studies from the 2014 Ebola outbreak have computed transmission rates from patients to healthcare workers as 0.27 (Hu et al., 2015; Pandey et al., 2014). Moreover, Rivers et al. (2014) estimate hospital transmission rates as 0.062 and 0.08 for Liberia and Sierra Leone, respectively.

In addition to reviewing several modeling approaches and data for Ebola, we have also included studies that have implemented effective containment of the Ebola epidemic. We provide the most-useful intervention strategies gathered from various studies in the following section.

4.5 Policy Recommendations

Today many policymakers and governmental officials in West Africa are being confronted with challenges including resources for controlling the complex infectious disease outbreaks ever taken place in the 21st century. For this reason, we conclude our study with a summary of policy recommendations from various literature on Ebola.

Community education and awareness

The community education and awareness of the disease is critical to identifying early signs of viral infectious diseases in order to seek immediate support for the sick (Frieden et al., 2014; Obilade, 2015). With appropriate community-based education and guidelines from healthcare managers to identify symptomatic individuals, the 2014 Ebola outbreak would, most likely, not have spread so widely. For instance, Nigeria demonstrated a swift implementation of intervention approaches to contain Ebola through early notification of the disease and education of their citizens regarding the disease with guidelines. In particular, the local healthcare workers monitored approximately $18,500$ suspected individuals for early Ebola symptoms (Fasina et al., 2014; Shuaib et al., 2014). In addition, through extensive community engagement and mobilization, the DRC was able to contain and quickly end all seven Ebola outbreaks they have experienced previously (Obilade, 2015).

Quarantine, hospitalization, and safe burial

Successful control intervention methods involve proper isolation, hospitalization of infected individuals, and safe burials of the deceased, in order to stop the disease from spreading in the community and surrounding areas. Our review suggests that the best way to eradicate Ebola from the West African region is to get the ongoing Ebola epidemic under control with proper and rapid intervention in place. In addition, the literature explains that immediate isolation and hospitalization of infected individuals at the onset of the disease are key strategies in controlling the Ebola epidemic (CDC, 2003; Chowell et al., 2004; Hu et al., 2015; Khan et al., 2015; WHO, 2014b). One particular example is the quick containment of Nigeria's 2014 EVD outbreak, which is the result of immediate implementation of control intervention including early establishment of the Ebola Emergency Center (EEC), which quickly isolates and quarantines suspected cases (Fasina et al., 2014; Shuaib et al., 2014). Furthermore, the immediate action taken by Nigeria's government to prevent burial rituals at funerals largely helped in decreasing the spread of Ebola in that country (Omonzejele, 2014).

Other studies also suggest to set up community-based clinics to ensure that sick individuals are locally isolated from the public in order to reduce the spread of the disease to other regions of the nation (Chen et al., 2014). For example, the implementation of diagnosis and hospitalization of Ebola-infected individuals by the Firestone Tire and Rubber Company in Liberia were successful in eradication of the disease from the community. The company's quick response identified 71 Ebola-infected individuals among a population of $80,000$ people within the community (Reaves et al., 2014). Finally, according to the WHO and CDC, the maintenance of a clean environment and practicing safe burial of the dead aids in prompt isolation of the virus from the community, thus reducing further spread of the disease.

International support and coordination

Government and local officials should encourage continuous international coordination and humanitarian aid in West Africa (Obilade, 2015). Specific examples of such aid for meeting the fundamental needs of populations during the Ebola crisis period include the following: (*i*) World Food Programme (WFP), which helps more than 1.3 million most-affected communities and families with their medical and food needs (Waddington, 2014); and (*ii*) Doctors Without Borders (Médecins Sans Frontiéres [MSF]), an active leading response organization employing approximately 700 foreign staff and operating six Ebola case management centers (ECMCs) in West Africa (Arie et al., 2014; Green, 2014; Philips and Markham, 2014). Furthermore, African countries that have experienced several Ebola epidemics in the past, and have been declared free of the virus, for example the DRC, can provide strong support to at-risk countries such as Guinea, Liberia, and Sierra Leone (Obilade, 2015).

Rebuilding infrastructure

The disease primarily impacted middle-aged citizens 15 to 44 years old (Meltzer et al., 2014; WHO, 2014b). Therefore, policymakers and government officials should promote programs aimed at closing the productivity gap due to the 2014 Ebola epidemic (Wilkinson and Leach, 2014). For example, the United Nations (UN) and other humanitarian support including the WBG and other international organizations have initiated programs such as the Ebola Recovery Assessment Program (ERAP) for purposes of promoting early post-Ebola recovery plans including food security and rebuilding of healthcare systems in Guinea, Liberia, and Sierra Leone (WBG, 2014).

Finally, in chapter 5 of the dissertation, we implement the insights and ideas we gain from review and studies of Ebola compartmental models as well as data analysis for estimation of transition parameters.

CHAPTER 5

A MIXED-INTEGER OPTIMIZATION APPROACH FOR ALLOCATION OF RESOURCES AND CONTROL OF THE DYNAMICS AND SPREAD OF THE 2014 EBOLA EPIDEMIC IN GUINEA, LIBERIA, AND SIERRA LEONE

5.1 Introduction

Ebola is a severe, often deadly, infectious disease caused by the Ebola virus (Baize et al., 2014). New patients of the Ebola virus disease are reported to have directly come in contact with body fluids, blood of an infectious person, or a contaminated objected from Ebola-infected fluid (WHO, 2014a). Therefore, the virus is known to primarily affect those family members who provide care and healthcare workers in close proximity to infected individuals, due to the cross-contamination of body fluids (Baron et al., 1983; Georges et al., 1999; Heymann et al., 1980). On the other hand, since Ebola-related dead bodies are highly infectious, traditional funeral rituals largely contribute to spread of the disease (Muyembe-Tamfum et al., 1999).

Today, many regions in West Africa have been hit hard by the EVD, considered one of the deadliest Ebola outbreaks ever known. According to the WHO, this 2014 West African EVD outbreak is the first ever, and in this case, the largest to occur in this part of the continent. Evidence also indicates that the majority of reported EVD cases and deaths in the currently affected countries appears to be in the middle-aged 15 to 44 years old (Meltzer et al., 2014).

Among the most severely affected countries faced with Ebola are the following: Guinea, Liberia, and Sierra Leone. Yet, it continues to spread to neighboring countries including Mali, Nigeria, and Senegal. According to Baize et al. (2014) and other studies on Ebola, the disease appears to have an associated case fatality rate of up to 90%. However, the WHO estimates that this high fatality rate would be reduced to around 60% for Ebola-infected individuals who seek immediate medical attention (WHO, 2014b). Following the fatality rate in Guinea, it is estimated that approximately 60% of total cases have been associated with traditional funerals of family members, where burial rituals involve touching the body of the deceased individual (Chan, 2014; Hewlett and Amola, 2003). On the other hand, the migration of individuals across geographic regions within affected countries also contributes to spread and growth of the deadly disease (Goufo and Maritz, 2015). Subsequently, an appropriate technique for modeling spatial spread of this infectious disease is desperately needed. For example, Sattenspiel and Dietz (1995) formulate a model for spread of infectious diseases by employing the migration of individuals between regions.

Presently, there is no known EVD treatment that has demonstrated success (Yazdanpanah et al., 2015). Yet reports state that patients who completely recover from Ebola receive aid from supportive therapy, such as maintenance of fluids and standard nursing care (Sanchez, 2001; Yazdanpanah et al., 2015). The current EVD outbreak also reveals the broken and poor healthcare system in the three affected nations. As Chan (2014) describes in his paper, poverty and the lack of medical facilities play a significant role in early spread of the disease. For instance, Liberia has 0.1 physicians, 2.7 nurses and 8, hospital beds per $10,000$ people (UN, 2014).

Financial support is the most needed aid during an epidemic in order to effectively ensure improving the prevention of disease outbreak. For instance, Bausch and Schwarz (2014); Green (2014) report that the current short-term economic impact of the outbreak is estimated to be \$130M in Guinea, \$66M in Liberia, and \$163M in Sierra Leone. Other studies, such as one by the CDC document the fact that a significant portion of the Ebola treatment cost is attributed to the cost of ETCs, and the availability of healthcare professionals. Therefore, the cost of Ebola diagnosis and treatment incurred by sick patients could amount to a major problem for individuals living in developing countries, especially in rural areas. In its 2015 economic growth report, the World Bank Group's estimates that the financial burden created by the Ebola epidemic across the three severely affected nations of Guinea, Liberia, and Sierra Leone is -2%, -2%, and 3% compared to 4.3%, 8.9%, and 6.8%, respectively, in the previous growth report before the crisis.

Mathematical models have been widely used to understand the dynamics of infectious diseases, including MIP models (Tao et al., 2004), stochastic simulation models (Eubank et al., 2004; Meltzer et al., 2014), and differential equations (Arreola et al., 1999; Chowell et al., 2004). These models could either be formulated as either continuous-time (Zhou and Fan, 2012) or discrete-time (Allen, 1994) models. Infectious disease models have been classified on the basis of their mode of spread, whereby the given population is partitioned into several compartment classes in proportion to the severity of the disease to be studied. For instance, the SIR (Rizkalla et al., 2007) and SEIR models (Chowell et al., 2004) have been studied to explain spread and control of the Ebola virus in a population. In fact, the difference between the two models is the the addition of the exposed compartment class represented by E, where individuals are infected but not contagious (Nåsell, 2001). Similarly, the purpose of infection control intervention is for the containment of an epidemic disease, thereby decreasing the total number of cases. Most recently, many Ebola epidemic models extend the basic SIR or SEIR model by including quarantine compartment (Arreola et al., 1999), treated compartment (Camacho et al., 2014), funeral (dead but unburied) compartment (Rivers et al., 2014), and burial compartment (Hu et al., 2015).

5.1.1 Contributions

We summarize the main contributions of this chapter as follows:

- While most Ebola epidemic models deal with the estimation of population dynamics of Ebola and its behavior in West Africa, they tend not to incorporate the spatial effects of epidemiology, which also influence the path of an outbreak. To deal with this, we develop an optimization mathematical approach to assess the 2014 Ebola epidemic in West Africa. We formulate an epidemic MIP model for Ebola, which involves management of the infectious disease and its timely intervention to minimize the total number of fatalities and cases. We also apply our SITR-FB compartmental epidemic model to study spread-and-control of Ebola because of its dynamics. Furthermore, the proposed model is used to allocate ETC facilities in Guinea, Liberia, and Sierra

Leone where they serve as both quarantine and treatment centers because the disease is transmitted through direct contact with an infected person (Arreola et al., 1999; Chan, 2014; Hewlett and Amola, 2003; Hu et al., 2015).

- We illustrate the performance of our SITR-FB compartmental epidemic model on a case study specific to the 2014 Ebola outbreak in Guinea, Liberia, and Sierra Leone. We gather our data from various sources including the following: The WHO Ebola response roadmap situation report, Ebola journal papers, and other published sources on the disease. First, we split the data into three categories: demographic characteristics in Guinea, Liberia, and Sierra Leone, compact published estimates for Ebola transition parameters, and data on costs of Ebola treatment. Second, based on the square footage of the three nations, we partition Guinea into three model regions: upper, mid and lower. Liberia into two model regions: northern and southern and Sierra Leone as one. Third, we incorporate the travel of susceptible and infected individuals between model regions of Guinea and Liberia in our MIP model, because we estimate migration rates by growth, birth, and death rates in selected countries.
- Lastly, we perform a computational study and numerical analysis to determine how several levels of control intervention and allocation of ETC facilities impact spread of the disease within model regions of the given countries. We also analyze model transition parameters in the absence and presence of control intervention for determining sensitive parameters in the SITR-FB epidemic model. Therefore, this approach allows policymakers to focus on key epidemic parameters such as transmission and recovery rates which are directly related to spread and dynamics of the disease.

The remainder of this chapter is structured as follows: In Section 5.2, we describe and explain the MIP epidemic model formulation with built-in migration of susceptible and infected individuals, allocation of limited ETC facilities, and control intervention over a planning horizon of sixty weeks. In Section 5.3, we illustrate our MIP model on a case study occurrence with data collected from the most-affected West African nations of Guinea, Liberia, and Sierra Leone, relating to the current 2014 Ebola outbreak to analyze different decisions. Data used in our computational analysis typically include fixed and variable costs of Ebola treatment, a model parameter estimation, and demographic characteristics of the three most-affected nations. In Section 5.4, we perform numerical analysis to determine the population transmission dynamics among geographic regions, optimal budget to determine minimum number of ETC facilities to be allocated to model regions and then study cost component analysis in each model region of selected countries. We also demonstrate results on spread of the virus with and without migration of susceptible and infected individuals between model regions of selected countries. Finally, we study sensitive model parameters regarding disease transmission for management and elimination of the disease.

5.2 Mixed-Integer Optimization Model Definition

To address the spread and control of the 2014 EVD in Guinea, Liberia, and Sierra Leone, we study the SITR-FB epidemic model that combines mixed-integer optimization approach with effective allocation of epidemic resources in a set population. The proposed model analyzes transitional flow of individuals within the six compartmental classes, as shown in Figure 5.1. We present this model as a decision-making policy for the managing the disease including optimally allocating ETC facilities in the form of available budget over a finite planning horizon of sixty weeks.

5.2.1 SITR-FB Compartmental Epidemic Model

This section presents description of the formulation of the SITR-FB compartmental epidemic model which involves the following features for modeling of epidemic disease such as the following: (*i*) transmission dynamics of the Ebola virus, (*ii*) built-in control interventions, (*iii*) migration of individuals between geographic regions of a selected country (Guinea, Liberia, and Sierra Leone), and (*iv*) optimal allocation of epidemic resources to six distinct model regions.

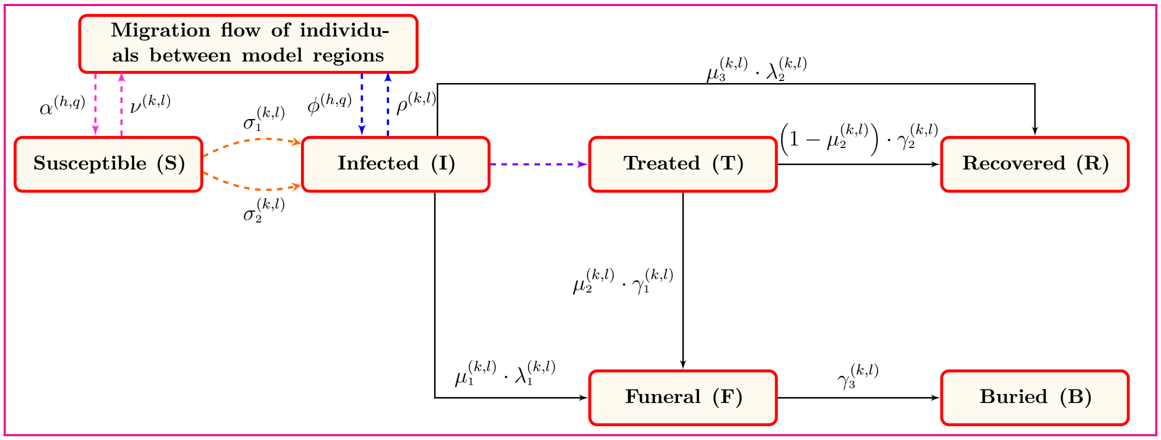

Figure 5.1: Network representation of transmission dynamics of Ebola and SITR-FB epidemic model for each model region (k, l). (Here we determine the number of individuals in each model region (k, l) who are susceptible (S), infected (I), treated (T), recovered with lifelong immunity (R), funerals (Ebola-related dead but unburied) (F), and who are safely buried (B))

Figure 5.1 determines the flow and the number of individuals in each of the six distinct SITR-FB epidemic Ebola categories and who are also identified by their compartmental class and model-based region (k, l) in which they are located. Additionally, the index j denotes the finite planning horizon over which the entire problem is solved. While we represent the ordered pair (k, l) as a model-based region, it is defined by row k and column l in each of the three most-affected West African nations. Moreover, the vertices between each of the six compartments represent the transition made by an individual from one compartment to the next with constant transition parameters over time period j until the sixtieth period.

We also assume that each individual in a set population is initially susceptible (S) to the disease and once infected with the virus immediately move to the infected (I) compartment at a rate of either $\sigma_1^{(k,l)}$ or $\sigma_2^{(k,l)}$, thus developing Ebola-related symptoms. Meanwhile, there is an ongoing migration of susceptible and infected individuals into and from compartments S and I at rates of $(\alpha^{(h,q)}, \nu^{(k,l)})$ and $(\phi^{(h,q)}, \rho^{(k,l)})$, respectively. At this period, a proportion, $\mu_1^{(k,l)}$, of individuals in compartment I will also die from the disease and progress to the funeral (F) compartment at a rate of $\lambda_1^{(k,l)}$. Subsequently, a proportion $(1 - \mu_1^{(k,l)} - \mu_3^{(k,l)})$ of individuals in compartment I are hospitalized for treatment (T), depending on the availability of beds in an ETC facility. For this reason, it is assumed that individuals who are not sent for treatment remain in the community to spread the disease, thus making it complex to eradicate the epidemic. Furthermore, individuals in the T compartment could either recover from the disease at a rate of $\gamma_2^{(k,l)}$ or die at a rate of $\gamma_1^{(k,l)}$. Finally, the buried (B) compartment provides the cumulative number of deceased individuals from the funeral compartment who are safely buried at a rate of $\gamma_3^{(k,l)}$.

5.2.2 Model Notations

The set of model notations for the description of the Ebola MIP model are as follows:

Indices:

j	Index for time period
n	Index for type of ETC facility
(k,l)	Index for model region where $k \in K$ and $l \in L$

Sets:

J	Set of time periods, $J = \{0, \cdots, \bar{J}\}$
N	Set of ETC types, $N = \{1, \cdots, \bar{N}\}$
K	Set of rows, $K = \{1, \cdots, \bar{K}\}$
L	Set of columns, $L = \{1, \cdots, \bar{L}\}$
$M_{(k,l)}$	Set of all surrounding regions (k,l)

Function:

$\mathscr{F}$	Function to represent force of infection

Ebola transition and migration parameters:

$\mu_1^{(k,l)}$	Fatality rate without treatment in region (k,l)
$\mu_2^{(k,l)}$	Fatality rate while receiving treatment in region (k,l)
$\mu_3^{(k,l)}$	Survival rate of infected individuals without treatment in region (k,l)
$\sigma_1^{(k,l)}$	Transmission rate per person due to community interaction in region (k,l)
$\sigma_2^{(k,l)}$	Transmission rate per person during traditional funeral ceremony in region (k,l)
$\left(\lambda_1^{(k,l)}\right)^{-1}$	Average time (in periods) it takes an infected individual to die without treatment in region (k,l)
$\left(\lambda_2^{(k,l)}\right)^{-1}$	Average time (in periods) it takes infected individual to recover without treatment in region (k,l)

Remaining parameters:

$\left(\gamma_1^{(k,l)}\right)^{-1}$	Average time (in periods) it takes individual to die while receiving treatment in region (k,l)
$\left(\gamma_2^{(k,l)}\right)^{-1}$	Average time (in periods) it takes individual to recover while receiving treatment in region (k,l)
$\gamma_3^{(k,l)}$	Safe burial rate of Ebola-related dead bodies in region (k,l)
$b_{1_j}^{(k,l)}$	Unit cost of treatment for infected individual in region (k,l) at end of period j
$b_{2_j}^{(k,l)}$	Unit cost of safe burial for dead individual in region (k,l) at end of period j
$g_{nj}^{(k,l)}$	Fixed cost of establishing a type n ETC in region (k,l) at the end of period j
κ_n	Capacity (number of beds) of a type n ETC
Ω_1	Total available budget for treatment
Ω_2	Total available budget for safe burial

Migration parameters:

$\alpha^{(h,q)\to(k,l)}$	Migration rate of susceptible individuals from surrounding regions (h,q) to region (k,l)
$\phi^{(h,q)\to(k,l)}$	Migration rate of infected individuals from surrounding regions (h,q) to region (k,l)
$\nu^{(k,l)\to(h,q)}$	Migration rate of susceptible individuals from region (k,l) to surrounding regions (h,q)
$\rho^{(k,l)\to(h,q)}$	Migration rate of infected individuals from region (k,l) to surrounding regions (h,q)

Linearization variables:

$U_j^{(k,l)}$	Continuous variable to represent nonlinear term $\left(C_j^{(k,l)} - T_j^{(k,l)}\right) \cdot z_j^{(k,l)}$ in region (k,l) at end of period j
$W_j^{(k,l)}$	Continuous variable to represent nonlinear term $I_j^{(k,l)} \cdot \left(1 - z_j^{(k,l)}\right)$ in region (k,l) at end of period j

$$z_j^{(k,l)} = \left[\begin{array}{ll} 1, & \text{if number of infected individuals in region } (k,l) \text{ are hospitalized at end} \\ & \text{ of period } j \text{ is equal to } \left(C_j^{(k,l)} - T_j^{(k,l)}\right) \\ 0, & \text{otherwise} \end{array}\right.$$

Decision variables:

$S_j^{(k,l)}$	Number of susceptible individuals in region (k,l) at end of period j
$I_j^{(k,l)}$	Number of infected individuals in region (k,l) end of period j
$T_j^{(k,l)}$	Number of individuals receiving treatment in region (k,l) at end of period j

Remaining decision variables:

$R_j^{(k,l)}$	Number of recovered individuals in region (k,l) at end of period j
$F_j^{(k,l)}$	Number of deceased individuals due to the epidemic in region (k,l) at end of period j
$B_j^{(k,l)}$	Number of buried individuals in region (k,l) at end of period j
$\hat{S}_j^{(k,l)}$	Number of susceptible individuals migrating from surrounding regions into region (k,l) at end of period j
$\tilde{S}_j^{(k,l)}$	Number of susceptible individuals migrating from region (k,l) to surrounding regions at end of period j
$\hat{I}_j^{(k,l)}$	Number of infected individuals migrating from surrounding regions into region (k,l) at end of period j
$\tilde{I}_j^{(k,l)}$	Number of infected individuals migrating from region (k,l) to surrounding regions at end of period j
$C_j^{(k,l)}$	Total capacity (number of beds) of established ETCs in region (k,l) at end of period j
$\bar{I}_j^{(k,l)}$	Number of infected individuals hospitalized in region (k,l) at end of period j
$y_{nj}^{(k,l)}$	Number of type n ETCs established in region (k,l) at end of period j

5.2.3 Model Assumptions

- All individuals are initially in the susceptible compartment with the exception of the already infected, dead, and buried individuals at the beginning of the time period in the planning horizon.
- Individuals in the recovered compartment are assumed to receive lifelong immunity, according to the studies of Griggs (2014).
- Migration of susceptible and infected individuals between model-based regions of a given country is also considered in this model to understand spread of the disease across regional borders. We note that spread of the Ebola virus from rural areas to cities is mostly related to individuals in search of better treatments and jobs (Goufo and Maritz, 2015; Ivorra et al., 2014).
- According to the studies of Pandey et al. (2014); Rivers et al. (2014), individuals who become infected with the Ebola virus are known to have come into direct contact with an infectious person. This could occur either in the community during socializing, at

traditional funerals where burial ceremony rites are performed (including kissing of the deceased), or in the hospital during treatment procedures. Despite these forms of Ebola transmission, we consider transmission as a result of community and traditional funeral interactions for the ease of computational difficulty.

- Three forms of control interventions for management and eradication of Ebola to evaluate the success of intervention policy are considered in this model. These include the following: availability of budget for ETC and IUC facilities for Ebola-infected individuals, safe burials for deceased individuals, and accounting for recovered individuals (Lekone and Finkenstädt, 2006).
- For the SITR-FB epidemic model, we assume approximation of the non-linear terms of the force of infections $\mathscr{F}(S, I)$ and $\mathscr{F}(S, F)$ as linear terms $\mathscr{F}(I)$ and $\mathscr{F}(F)$, respectively, to ease computational difficulty.

5.2.4 Mixed-Integer Optimization Approach and Epidemic Model Formulation

We formulate the following problem as an MIP model using the general principles of epidemic modeling based on the above assumptions, notations, and relationships among six distinct Ebola epidemic compartments, as shown in Figure 5.1.

$$\min \sum_{j\in J}\sum_{k\in K}\sum_{l\in L}\left[1+\mu_{1}^{(k,l)}\cdot\lambda_{1}^{(k,l)}\right]\cdot I_{j}^{(k,l)} \tag{5.1}$$

subject to:

$$\sum_{j\in J}\sum_{k\in K}\sum_{l\in L}\sum_{n\in N}\left[g_{nj}^{(k,l)}\cdot y_{nj}^{(k,l)}+{b_1}_{j}^{(k,l)}\cdot T_{j}^{(k,l)}\right]\leq\Omega_1 \tag{5.2a}$$

$$\sum_{j\in J}\sum_{k\in K}\sum_{l\in L}\gamma_{3}^{(k,l)}\cdot {b_2}_{j}^{(k,l)}\cdot F_{j}^{(k,l)}\leq\Omega_2 \tag{5.2b}$$

$$\begin{aligned} S_{(j+1)}^{(k,l)} &= S_{j}^{(k,l)}+\hat{S}_{j}^{(k,l)}-\tilde{S}_{j}^{(k,l)}-\mathscr{F}(S_{j}^{(k,l)},I_{j}^{(k,l)})-\mathscr{F}(S_{j}^{(k,l)},F_{j}^{(k,l)}),\\ &\forall j\in J\backslash\bar{J},\forall k\in K,\forall l\in L \end{aligned} \tag{5.3}$$

$$I_{(j+1)}^{(k,l)} = I_j^{(k,l)} + \hat{I}_j^{(k,l)} - \tilde{I}_j^{(k,l)} + \mathscr{F}(S_j^{(k,l)}, I_j^{(k,l)}) + \mathscr{F}(S_j^{(k,l)}, F_j^{(k,l)})$$

$$- \Big[\mu_{_1}^{(k,l)} \cdot \lambda_{_1}^{(k,l)} + \mu_{_3}^{(k,l)} \cdot \lambda_{_2}^{(k,l)}\Big] \cdot I_j^{(k,l)} - \bar{I}_j^{(k,l)} \tag{5.4}$$

$$\forall j \in J \backslash \bar{J}, \forall k \in K, \forall l \in L$$

$$T_{(j+1)}^{(k,l)} = T_j^{(k,l)} + \bar{I}_j^{(k,l)} - \Big[\mu_{_2}^{(k,l)} \cdot \gamma_{_1}^{(k,l)} + \Big(1 - \mu_{_2}^{(k,l)}\Big) \cdot \gamma_{_2}^{(k,l)}\Big] \cdot T_j^{(k,l)},$$

$$\forall j \in J \backslash \bar{J}, \quad \forall k \in K, \forall l \in L \tag{5.5}$$

$$R_{(j+1)}^{(k,l)} = R_j^{(k,l)} + \Big(1 - \mu_{_2}^{(k,l)}\Big) \cdot \gamma_{_2}^{(k,l)} \cdot T_j^{(k,l)} + \mu_{_3}^{(k,l)} \cdot \lambda_{_2}^{(k,l)} \cdot I_j^{(k,l)},$$

$$\forall j \in J \backslash \bar{J}, \forall k \in K, \forall l \in L \tag{5.6}$$

$$F_{(j+1)}^{(k,l)} = F_j^{(k,l)} + \mu_{_1}^{(k,l)} \cdot \lambda_{_1}^{(k,l)} \cdot I_j^{(k,l)} + \mu_{_2}^{(k,l)} \cdot \gamma_{_1}^{(k,l)} \cdot T_j^{(k,l)} - \gamma_{_3}^{(k,l)} \cdot F_j^{(k,l)},$$

$$\forall j \in J \backslash \bar{J}, \forall k \in K, \forall l \in L \tag{5.7}$$

$$B_{(j+1)}^{(k,l)} = B_j^{(k,l)} + \gamma_{_3}^{(k,l)} \cdot F_j^{(k,l)}, \quad \forall j \in J \backslash \bar{J}, \forall k \in K, \forall l \in L \tag{5.8}$$

$$\bar{I}_j^{(k,l)} = \begin{bmatrix} I_j^{(k,l)}, & \textit{if } \; I_j^{(k,l)} \le C_j^{(k,l)} - T_j^{(k,l)}; \\ C_j^{(k,l)} - T_j^{(k,l)}, & \textit{otherwise}; \quad \forall j \in J \backslash \bar{J}, \forall k \in K, \forall l \in L \end{bmatrix} \tag{5.9}$$

$$y_{nj}^{(k,l)} \le I_j^{(k,l)}, \quad \forall n \in N, \forall j \in J, \forall k \in K, \forall l \in L \tag{5.10}$$

$$C_j^{(k,l)} = \sum_{r=0}^{j} \sum_{n \in N} \kappa_n \cdot y_{nr}^{(k,l)}, \quad \forall j \in J, \forall k \in K, \forall l \in L \tag{5.11}$$

$$\Big(S_j^{(k,l)},\, I_j^{(k,l)},\, \bar{I}_j^{(k,l)},\, T_j^{(k,l)},\, R_j^{(k,l)},\, F_j^{(k,l)},\, B_j^{(k,l)}\Big) \ge 0, \quad \forall j \in J, \forall k \in K, \forall l \in L \tag{5.12}$$

$$y_{_{nj}}^{(k,l)} \in \{0, 1, 2, \cdots\}, \quad \forall n \in N, \forall j \in J, \forall k \in K, \forall l \in L \tag{5.13}$$

where $\mathscr{F}(S_j^{(k,l)}, I_j^{(k,l)}) \approx \mathscr{F}(I_j^{(k,l)}) = \sigma_{_1}^{(k,l)} \cdot I_j^{(k,l)}$ and

$$\mathscr{F}(S_j^{(k,l)}, F_j^{(k,l)}) \approx \mathscr{F}(F_j^{(k,l)}) = \sigma_{_2}^{(k,l)} \cdot F_j^{(k,l)}, \quad \forall j \in J \backslash \bar{J}, \forall k \in K, \forall l \in L$$

- The relation to define migration of susceptible and infected individuals is

$$\hat{S}_j^{(k,l)} = \sum_{(h,q)\in M_{(k,l)}} \alpha^{(h,q)\to(k,l)} \cdot S_j^{(h,q)}, \quad \forall j \in J, \forall k \in K, \forall l \in L$$

$$\hat{I}_j^{(k,l)} = \sum_{(h,q)\in M_{(k,l)}} \phi^{(h,q)\to(k,l)} \cdot I_j^{(h,q)}, \quad \forall j \in J, \forall k \in K, \forall l \in L$$

$$\tilde{S}_j^{(k,l)} = \sum_{(h,q)\in M_{(k,l)}} \nu^{(k,l)\to(h,q)} \cdot S_j^{(k,l)}, \quad \forall j \in J, \forall k \in K, \forall l \in L$$

$$\tilde{I}_j^{(k,l)} = \sum_{(h,q)\in M_{(k,l)}} \rho^{(k,l)\to(h,q)} \cdot I_j^{(k,l)}, \quad \forall j \in J, \forall k \in K, \forall l \in L$$

The objective function (5.1) of the model minimizes the total number of infected individuals and fatalities over all regions (k, l) over the finite planning horizon. The budget constraint comprises two distinct components. The first term of the budget constraint (5.2a) ensures that the total fixed costs for setting up either a 50- or 100-bed ETC facility and variable cost for treating Ebola-related patients over all regions (k, l) is equal to or less than the available treatment budget. Similarly, the second term of the budget constraint (5.2b) ensures that all Ebola-related fatalities are safely buried in region (k, l) and is equal to or less than the budget allocated for safe burial. The set of constraints (5.3) to (5.8) maintain the flow of individuals through the SITR-FB compartmental classes by describing the transmission dynamics of Ebola in a set population, in region (k, l) at the end of period j as shown in Figure 5.1.

Constraint (5.3) defines the number of susceptible individuals in region (k, l) where a portion becomes infected with the virus either at the community level or at traditional funerals at the end of time period j. Further, these infected individuals immediately move from compartment S to I. Constraint (5.4) then determines the number of infected individuals in region (k, l) at the end of time period j, where a fraction of these infected individuals either leave for treatment in an ETC facility, recover naturally, or die from the disease. We also assume the migration of susceptible and infected individuals from and into compartments S and I while the epidemic spreads. Constraint (5.5) represents individuals who are receiving treatment from an ETC facility in region (k, l) at the end of time period j. A portion of these individuals may either die from the disease and move into compartment F, or recover from the disease and transition into compartment R at the end of time period j. Constraint (5.6) relates to the total number of recovered individuals coming from both I and T compartments in region (k, l) at the end of time period j. Constraint (5.7) updates the total number of unburied Ebola-related deaths as a result of untreated infection or individuals not responding to treatments in region (k, l) at end of time period j. Constraint (5.8) provides the total number of Ebola-related deaths transitioning from compartment F who are safely buried in region (k, l) at the end of time period j.

Constraint (5.9) ensures that Ebola-infected individuals are hospitalized for treatment on the basis of available beds in treatment facilities in region (k, l) at the end of period j. For constraint (5.9) in this model, we linearize it by substituting it with equations (5.10b) to (5.10i) in order to reduce computational difficulty at the end of time period j. Constraint (5.10) provides a bound on the number of ETC facilities to be set up, because as these depend on the number of individuals to be infected in region (k, l) at the end of period j. Constraint (5.11) determines the total number of beds (capacity) in each of the 50- or 100-bed ETC facilities in region (k, l) at the end of time period j. Constraint (5.12) states that the number of susceptible, infected, treated, funeral, buried, and recovered individuals are non-negative integers. Finally, constraint (5.13) ensures that the number of type n ETC facilities to be opened in region (k, l) at the end of time period j are non-negative integers.

5.2.5 Linearizing Conditional Function

We start the linearization process of the logical constraint (5.9) by performing the following steps. First, we express constraint (5.9) as a function of a binary variable and its conjugate by rewriting it as

$$\bar{I}_j^{(k,l)} = \underbrace{\left(C_j^{(k,l)} - T_j^{(k,l)}\right) \cdot {z_j}^{(k,l)}}_{Quadratic\ term\ 1} + \underbrace{I_j^{(k,l)} \cdot \left(1 - {z_j}^{(k,l)}\right)}_{Quadratic\ term\ 2}, \quad \forall j, k, l \tag{5.10a}$$

where ${z_j}^{(k,l)}$ denotes a binary variable $(0, 1)$. Further, according to equation (5.10a), when ${z_j}^{(k,l)} = 1$, $\bar{I}$ becomes $C_j^{(k,l)} - T_j^{(k,l)}$, as expected, we observe that the number of infected individuals to be hospitalized will depend on the number of beds available in ETC facilities. Likewise, when ${z_j}^{(k,l)} = 0$, $\bar{I}$ becomes I, as expected, we also see that all infected individuals will be hospitalized for treatment in ETC facilities due to the available capacity as $C_j^{(k,l)} \geq I_j^{(k,l)}$. Therefore, the minimum of $\left(C_j^{(k,l)} - T_j^{(k,l)}\right)$ and $I_j^{(k,l)}$ determines the value of ${z_j}^{(k,l)}$.

Second, to improve the linearization process of equation (5.10a), we then represent (5.10a) as the sum of two auxiliary (continuous) variables where we introduce two continuous variables: ($U_j^{(k,l)}$ and $W_j^{(k,l)}$). By doing this, we eliminate computational difficulty resulting from the multiplication of the continuous and binary variables. To finalize this process, we let $U_j^{(k,l)} = \left(C_j^{(k,l)} - T_j^{(k,l)}\right) \cdot {z_j}^{(k,l)}$ and then assume that $H_{LB} \leq C_j^{(k,l)} - T_j^{(k,l)} \leq H_{UB}$, where H_{LB} and H_{UB} as lower and upper bounds, respectively, for $C_j^{(k,l)} - T_j^{(k,l)}$. This leads to the set of inequalities (5.10b) to (5.10e) as it enforces $U_j^{(k,l)}$ to be equal to $\left(C_j^{(k,l)} - T_j^{(k,l)}\right) \cdot {z_j}^{(k,l)}$.

$$U_j^{(k,l)} \leq H_{UB} \cdot {z_j}^{(k,l)}, \quad \forall j, k, l \tag{5.10b}$$

$$U_j^{(k,l)} \geq H_{LB} \cdot {z_j}^{(k,l)}, \quad \forall j, k, l \tag{5.10c}$$

$$U_j^{(k,l)} \leq \left(C_j^{(k,l)} - T_j^{(k,l)}\right) - H_{LB} \cdot \left(1 - {z_j}^{(k,l)}\right), \quad \forall j, k, l \tag{5.10d}$$

$$U_j^{(k,l)} \geq \left(C_j^{(k,l)} - T_j^{(k,l)}\right) - H_{UB} \cdot \left(1 - {z_j}^{(k,l)}\right), \quad \forall j, k, l \tag{5.10e}$$

Similarly, we let the continuous variable $W_j^{(k,l)} = I_j^{(k,l)} \cdot \left(1 - {z_j}^{(k,l)}\right)$ and then assume that $I_{LB} \leq I_j^{(k,l)} \leq I_{UB}$, where I_{LB} and I_{UB} represent the lower and upper bounds for, respectively, $I_j^{(k,l)}$. This results in the set of inequalities (5.10f) to (5.10i), which ensures that the value of $W_j^{(k,l)}$ is equal to $I_j^{(k,l)} \cdot \left(1 - {y_j}^{(k,l)}\right)$.

$$W_j^{(k,l)} \leq I_{UB} \cdot \left(1 - {z_j}^{(k,l)}\right), \quad \forall j, k, l \tag{5.10f}$$

$$W_j^{(k,l)} \geq I_{LB} \cdot \left(1 - {z_j}^{(k,l)}\right), \quad \forall j, k, l \tag{5.10g}$$

$$W_j^{(k,l)} \leq I_j^{(k,l)} - I_{LB} \cdot {z_j}^{(k,l)}, \quad \forall j, k, l \tag{5.10h}$$

$$W_j^{(k,l)} \geq I_j^{(k,l)} - I_{UB} \cdot {z_j}^{(k,l)}, \quad \forall j, k, l \tag{5.10i}$$

Finally, equation (5.10a) becomes exactly equal to the logical constraint expressed in the summation form: $\bar{I}_j^{(k,l)} = U_j^{(k,l)} + W_j^{(k,l)}$, where $U_j^{(k,l)}$ and $W_j^{(k,l)}$ are limited by equations (5.10b) to (5.10i).

5.3 Case Study Data and Parameter Estimation of 2014 Ebola Epidemic

This section presents case study occurrence data to illustrate the performance of our epidemic disease model specific to the 2014 Ebola epidemic in Guinea, Liberia, and Sierra Leone. Specifically, we utilize published data from the WHO Ebola response roadmap situation report and Ebola journal papers in order to emphasize differences among the transmission dynamics of Ebola and to address policy-making issues in Guinea, Liberia, and Sierra Leone. In this case study, we consider the economic data provided in Table 5.1 and the demographic data specific to each of the three most-affected nations given in Table 5.2. Transition rates from published data are in days; however, the weekly estimated transition parameters (epidemiological data) used in the MIP model are shown in Table 5.3.

5.3.1 Assessment Study of Treatment Cost of 2014 Ebola Epidemic

This section provides the initial cost assumptions based on the 2014 Ebola epidemic in Guinea, Liberia, and Sierra Leone. Here, we develop three distinct cost components: These are fixed, variable treatment, and safe burial costs. The fixed cost incurred includes a one-time cost for establishing the ETC facility, IUC, and laboratory diagnosis, while the variable cost of treatment includes the cost for operating a 50- or 100-bed ETC facility, cost of treatment for infected individuals, and safe burial for funerals as a result of Ebola-related deaths. That being said, the inadequacy of required resources can severely delay progress of the outbreak response (see, e.g., Bloom, 2003; Kalra et al., 2014).

To apply the case study data to our optimization model, we convert both the daily transition and monthly cost data parameters into weekly parameters. In addition to estimating the weekly variable costs, we also estimate the weekly variable cost per infected individual. Next, we describe each of the cost components in detail and use the data to validate our model. We classify our fixed costs according to ETCs, IUCs, and laboratory diagnosis, as shown in Table 5.1.

Table 5.1: Economic Impact and Cost of 2014 Ebola Epidemic (WHO, 2014b)

Cost explanation	Fixed cost	Variable treatment cost †	Burial cost †
Ebola treatment center	$386,000	$4,405	
Isolation unit center (IUC)	$112,500	$566.41	
Laboratory Diagnosis	$100,000	$270	
Subnational Technical		$1,125	
Contact tracing		$563.63	
Safe burial			$563.63
Total	**$598,500** (**$1,077,300**) *	**$6,930.04**	**$563.63**

† values for variable treatment and safe burial cost is per week.
* cost value in parenthesis represents total fixed cost for a 100-bed ETC.

Fixed cost

We researched the WHO roadmap situation report for the estimation of both fixed and variable costs for the economic data in the case study.

- Fixed cost is one of the initial cost and one-time costs involved with the setting up of ETC facility. The fixed cost for setting up a 50-bed ETC facility in any of the three at-risk countries is estimated to be approximately $386,000, while the fixed cost for opening a 100-bed ETC facility is assumed to be $1,077,300 $(1.8 * \$598,500)$ for the hospitalization of Ebola patients.
- The IUC facility located inside the ETC where suspected infected individuals are quarantined is an important component in reducing the risk of spreading the disease. This facility is estimated to have a fixed cost in the range of $112,500.
- Laboratory diagnosis is performed to confirm the Ebola status of individuals who are suspected of having the virus. In addition to the other fixed costs, the laboratory diagnostic cost estimated by the WHO is $100,000.

Variable treatment cost

For this model, variable treatment cost accounts for following provided services for Ebola-infected individuals to manage further spread of the disease: cost for operating ETC facility, IUC facility, laboratory diagnosis, and subnational technical coordination.

- According to the WHO, the treatment cost for an Ebola-infected individual in a 50 ETC facility is estimated as $\$881,000$ per month. Therefore, an estimate of the treatment cost for an individual per week is obtained by the following computation: $\left[\frac{\$881{,}000}{4*50}\right] = \$4,405$.
- The cost for operating the IUC is also estimated to be $\$181,250$ per month, which can accommodate only 80 infected individuals.
- It is also estimated that $\$129,600$ would be required to operate the diagnostic laboratory that performs 600 procedures on Ebola victims per month.
- Lastly, we use the subnational level technical (information management and technical expertise) cost based on the WHO situation report estimation. An amount of $\$450,000$ each month is needed to manage ten office setups to coordinate and support ETC activities. This is necessary because studies reported by Okware et al. (2002) indicate that community mobilization and logistic management were a key factors in minimizing the Ebola epidemic outbreak in Uganda in 2000.
- In this section, we define tracing as the identification of suspected new cases for immediate isolation and eradication of spread of the disease. On average, $\$225,450$ is needed each month to trace $1,000$ suspected Ebola-infected individuals by a trained team of 100 people.
- The variable subnational-level technical cost is estimated to be $\$450,000$ per month, while we assume that this fee covers a 100-bed ETC facility. Thus, the related cost for an individual is obtained by the following computation: $\left[\frac{450{,}000}{100*4}\right] = \$1,125$.

Safe burial cost

Safe burial and household disinfection procedures are the most hygienic approach to stopping the spread of Ebola epidemic in Guinea, Liberia, and Sierra Leone (Lamunu et al., 2004; Meltzer et al., 2014). According to the WHO report, approximately $225,450 each month is required to safely bury 100 Ebola-related deceased bodies performed by fully trained teams.

5.3.2 Geographic and Demographic Data From Guinea, Liberia, and Sierra Leone

Table 5.2 shows Guinea, Liberia, and Sierra Leone by geographic information including total land area in square miles, population sizes, and migration rates. The case study data categorizes the three countries into six distinct model regions according to their land area, with Sierra Leone being the base case. Therefore, Guinea is divided into three model regions, Liberia is split into two model regions, and Sierra Leone is classified as its own model region. Additionally, migration rates are also calculated from growth, birth, and death rates of selected countries between the years 1996 and 2014 (GeoHive, 2014).

Table 5.2: Geographic and Demographic Characteristics in Guinea, Liberia, and Sierra Leone

Country	Guinea			Liberia		Sierra Leone
Total population	10,628,978			3,476,608		4,976,871
Total area size †	94,926			43,000		27,699
Model region	Upper (G_1)	Mid- (G_2)	Lower (G_3)	Northern (L_1)	Southern (L_2)	(SL)
Geographic region	Boké	Labé	Kankan	Northwest	Southeast	Northern
	Conakry	Mamou	N'zérékoré	Central	South	Southern
	Kindia	Faranah			Southwest	Eastern
						Western
Population size	4,308,494	2,670,567	3,649,911	2,233,091	1,243,517	4,976,871
Population ratio	0.41	0.25	0.34	0.64	0.36	1
Migration rate *	1.1×10^{-4}	-1.3×10^{-4}	1×10^{-4}	4.5×10^{-5}	-1.1×10^{-4}	–

† size of country in square miles.

* migration rate is computed from this formula: growth rate − (birth rate − death rate).

Guinea

The first case of the 2014 Ebola outbreak was identified in a Meliandou village of Guinea on December 26, 2013. The two-year individual died two days after being hospitalized for treatment (Baize et al., 2014). That being said, intensive control intervention to eradicate the disease started in March 22, 2014 when 49 cases with 29 deaths were identified (Althaus, 2014; Ivorra et al., 2014). The West African nation of Guinea has a population of approximately $10,628,972$, the highest among the three nations, which stretches over $94,926$ square miles. The three model regions of Guinea discussed in this chapter are upper (G_1), mid- (G_2), and lower (G_3). Upper Guinea represents the geographic regions Boké, Conakry, and Kindia, with a total population of $4,308,494$, whereas mid-Guinea represents the geographic regions Labé, Mamou, and Faranah, with an overall population of $2,670,567$, and lower Guinea represents the geographic regions of Kankan and N'zérékoré, with an overall population of $3,649,911$.

Liberia

The disease quickly spread to Monrovia in Liberia where major control intervention was received in August of 2014 (Ivorra et al., 2014). The population size of Liberia which shares border with Guinea is estimated to be $3,476,608$, while its area size is given as $43,000$ square miles. We group the country into two model regions. Bomi, Bong, Gbarpolu, Grand Cape Mount, Lofa, Margibi, and Montserrado counties (northwest and central) are classified as northern (L_1), with an overall population of $2,233,091$. Similarly, we list Grand Bassa, Grand Gedeh, Grand Kru, Maryland, Nimba, River Cess, River Gee, and Senoe counties (southeast, south, and southwest) as southern (L_2), with an approximate population of $1,243,517$.

Sierra Leone

According to the WHO, the EVD immediately spread to Sierra Leone by May of 2014 through a young lady who later recovered from the disease. In July of 2014, epidemic control intervention was later deployed to seriously deal with eradication of the virus (Ivorra et al., 2014). Sierra Leone, which has northern, southern, eastern, and western geographic provinces, is the smallest country with a total population of $4,976,871$

covering an area of $27,699$ square miles and is categorized as its own model region (SL).

5.3.3 Epidemiological Attributes of 2014 Ebola Epidemic

Table 5.3 provides information for weekly Ebola transition parameters in our model for the case study. This is based on the estimation we develop from several sources including the WHO and published estimates from Ebola journal papers. Some of the data values obtained from the literature are refined based on the model fit to the original outbreak data within reasonable ranges defined in the literature.

Table 5.3: Summary of Model Parameters Obtained from Literature for 2014 Ebola Epidemic

Parameter	Description	Guinea	Liberia	Sierra Leone	Reference
$\left(\lambda_1^{(k,l)}\right)^{-1}$	Infection to funeral	0.91	1.13	1.23	(Team, 2014)
$\left(\lambda_2^{(k,l)}\right)^{-1}$	Infection to recovery	2.50	2.14	2.86	(Rivers et al., 2014)
$\left(\gamma_1^{(k,l)}\right)^{-1}$	Treatment to funeral	0.84	1.44	0.89	(Rivers et al., 2014; Team, 2014)
$\left(\gamma_2^{(k,l)}\right)^{-1}$	Treatment to recovery	1.57	2.27	2.27	(Rivers et al., 2014; Team, 2014)
$\mu_1^{(k,l)}$	CFR without treatment	0.71	0.71	0.71	(Althaus, 2014)
$\mu_2^{(k,l)}$	CFR with treatment	0.60	0.61	0.60	(WHO, 2014b)
$\mu_3^{(k,l)}$	Survival rate without treatment	0.26	0.29	0.27	Estimate Value
$\gamma_3^{(k,l)}$	Safe burial rate	0.71	0.71	0.71	Estimate value
$\sigma_1^{(k,l)}$	Community transmission rate	0.27	0.36	0.45	(Althaus, 2014)
$\sigma_2^{(k,l)}$	Funeral transmission rate	0.68	0.78	0.60	(Camacho et al., 2014)

Case fatality rate without treatment

The CFR data has fluctuated among Ebola outbreaks, including those in the DRC and Sudan, with CFRs of around 88% and 66%, respectively (Arreola et al., 1999; CDC, 2003; Chowell et al., 2004; Okware et al., 2002). Similarly, the WHO reported that the CFR for past Ebola outbreaks is observed to be approximately between 25% and 90% (WHO, 2003). The recent 2014 Ebola outbreak in West Africa has an estimated CFR in the range of 50% to 90%, with specific CFRs for Guinea, Liberia, and Sierra Leone of $74\%, 71\%$, and 48%, respectively (Althaus, 2014; Fowler et al., 2014). However, for our

MIP model, we set a CFR of 71% for all three countries based on the model calibration with respect to original outbreak data.

Case fatality rate with treatment

According to the 2014 WHO Ebola response roadmap situation report, the CFR for hospitalized individuals varies from 60% to 61% in Guinea, Liberia, and Sierra Leone. This data is then developed for our case study.

Average time from onset of symptoms to funeral

Several Ebola reports state that, once an individual gets infected with the virus and become infectious, it takes the individual four to ten days (0.57 to 1.43 weeks) to die depending on several factors. Data employed for this model includes the mean values from the data analysis in the study of Team (2014) that provide average estimates for the three at-risk countries as follows: Guinea, Liberia, and Sierra Leone being 6.4 ± 5.3 days (0.91 ± 0.76 weeks), 7.9 ± 8.0 days (1.13 ± 1.14 weeks), and 8.6 ± 6.9 days (1.23 ± 0.99 weeks), respectively.

Average time from onset of symptoms to recovery

To be consistent in this chapter, we use average length of Ebola infection to represent the average time it takes an infectious individual to recover without any medical treatment. Other studies have shown that the 2014 Ebola outbreak has an expected recovery time (mean infection length) in the range of approximately 15 (2.14 weeks) and 20 days (2.86 weeks), using fitted values for Liberia and Sierra Leone (Rivers et al., 2014). Furthermore, studies on Ebola estimate the daily rate of recovery in the community and hospital in the range of 0.05 and 0.18 (Althaus, 2014; Gomes et al., 2014; Legrand et al., 2007; Towers et al., 2014). However, for Guinea, an average value of 17.5 days (2.5 weeks) is used in the case study.

Average time from treatment to funeral

For the estimation of the time from treatment to funeral, 10.38 days (1.48 weeks) and 13.31 days (1.90 weeks) are assumed to be the average time for infected individuals in Liberia and Sierra Leone to transition from ETC facilities to funeral, respectively (Rivers et al., 2014). At the same time, this chapter uses the extreme value of $(2.5 \pm 3.4$ days) which result in 5.9 days (0.84 weeks) in Guinea according to the work of Team (2014).

Average time from treatment to recovery

The expected amount of time it takes an Ebola-infected individual to recover while receiving treatment is estimated to be 15.88 days (2.27 weeks) in both Liberia and Sierra Leone (Rivers et al., 2014). For Guinea, we use the estimate 11 ± 5.4 days (1.57 weeks) provided in the studies of Team (2014).

Average time from funeral to traditional burial (Safe burial rate)

Rivers et al. (2014) indicate that the mean time from traditional funerals to safe burials by trained teams in Guinea, Liberia, and Sierra Leone varies between 2.01 days and 4.05 days. According to Eisenberg et al. (2015), the time from death until burial is also estimated to be one to three days. Meanwhile, previous studies on past Ebola outbreaks in DRC and Sudan suggest that the time to safe burial is approximately 2 days (Gomes et al., 2014; Legrand et al., 2007; Pandey et al., 2014). Based on these data, this chapter assumes a safe burial rate of 0.71 for all three countries because we assume that on average, dead individuals are safely buried within 5 days (0.71 week) after death.

Transmission rate at community level

Transmission rates at the community level are seen to be higher for individuals than the other two transmission rates: at funerals and in hospital settings. According to a study by Althaus (2014), transmission rates via person-to-person contact during community interaction are reported to be 0.27 in Guinea, 0.28 in Liberia, and 0.45 in Sierra Leone.

Transmission rate at traditional funerals

Transmission rates at traditional funerals are assumed to vary in the range of 0.08–2.00, as traditions pertaining to burial change across West African nations (Camacho et al., 2014). We set the transmission rates by examining model results with respect to the original outbreak data within the presented range 0.08–2.00.

5.3.4 SITR-FB Epidemic Model Implementation and Experimental Design

In this section, we present numerical results using the proposed MIP model for all three most-affected West African nations with Ebola. For the MIP model, we describe the six distinct model regions in the form of a two-by-three matrix. All case study data required for this model application with parameter settings are provided in Tables 5.1 to 5.3. On the other hand, we assume zero for both the initial number of recovered and treated individuals because there is no available data. Furthermore, we use the population ratio in the given model regions in each country to compute their initial number of cases and deaths.

Given these parameters, we perform all of the computational experiments on a desk-top computer equipped with Windows 7, 1.50 GHz CPU and 4 GB memory. We model the problem using $C++$ as a front-end interface to CPLEX, which is used for solving the MIP model over a sixty-week horizon period. For the base case our SITR-FB epidemic model is solved starting on the June 16, 2014 and run until August 15, 2015 in order to fully assess transmission dynamics of the 2014 Ebola epidemic. Therefore, we provide the initial conditions for our case study in Table 5.4, which corresponds to the state of our SITR-FB epidemic disease model at the end of time period zero.

On the other hand, we retrieve only the cumulative number of cases and deaths for Guinea, Liberia, and Sierra Leone represented from studies of Althaus (2014) and the WHO, however, we estimate the number of individuals $I_0^{(k,l)}$, $T_0^{(k,l)}$, $R_0^{(k,l)}$, and $F_0^{(k,l)}$ in their respective compartments as follows.

- We estimate the initial number of individuals in compartment F as one in all three countries and compute $F_0^{(k,l)}$ by considering the respective population ratio for each model region shown in Table 5.2.
- For the initial number of individuals in compartment B, we use the exact cumulative number of deaths reported in Althaus (2014) and by the WHO.

- We estimate $T_0^{(k,l)}$ and $R_0^{(k,l)}$ as zero, since the initial number of treated and recovered individuals as of June 16, 2014, was not reported.
- We compute the initial number of infected individuals in compartment I by subtracting the reported cumulative number of cases on June 15, 2014 from the cumulative number of cases on June 16, 2014. We then estimate $I_0^{(k,l)}$ in each model region by taking into account their corresponding population ratio, as shown in Table 5.2.

Table 5.4: Baseline Case Study Initiated on June 16, 2014 (Althaus, 2014; GeoHive, 2014)

	Guinea			Liberia		Sierra Leone
Parameter explanation	G_1	G_2	G_3	L_1	L_2	SL
$S_0^{(k,l)}$	$4,308,333$	$2,670,467$	$3,649,774$	$4,976,775$	$2,233,070$	$1,243,505$
$I_0^{(k,l)}$	54	34	46	49	6	3
$T_0^{(k,l)}$	0	0	0	0	0	0
$R_0^{(k,l)}$	0	0	0	0	0	0
$F_0^{(k,l)}$	0.41	0.25	0.34	0.64	0.36	1
$B_0^{(k,l)}$	107	66	91	48	15	9
$C_0^{(k,l)}$	0	0	0	0	0	0

5.4 Numerical Results and Analysis of SITR-FB Epidemic Model

This section illustrates computational results and data analyses to evaluate the performance of the optimization-based Ebola epidemic model using the data provided in Tables 5.1 to 5.3 over a sixty-period (weeks) time horizon. Our numerical results regarding the set of experiments are provided to explain the epidemic growth with and without the introduction of control intervention. We also present other results such as the effects of migration on the spread of the disease and the analysis of Ebola treatment cost in the content of this chapter. Finally, our Ebola parameter sensitivity analysis results discuss the impact of sensitive parameters on possible strategies for containing EVD.

5.4.1 Examining Impact of Non-Control Intervention on 2014 Ebola Epidemic

This section presents the Ebola SITR-FB epidemic model solution using the June 16, 2014, base case data defined in Table 5.4. We explain the spread of Ebola without the presence of any control intervention such as available budget for an ETC facility and safe burial, as our two main intervention approaches. Figure 5.2 shows that the total number of infected and funeral individuals increase significantly and thus follow an exponential function from the start of the model-based epidemic until the sixtieth time period (August 15, 2015). Further, the result describes the transmission dynamics of Ebola in each of the six distinct model-based regions in the case of zero available budget for treatment and ample budget for safe burial at all experiments over a sixty period horizon.

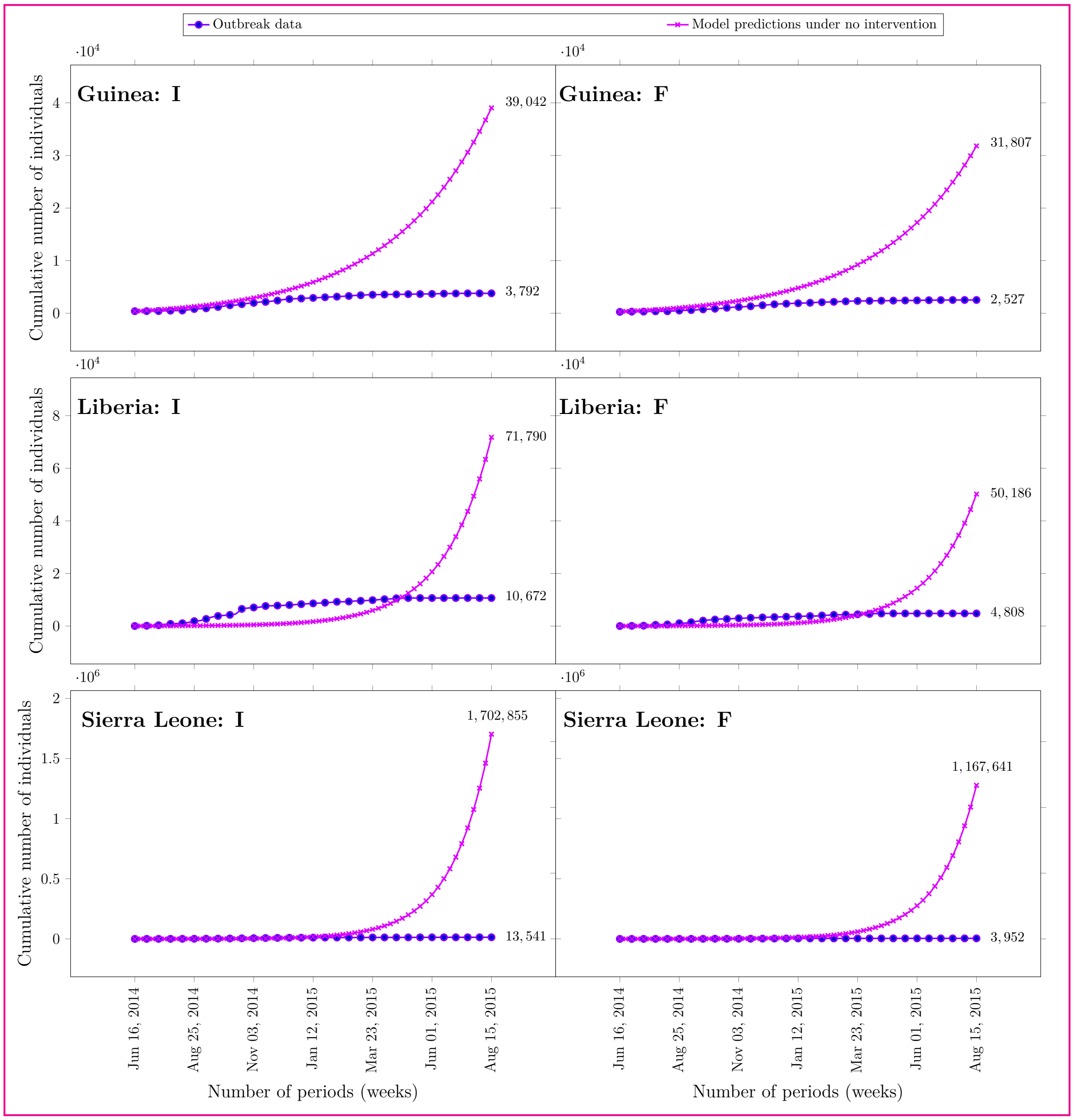

Figure 5.2: Examining impacts of non-control intervention on actual data and SITR-FB epidemic model prediction for cumulative number of cases (I) and funerals (F) of 2014 Ebola outbreak in Guinea, Liberia, and Sierra Leone

Figure 5.2 indicates that the non-control intervention case in the epidemic model solution predicts the total number of infected individuals in Guinea, Liberia, and Sierra Leone, to be $39,042$, $71,790$, and $1,702,855$, respectively, over the sixty-period planning horizon (August 15, 2015). Comparing both the actual and model-based outbreak curves, we notice how close both curves follow the same path. However, Liberia experiences changes in actual data between June 16, 2014 (in period 10) and March 23, 2015 (in period forty). It is also observed that the cumulative number of cases in Sierra Leone accounts for more than 22 times the numbers in Guinea and double the numbers in Liberia. Similarly, Sierra Leone deflects from the path of the actual data by March 23, 2015, and then follows the path of an exponential curve. This difference in cumulative cases can be explained by changes in human behavior due to cultural practices at traditional funerals and at community activities, thus increasing transmission rates and fatalities. More specifically, it is assumed that the high community transmission rate in Sierra Leone contributes to the increasing number of infections since citizens have not been educated enough about the Ebola epidemic.

Moreover, the model estimates that the total number of infected individuals to be far higher than the total number of funerals at the end of the sixtieth time period in all three countries. For example, Liberia and Sierra Leone indicate more than 40% more infections than deaths, while this drops to 23% in Guinea. This can be explained by the actual control intervention strategies implemented in these countries.

On the other hand, Figure 5.2 shows that the total number of funerals for Guinea, Liberia, and Sierra Leone by August 15, 2015, is estimated at $31,807$, $50,186$, and $1,167,641$, according to the epidemic model solution. The curves and growth for the total number of funerals in all three countries behaves similarly as the cumulative number of cases. Therefore, our analyses indicate that several control intervention approaches should be considered during the early stages of epidemics of this magnitude, including education and social distancing.

5.4.2 Analyzing Spatial Distribution of 2014 Ebola in Guinea, Liberia, and Sierra Leone: August 25, 2014, to August 15, 2015

Geographic mapping of infectious diseases are designed to provide information on the spatial pattern of the disease to inform policymakers where epidemic resources are most needed. A spatial study of Ebola can aid decision-makers to identify other geographic factors in addition to transmission rates that impact spread of the virus. For example, Snow (1855) implements a spatial distribution of cholera in his paper to examine the relationship between sources of sanitized water and cholera disease.

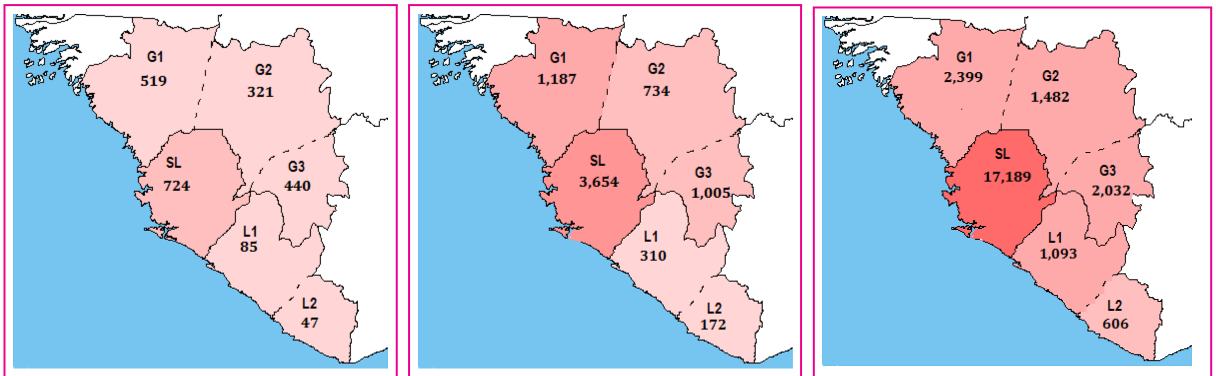

(a) August 25, 2014 (b) November 03, 2014 (c) January 12, 2015

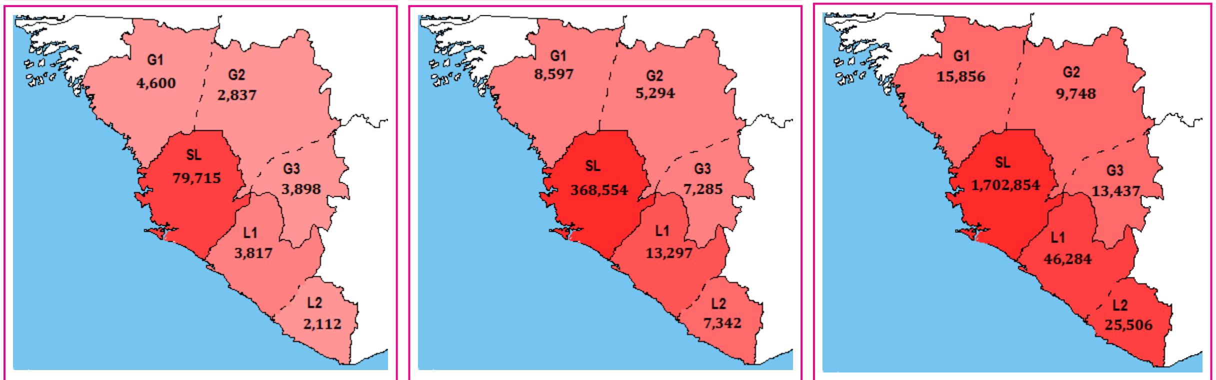

(d) March 23, 2015 (e) June 01, 2015 (f) August 15, 2015

🟥	1-500	🟥	501-1,000	🟥	1,001-2,500	🟥	2,501-5,000	🟥	5,001-10,000
🟥	10,001-25,000	🟥	25,001-50,000	🟥	50,001-200,000	🟥	200,001+		

Figure 5.3: Analyzing size of Ebola outbreaks and spatial spread by model region at end of August 25, 2014 to end of August 15, 2015 in absence of control intervention (changes in cumulative number of cases represented by different shades of the color pink)

We investigate the increase in the cumulative number of cases under non intervention case (no treatment budget case) in each of the six model regions (geographical display) in equal intervals of ten weeks over the entire planning horizon from the epidemic point of view. The purpose of this result is to inform decision- and policymakers about the number of treatment facilities and the educational guidelines required in order to contain the EVD on community-based levels. Figures 5.3a to 5.3f confirm the results shown in Figure 5.2: the absence of control intervention indicates significant changes in transmission dynamics of the EVD, thus increasing the combined number of cases and deaths to further spread the disease. These output shows that delay in control intervention strategies further hurt at-risk nations from recovering and hinder progress.

Additionally, Figure 5.3 provides the case numbers by which the disease is expected to grow exponentially by end of each tenth week over the planning horizon (August 15, 2015). For instance, in Guinea and Liberia, the model estimates the cumulative number of cases to double and quadruple every tenth week starting at the end of August 25, 2014 and run until the end of August 15, 2015, respectively. However, this type of significant increase in the number of infections slightly lessens as time passes as the citizens of these countries are educated about the deadly disease. Moreover, the exponential growth of the disease in Guinea and Liberia can be explained by the impact of immigration of susceptible and infected individuals across model regions. At the same time, the cumulative number of cases in Sierra Leone alone is observed to grow sharply between the end of March 23, 2015 and of August 15, 2015. Therefore, the increase in the total number of cases in Sierra Leone is approximately 15 times more than the total number of cases predicted from both Guinea and Liberia at the end of the finite planning horizon.

5.4.3 Examining Effect of Control and Non-Control Intervention on 2014 Ebola Epidemic

In Table 5.5, we study the transmission dynamics of the EVD among the six model regions of Guinea, Liberia, and Sierra Leone when control intervention is introduced.

Table 5.5: Effect of Control and Non-Control Intervention on 2014 Ebola Epidemic

Total	Budget^1	Objective	Reg^2	OptBudget^3	50-Bed ^{4}	100-Bed^5	Infected^6	Funeral^7	Recovered^8
	$0	3,922,070	G_1	$0	0	0	15,856	12,918	1,902
			G_2	$0	0	0	9,748	7,940	1,169
			G_3	$0	0	0	13,437	10,948	1,612
			L_1	$0	0	0	46,284	32,358	7,055
			L_2	$0	0	0	25,506	17,828	3,887
			SL	$0	0	0	1,702,855	1,167,641	203,556
Total			–	**$0**	**0**	**0**	**1,813,687**	**1,249,635**	**219,184**
	$5M	3,755,830	G_1	$0	0	0	15,848	12,912	1,901
			G_2	$2,010,485	1	0	473	392	78
			G_3	$0	0	0	13,430	10,942	1,611
			L_1	$1,549,732	1	0	166	128	35
			L_2	$1,182,396	1	0	102	79	21
			SL	$0	0	0	1,702,855	1,167,641	203,556
Total			–	**$4,742,534**	**3**	**0**	**1,732,877**	**1,192,095**	**207,207**
	$10M	77,360	G_1	$0	0	0	15,856	12,918	1,902
			G_2	$0	0	0	9,748	7,940	1,169
			G_3	$1,638,923	1	0	13,372	10,897	1,620
			L_1	$1,549,732	1	0	166	128	35
			L_2	$1,182,396	1	0	102	79	21
			SL	$5,621,480	1	0	1,122	917	193
Total			–	**$9,992,532**	**4**	**0**	**40,366**	**32,882**	**4,944**
	$15M	21,724	G_1	$3,542,595	2	0	779	646	130
			G_2	$0	0	0	9,784	7,971	1,174
			G_3	$2,585,995	1	0	660	547	110
			L_1	$1,549,732	1	0	166	128	35
			L_2	$1,182,396	1	0	102	79	21
			SL	$5,621,480	1	0	1,122	917	193
Total			–	**$14,482,200**	**6**	**0**	**12,616**	**10,291**	**1,667**
	$20M	2,978	G_1	$2,936,446	1	0	777	645	130
			G_2	$2,044,684	1	0	481	399	80
			G_3	$2,579,249	1	0	658	546	110
			L_1	$1,547,732	1	0	166	128	35
			L_2	$1,182,396	1	0	102	79	21
			SL	$5,621,480	1	0	1122	917	194
Total			–	**$15,913,989**	**6**	**0**	**3,309**	**2,716**	**573**

[1] overall budget in US $ million for controlling epidemic outbreak, [2] number of model-based regions within each country, [3] optimal total budget allocation over all time periods,
[4] total number of 50-bed ETC facilities established, [5] total number of 100-bed ETC facilities established,
[6] cumulative number of infected individuals, [7] cumulative number of dead individuals,
[8] cumulative number of recovered individuals.

The SITR-FB epidemic model has built-in control interventions intended to inform policymakers concerning the number of treated, recovered, and funeral individuals. Therefore, policymakers need these case data information in order to make decisions about ETC facilities, number of healthcare workers, safe burial practices, and other educational guidelines for the eradication and control of the EVD.

Next, the columns in Table 5.5 provide the following information: Overall budget, objective function value, country, model region, optimal budget, number of type of ETC facility, total number of infected, funeral, and recovered individuals. Table 5.5 shows the comparison between non-control intervention (zero budget) and control intervention (available budget) cases at the start of the epidemic in June 16, 2014, to August 15, 2015. For the control intervention case, we allocate limited budgets ranging from $5M to $20M to study how the SITR-FB epidemic model controls the spread of Ebola by allocating resources among six model regions of Guinea, Liberia, and Sierra Leone.

It is also observed that the increase in available budget from $5M to $20M significantly reduces the number of infected individuals, increases the number of susceptible individuals, and subsequently reduces the number of funerals by increases in number of ETC facilities. Under the non-control intervention case in the SITR-FB epidemic model, it can be seen that approximately 12% of the total number of infected individuals during the Ebola epidemic recover from the disease, while nearly 70% of those cases die (funeral) from the disease. However, these numbers slightly change within specific countries. For example, in Liberia (northern and southern), 15% of the recorded number of cases recover and in Guinea (upper, mid and lower), 81% of the cases are estimated to be the number of deaths.

For control intervention in the amount of $5M, the model tends to choose Guinea's model region G_2 and Liberia model regions L_1 and L_2 among all three countries with an optimal budget of $4.7M in order to fully optimize its treatment resources. This results in the effective reduction of the number of infections and fatalities by nearly 99.5% compared to the non-control intervention case.

However, when control intervention in the amount of \$10M is introduced, the model optimally applies \$5.6M of the budget to significantly control the number of cases and deaths in SL because of its high EVD infection and fatality rates. Next, it can be seen that Liberia receives its portion of intervention (\$2.7M) with similar results as in the case of \$5M intervention. Obviously, the remaining \$1.6M of the budget establishes a 50-bed ETC facility in Guinea but is found insufficient to treat all infected individuals in this country.

Finally, \$15M and \$20M budgets in the form of control intervention reduce the objective function value by nearly 99% through six 50-bed ETC facilities. Table 5.5 also indicates that out of a \$20M overall budget, the model optimally utilized \$15.9M for control of Ebola over the sixty-period horizon. Our analysis shows that our model-based control interventions are successful at decreasing the number of infections from 1.8 million without any control intervention to three thousand. This suggests that our decision-making and control intervention strategy focuses on early-stage intervention and optimal allocation of treatment resources while the following strategies enhance the effectiveness of the treatment intervention.

- The first approach is to properly isolate individuals suspected of the disease and infectious individuals and keep them away from susceptible individuals through improved quarantine and infection-control practices. On the other hand, deceased individuals must be immediately removed from the community within a few hours of death (Hu et al., 2015). By considering these practices, the number of infections in the community can be reduced with time.
- The second approach is to focus on making treatment facilities more accessible to individuals in villages and communities. This is because the 2006 Ebola outbreak in the DRC experienced a significant decrease in transmission rates as a result of increased control interventions (Lekone and Finkenstädt, 2006).

5.4.4 Assessing Impact of Control Intervention on 2014 Ebola Epidemic

In this Section, we further investigate the transmission dynamics and spread of the EVD in terms of cumulative number of cases and deaths in addition to June 16, 2014 intervention, over a sixty-period time horizon in the presence of control intervention. In particular, we analyze other starting dates for intervention on June 30, July 30, August 29, and September 29 of 2014 to assess optimal strategies for the eradication of Ebola.

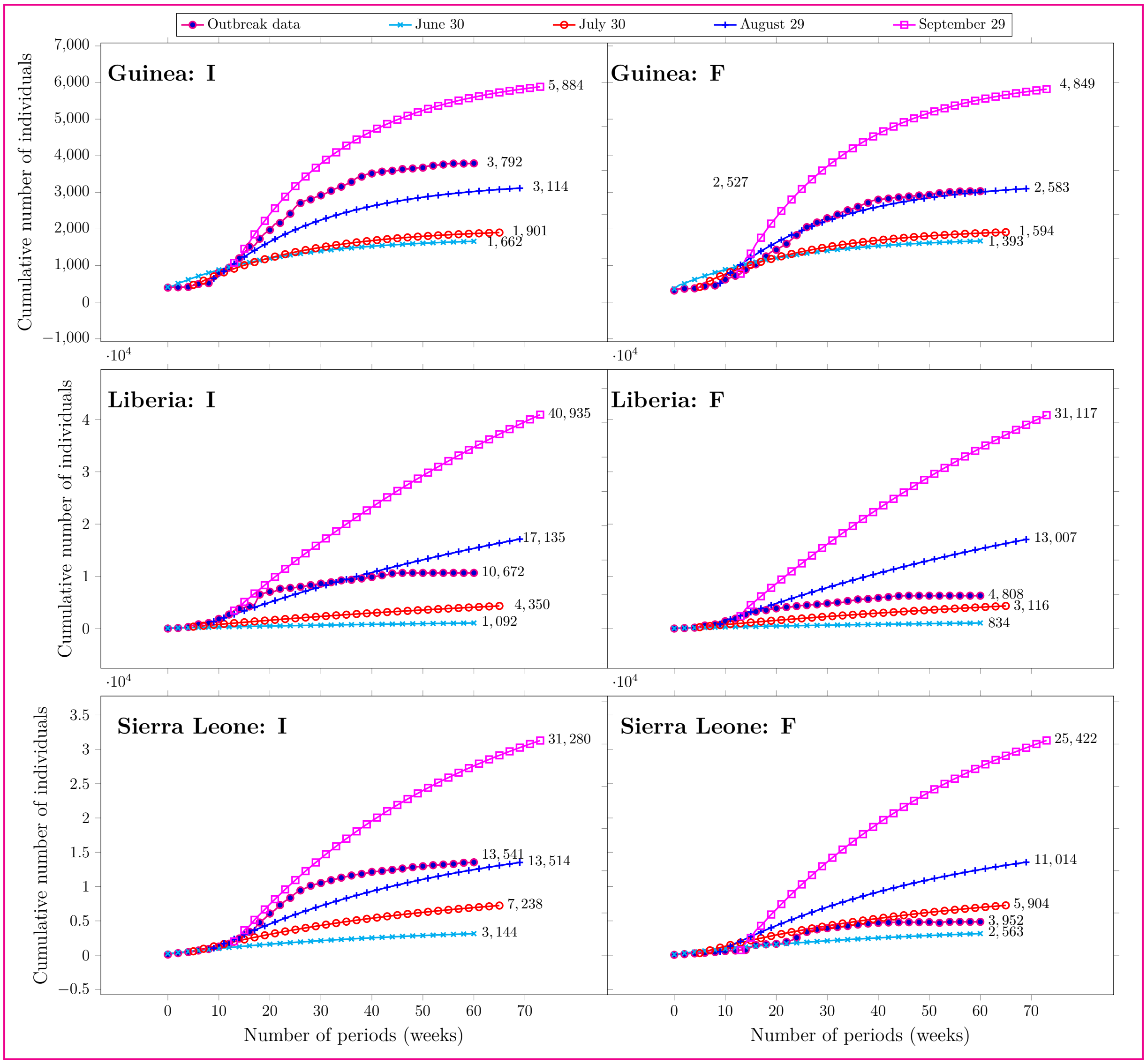

Figure 5.4: Assessing actual outbreak data and model predictions for cumulative number of cases (I) and funerals (F), in presence of control intervention

The introduction of control intervention on all four different starting dates among Guinea, Liberia, and Sierra Leone are observed to reduce the cumulative number of cases and deaths. However, the early stage intervention analysis, as shown in Table 5.5, is key to successful containment of the Ebola epidemic.

First, we notice that early-stage control intervention on July 30 requires an optimal budget of $78.5M for control of the disease, while the presence of control interventions on both August 29 and September 29 are estimated to be $203.6M and $474M, respectively. This clearly explains the idea behind early timing of control intervention.

Second, we also present comparison between the SITR-FB epidemic model outbreak data from all four cases and the actual outbreak data (WHO, 2014c), in order to assess SITR-FB epidemic model performance with its optimal allocation of epidemic resources. For example, Figure 5.4 shows that the introduction of control intervention on June 30 and July 30, 2014, among Guinea and Liberia are observed to be successful, as their epidemic growth curves lie below the actual outbreak data curve. For example, intervention introduced in Guinea on June 30 and July 30 reduces the cumulative number of cases and deaths from the actual outbreak by an average of 53% and 41%, respectively. This is quite different as the trend changes for the cumulative number of deaths comparison starting on July 30 in Sierra Leone. This can be explained by the high community transmission rate of 0.45; therefore, control intervention on July 30 was too late to create an impact on the funeral growth curve in Sierra Leone.

Third, in Guinea, the presence of control intervention on August 29, suppresses an increase in the cumulative number of cases and deaths, while the trend seems quite out of line in the cases for Liberia and Sierra Leone. We observe the epidemic growth curves in all cases to lie above the curve for the actual outbreak data for the cumulative number of deaths.

Lastly, late introduction of control intervention on September 29 is obviously illustrated in epidemic growth curves shown in Figure 5.4. The epidemic growth curve rises highly above the actual data outbreak curve on all six graphs. For instance, the late control intervention that began on September 29 in Guinea results in an approximate 55% and 78% increase in the cumulative number of cases and deaths, respectively, when compared to actual outbreak data. Overall, the SITR-FB epidemic model solution analysis, which is similar to earlier results in this chapter shows that early implementation of control intervention is more successful than late-stage intervention.

5.4.5 Understanding Treatment Cost Components of 2014 Ebola Epidemic

Figure 5.5 shows an analysis of cost components for introducing control intervention on different starting dates: June 30, July 30, August 29, and September 29, 2014, over the finite planning horizon with regard to the SITR-FB Ebola epidemic model. The following cost components include fixed, variable treatment, and safe burial costs.

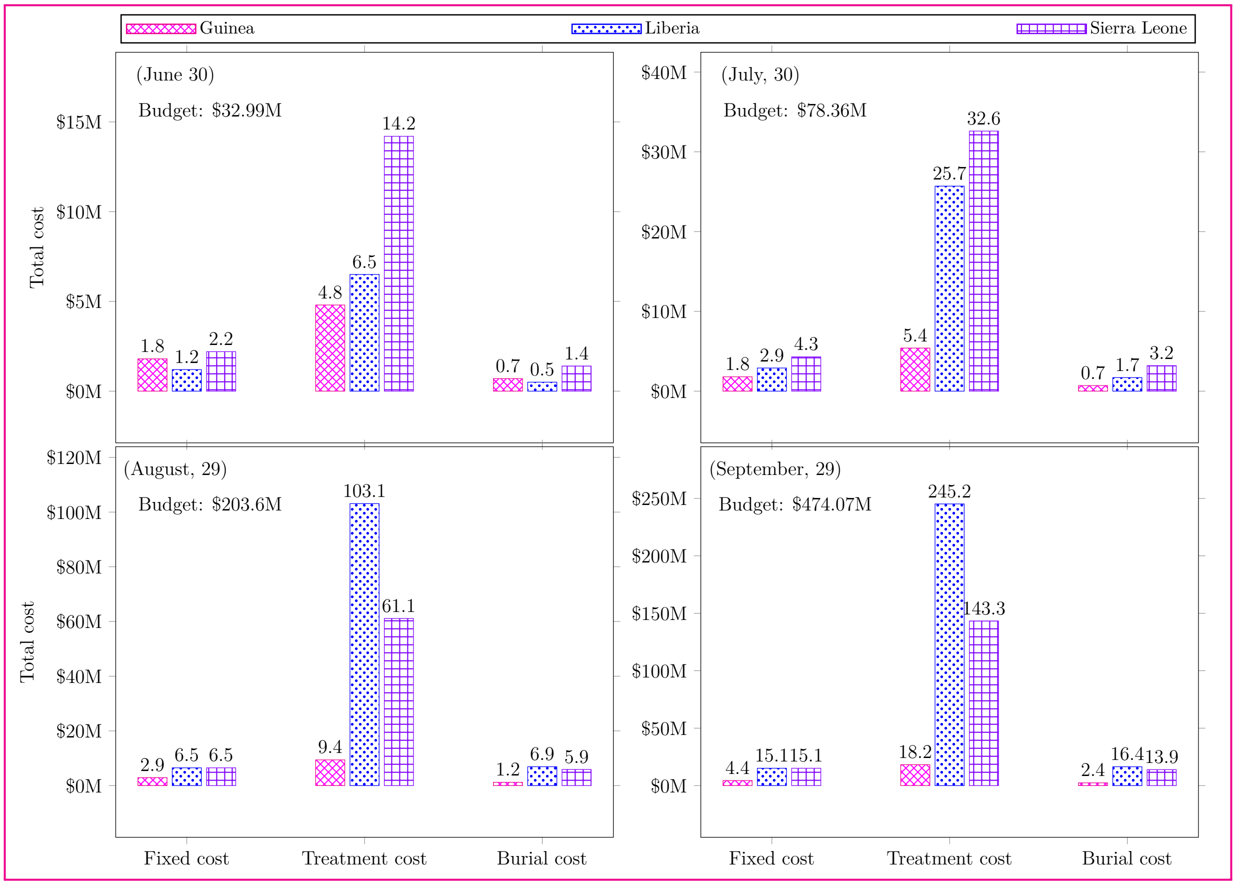

Figure 5.5: Understanding cost components for different starting dates of implementing control intervention

Figure 5.5 shows that variable treatment cost is observed as a major cost driver accounting for, on average, 82% of the available budget in the presence of control intervention. Fixed cost is the next major cost component, followed by the safe burial cost. Figure 5.5 also summarizes cost components for all three countries at different intervention starting dates. For example, for an optimal budget of $33M introduced on June 30, we observe the following: 77% of the budget accounts for treatment cost, whereas 15.6% contributes to fixed cost (initial set up cost) for five 50-bed and two 100-bed ETC facilities with 7.4% of the total budget allocated to safe burial. Further, Sierra Leone accounts for 43.2% of the treatment cost, which is more than twice the percentage cost in Liberia and three times that in Guinea.

We introduce control intervention on July 30 and notice that the variable cost of treatment in Liberia is four times higher than its cost on July 7. This can be explained by the high community transmission and migration rates. Also, cost percentages in Guinea remain exactly the same, with the exception of variable treatment cost which increase by 0.1%. This means that Liberia and Sierra Leone form a major drive of the total cost of Ebola treatment while fixed and safe burial costs account for approximately 19% of the 78.4M budget.

Additionally, the dynamics of the cost-components percentages change significantly during implementation of interventions on August 29 and September 29, with optimal budgets of $203.6M and $474M, respectively. For these late stage control intervention cases, it is clearly seen that variable treatment costs in Liberia account for more than 50% of the optimal budget and nearly 1.6 times the treatment cost in Sierra Leone. On the other hand, the variable cost of treatment increase by 15% on September 29 compared to June 30. Hence, this section establishes the fact that late implementation of control intervention during an epidemic of infectious disease incurs huge cost and sometimes becomes unsuccessful. Finally, the comparisons of control and non-control intervention cases reveal the importance of timing and resources allocated for treatment during an Ebola epidemics (Bartsch et al., 2015; Legrand et al., 2007).

5.4.6 Studying Optimal Allocation of Treatment Facilities to Model Regions

In this section, we discuss the optimal allocation of ETC facilities among six distinct model regions without migration. The discussion describes how the proposed optimization model for epidemic control allocates either 50-bed or 100-bed ETC facilities to each of the model regions depending on its cumulative number of cases and deaths. This analysis follows similar results encountered in the previous sections on how control interventions alter transmission dynamics and spread of the EVD. All results are provided in Figure 5.6 using a demographic representation of the six model regions in Guinea, Liberia, and Sierra Leone over periods one and two.

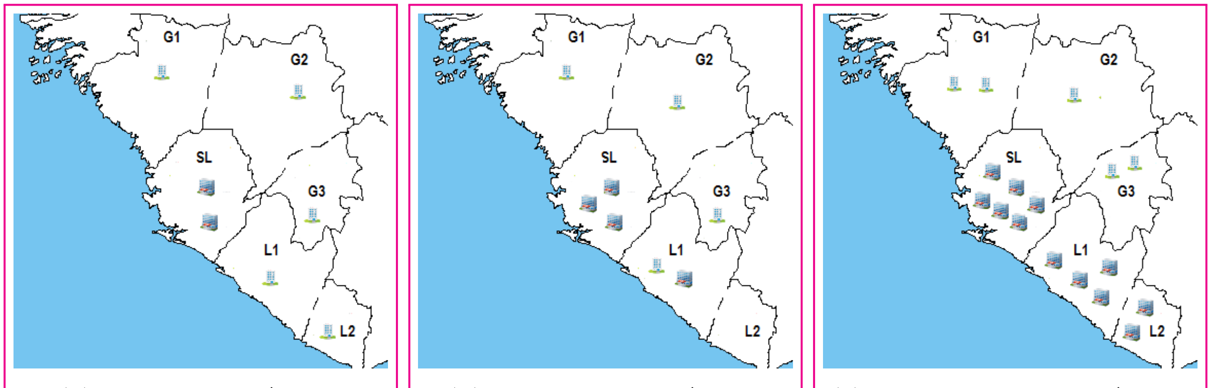

(a) `July 07 (1st wk)` (b) `August 06 (1st wk)` (c) `September 06 (1st wk)`

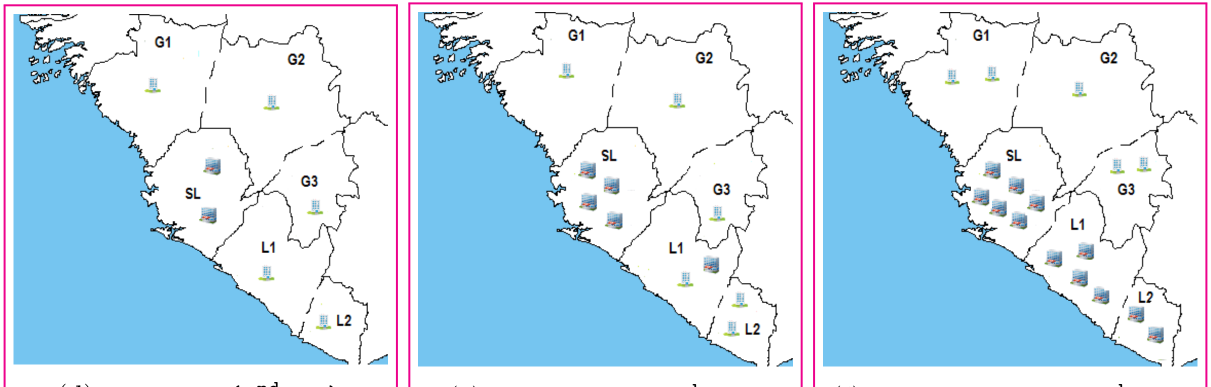

(d) `July 14 (2nd wk)` (e) `August 13 (2nd wk)` (f) `September 13 (2nd wk)`

🏢	50-bed ETC	🏬	100-bed ETC

Figure 5.6: Spatial allocation of ETC facilities (50- and 100-bed) by model region at end of first and second weeks (wks) when control intervention begins on June 30, July 30, and August 29, 2014

We examine analysis of optimal ETC facilities distribution in the presence of control intervention under different starting dates: June 30, July 30, and August 29, 2014. First, Figure 5.6 shows that early introduction of model-based control intervention allocates two 100-bed ETC facilities (optimal budget: $17.4M) to Sierra Leone while a single 50-bed center is established in each of the remaining model regions for starting date in June 30 (periods 1 and 2). We chose periods 1 and 2 because decisions about allocation of resources are made early in the experimental runs. Therefore, the SITR-FB epidemic model makes these expected decisions early to prevent further spread of the epidemic in all three at-risk countries with Ebola.

Furthermore, for starting dates on July 30 and August 29, we notice a significant increase in the number of ETC facilities allocated to model regions (L_1, L_2, and SL) with high levels of infections and fatalities. For example, the number of ETC facilities in model region L_2 in Liberia is seen to increase from a 100-bed ETC facility to four 100-bed ETC facilities. Meanwhile, Guinea, with fewer number of infections and fatalities, attracts on average, two ETC facilities in each model region. Thus, this analysis of ETC facility allocation among the six model regions under a limited budget shows the importance of early intervention.

5.4.7 Examining Optimal Allocation of Treatment Facilities to Model Regions Without Migration

In this section, we consider the optimal distribution of ETC facilities to all six model regions of Guinea, Liberia, and Sierra Leone and estimate its impact on the cumulative number of cases in the absence of migration. Figure 5.7 shows the geographic allocation of ETC facilities (control intervention) according to the SITR-FB epidemic model solution at the end of the first, second, and fifth weeks of the finite planning horizon.

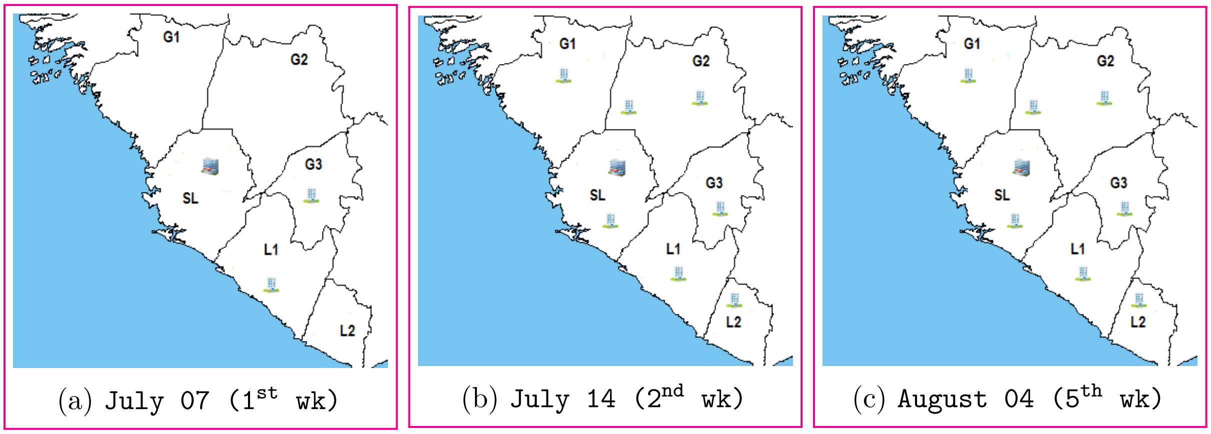

(a) `July 07 (1st wk)` (b) `July 14 (2nd wk)` (c) `August 04 (5th wk)`

Figure 5.7: Spatial allocation of ETC facilities at end of first, second, and fifth weeks (wks) with an optimal budget of $38.7M when control intervention begins on June 30

In this analysis, we study the optimal allocation of ETC (50- or 100-bed) facilities to six distinct model regions of Guinea, Liberia, and Sierra Leone when we assume that borders between model regions are closed. The allocation of the epidemic resources in the form of the treatment centers requires an optimal budget of $38.7M during the first, second, and fifth weeks in a sixty-period planning horizon. With no migration of susceptible and infected of individuals across model regions, fewer treatment centers are established. As an example, this illustration explains the impact of migration on dynamics and spread of the 2014 Ebola epidemic from Guéckédou to Macenta in Guinea (see, e.g., Baize et al., 2014).

Furthermore, a comparison of the Ebola epidemic control interventions cases in both Figures 5.6 and 5.7 over a two-week time period suggests that only a single 50-bed ETC is established until the end of July 14 to contain and prevent spread of the virus.

5.4.8 Examining Impact of Control Intervention on Spatial Distribution of the 2014 Ebola Epidemic

Section 5.4.8 describes the gradual reduction in number of Ebola infections within the three countries according to the SITR-FB epidemic model solutions when we introduce control intervention on July, 30, 2014. Figure 5.8 shows the impact of an optimal intervention strategy in equal intervals of ten periods (weeks) until October 24, 2015. This discussion reveals the impact of control intervention on the outcome of the number of infections in each of the six model regions in Guinea, Liberia, and Sierra Leone. Figure 5.8 shows that early implementation of control interventions (SITR-FB epidemic model-based) such as isolation of suspected infected individuals with corresponding treatment centers reduce the size of the outbreak by 99%. For example, model regions G_1, G_2, and G_3 in Guinea with 51, 31, and 43 initial cases, respectively, experience a decrease by nearly 88% at the end of period twenty. This subsequent reduction of cases continues periodically until end of period sixty in which, one infected individual is reported in each model region. However, the percentage decrease in the number of cases in Liberia is quite different from that reported in Guinea. This is because Liberia has, on average, considerably higher transmission rates both in the community and at traditional funerals than those in Guinea.

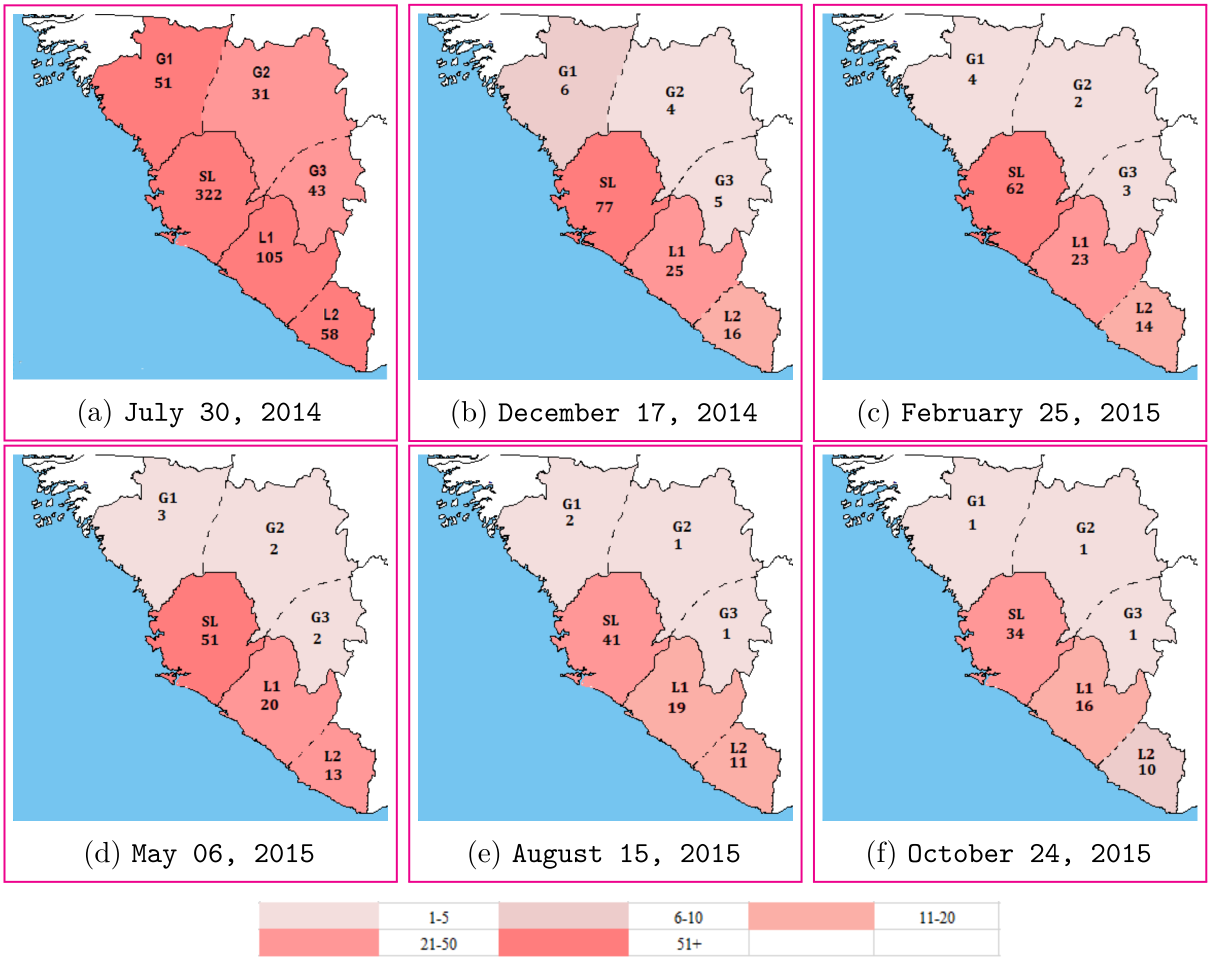

(a) `July 30, 2014` (b) `December 17, 2014` (c) `February 25, 2015`

(d) `May 06, 2015` (e) `August 15, 2015` (f) `October 24, 2015`

Figure 5.8: Examining size of Ebola outbreaks and spatial spread by model region at end of July 30, 2014 to end of October 24, 2015, (changes in number of cases is represented by different shades of the color pink)

In Figure 5.8, we observe a significant reduction (by 99% on average) in the total number of cases and infections by the end of the planning horizon when control intervention starts on July 30 compared to the no-intervention case. Isolating and treating infected individuals in ETCs early in the planning horizon eventually reduces the number of infections to very low levels in all regions. For instance, region G_1 in Guinea with an initial number of infected individuals of 51 is seen to exponentially decrease to 1 at the end of the planning horizon. By the end of September 29, 2015, only one individual is left in each of the regions G_1, G_2, G_3 and more than ten individuals in regions L_1, L_2, and SL under the control intervention. Therefore, although none of the regions are completely cleared of the disease, it is conceivable to control the EVD in the near future with the optimal number of ETCs established as well as continuing treatment and isolation efforts. Our detailed analysis show that early containment of the disease can stop the outbreak from getting worse and eventually eliminate the disease. This analysis supports the fact that timely provision and optimal allocation of adequate medical facilities have a significant role in intervening the outbreak and reducing fatalities caused by it.

5.4.9 Analyzing Effect of Non-Control and Control Intervention on 2014 Ebola Transition Parameters: Sensitivity Analysis 1 and 2

This section discusses the SITR-FB epidemic model parameters and their impact on the objective function value as they vary within 1% of the base case data. We perform parameter sensitivity analysis without and with control intervention and provide results in Tables 5.6 and 5.7, respectively.

This is to evaluate the importance of SITR-FB epidemic model parameters on the objective function for the assessment of control intervention for Ebola epidemics. Specifically, we vary a single or two model parameters within 1% change in the base case, while the other model parameters are kept constant. In Tables 5.6 and 5.7, we categorize the columns as follows: Description of model, Guinea, Liberia, Sierra Leone, and objective function values.

Table 5.6: Parameter sensitivity analysis in absence of control intervention

Description	Parameter (Δ1%)		Guinea		Liberia		Sierra Leone		Objective †
Transmission rates	$\sigma_1^{(k,l)}$	$\sigma_2^{(k,l)}$	0.25	0.66	0.34	0.70	0.43	0.58	1.3×10^6
			0.26	0.67	0.35	0.71	0.44	0.59	2.3×10^6
			0.27	0.68	0.36	0.72	0.45	0.6	3.9×10^6
			0.28	0.69	0.37	0.73	0.46	0.61	6.6×10^6
			0.29	0.7	0.38	0.74	0.47	0.62	1.1×10^7
Community rate [a]	$\sigma_1^{(k,l)}$		0.25		0.34		0.43		2×10^6
			0.26		0.35		0.44		2.8×10^6
			0.27		0.36		0.45		3.9×10^6
			0.28		0.37		0.46		5.4×10^6
			0.29		0.38		0.47		7.4×10^6
Funeral rate [b]	$\sigma_2^{(k,l)}$		0.66		0.70		0.58		2.5×10^6
			0.67		0.71		0.59		3.1×10^6
			0.68		0.72		0.6		3.9×10^6
			0.69		0.73		0.61		4.8×10^6
			0.7		0.74		0.62		5.9×10^6
Rate from I to F	$\mu_1^{(k,l)} \cdot \lambda_1^{(k,l)}$		0.76		0.60		0.56		4.7×10^6
			0.77		0.61		0.57		4.3×10^6
			0.78		0.62		0.58		3.9×10^6
			0.79		0.63		0.59		3.5×10^6
			0.80		0.64		0.60		3.2×10^6
Rate from I to R	$\mu_3^{(k,l)} \cdot \lambda_2^{(k,l)}$		0.09		0.11		0.08		7.4×10^6
			0.10		0.12		0.09		5.4×10^6
			0.11		0.13		0.10		3.9×10^6
			0.12		0.14		0.11		2.8×10^6
			0.13		0.15		0.12		2×10^6
Burial rate	$\gamma_3^{(k,l)}$		0.69		0.69		0.69		5.2×10^6
			0.7		0.7		0.7		4.5×10^6
			0.71		0.71		0.71		3.9×10^6
			0.72		0.72		0.72		3.4×10^6
			0.73		0.73		0.73		2.9×10^6

[a] transmission rate due to community interaction, [b] transmission rate at traditional funerals,
† objective function value, Δ changes in baseline data values by amount next to it,
underlined data values are initial values used for baseline case.

We study the effects of model parameters on the cumulative number of cases and deaths. As we change $\left(\sigma_1^{(k,l)}, \sigma_2^{(k,l)}\right)$ by 1% from the base case data, the objective function value is observed to change by an average of 71%. This is due to that fact that the cumulative number of cases and deaths vary directly as Ebola transmission rates vary. Similarly, a 1% increase in $\sigma_1^{(k,l)}$ or $\sigma_2^{(k,l)}$ results in 1.4 and 1.3 times increase in the objective function value, respectively. Thus, transmission rates due to community interaction is relatively more important to Ebola eradication than transmission rates at traditional funerals in Guinea, Liberia, and Sierra Leone.

For a one percent change in $\mu_1^{(k,l)} \cdot \lambda_1^{(k,l)}$, we observe the objective function value to be altered by approximately 10%. Meanwhile, a similar variation in $\mu_3^{(k,l)} \cdot \lambda_2^{(k,l)}$ causes a 39% change on average in the objective function value. This can be explained by the fact that the fatality rate and number of infections are inversely proportional. Clearly, Table 5.6 shows that as the number of recovered individuals increase, we observe fewer number of infections and fatalities. Therefore, the recovery rate analysis indicates that the increase in the rate of recovery decreases the time period of infection (Rivers et al., 2014).

According to a study by Chowell and Nishiura (2014), $\gamma_3^{(k,l)}$ is a major contributing factor to the Ebola transmission due to traditional funeral and burial practices. Thus, as we increase or decrease $\gamma_3^{(k,l)}$ by 1%, the objective function is expected to decrease or increase significantly in order to change by nearly 16%. This shows that safe burial practices must be utilized for every Ebola-related death.

Table 5.7: Parameter sensitivity analysis in presence of control intervention

Description	Parameter (Δ1%)	Guinea	Liberia	Sierra Leone	Objective †
CFR with treatment	$\mu_2^{(k,l)}$	0.58	0.59	0.58	2.7×10^3
		0.59	0.60	0.59	2.8×10^3
		0.60	0.61	0.60	2.9×10^3
		0.61	0.62	0.61	3×10^3
		0.62	0.63	0.62	3.1×10^3
Rate from T to F	$\mu_2^{(k,l)} \cdot \gamma_1^{(k,l)}$	0.69	0.40	0.65	2.8×10^3
		0.70	0.41	0.66	2.9×10^3
		0.71	0.42	0.67	2.9×10^3
		0.72	0.43	0.68	3×10^3
		0.73	0.44	0.69	3×10^3
Rate from T to R	$(1 - \mu_2^{(k,l)}) \cdot \gamma_2^{(k,l)}$	0.23	0.15	0.15	3.2×10^3
		0.24	0.16	0.16	3×10^3
		0.25	0.17	0.17	2.9×10^3
		0.26	0.18	0.18	2.8×10^3
		0.27	0.19	0.19	2.7×10^3

† objective function value, Δ changes in baseline data values by amount next to it,
underlined data values are initial values used for baseline case.

Next, we explain sensitivity analysis of parameters with control intervention as provided in Table 5.7. This table examines the impact of case fatality rate as well as transition parameters from treatment to either funeral or recovery on the SITR-FB epidemic model solution.

Our results show that $\mu_2^{(k,l)}$ and $\mu_2^{(k,l)} \cdot \gamma_1^{(k,l)}$ relate directly to the objective function (number of infections and fatalities) value but have a lower impact (on average 3.5%) on the output values, compared to output values, from the other model parameters as shown in Table 5.6. Meanwhile, a 1% increase in $(1 - \mu_2^{(k,l)}) \cdot \gamma_2^{(k,l)}$ results in a decrease in the objective function value by 4.3%. This occurs because the increasing recovery rate reduces the number of infections but has less impact compared to other SITR-FB epidemic model parameters. This implies that controlling these factors alone during an Ebola epidemic would not be enough to minimize spread of the disease but rather a combined effect from all SITR-FB epidemic model parameters.

CHAPTER 6

CONCLUSIONS AND FUTURE STUDY

In this dissertation, we present mixed integer optimization approaches and models for studying resource allocation problems with applications in healthcare asset-replacement problems and epidemics.

First, we introduce a model formulation of resource allocation problem as a 0–1 KP by deriving valid inequalities. Second, we develop a decision-making tool for healthcare asset-replacement problem under technological change and deterioration. Third, we study mathematical modeling and data analysis of Ebola epidemics and then provide effective control interventions and procedures for controlling the spread of the 2014 Ebola epidemic in Guinea, Liberia, and Sierra Leone.

6.1 Valid Inequalities for 0–1 Knapsack Formulation

In Chapter 2, we define three forms of valid inequalities for solving the large-size 0–1 KP. These inequalities are developed through iterative solutions of the primal DP formulation algorithm to produce tight upper bounds on the objective function. These valid inequalities attempt to strengthen the 0–1 KP to yield a reasonable solution time of the problem. The effectiveness of the valid inequalities through several experimental studies on difficult data instances generated using the Glover and Kochenberger (1996) generator with varying tightness ratios is also demonstrated. Comparative analyses are presented to show the effectiveness of these valid inequalities. Three forms of valid inequalities that are generated for the 0–1 KP are proven to be effective in terms of solution times. As a future research study, extensions of these solution tools would enable us to generate similar inequalities for the 0–1 MKP.

6.2 Optimizing New Technology Investments Under Deterioration

In Chapter 3 of this dissertation, we propose an MIP model for the optimal replacement of assets with multiple styles and types under a limited budget in the presence of technological change, deterioration, both, and neither. The introduction of a fixed purchasing cost requires replacement decisions to be made collectively in each period in order to benefit from the economies of scale. This model minimizes the weighted sum of penalty costs for unmet demand and other incurred costs, including fixed cost, unit purchase cost, unit inventory holding cost, and O&M cost minus salvage value.

A case study with specific reference to healthcare assets, namely 1.5 T and 0.5 T MRI and eMRI scanning machines, is considered to illustrate how the model could be used to provide insight into an optimal MRI replacement policy under four cases of technological change and deterioration. Optimal solutions and graphical analysis in all four cases show that the frequency of asset-replacement depends heavily on the capacity gains and losses due to technological change and deterioration.

All results from the case study consistently show that technological advances reduce total cost, while deterioration increases both penalty and replacement costs. We observe from sensitivity analysis that O&M cost, demand, budget, and unit purchase cost form the major cost drivers. In contrast, salvage value, fixed cost, and inventory holding cost have a lower impact on results, compared to the O&M cost and unit purchase expenses in the healthcare imaging machine replacement. Graphical analysis is also performed to provide the budget amount for different demand levels in order to satisfy all demand and thus pay no penalty for the unmet demand. This study shows that as demand rises, the budget is expected to increase in order to control the overall penalty incurred for failing to meet demand. Therefore, it is suggested that certain parameters, such as demand, should be monitored, and the budget should be adjusted accordingly because a variation in such parameters can significantly impact the optimal asset replacement decisions and total cost.

Budget and demand are key parameters in the MST-PRES; therefore, we perform a two-parameter sensitivity analysis for these two parameters, and observe changes in the objective function values and average replacement age of the assets over the entire planning horizon. Results show that increasing the demand with the same budget level leads to significant increases in the penalty cost. Finally, we briefly consider a Pareto front containing Pareto optimal solutions to illustrate the nature of trade-offs between penalty and costs using a weighted sum approach.

In summary, the overall analysis illustrates the following points:

- The MST-PRES model tends to replace more 0.5 T MRI than 1.5 T MRI units because the latter have a larger utilization due to higher capacity and are more expensive to acquire. For instance, in case 1, four 0.5 T MRI units are purchased compared to two 1.5 T MRI units throughout the planning horizon.
- O&M cost, unit purchasing cost, demand, and budget are key drivers in the optimal asset replacement policy.
- Incorporating technological change reduces the average number of assets in operation and in inventory because increased capacity allows fewer assets to satisfy the same demand, compared to the base case. On the other hand, the average number of assets in operation increases while the average inventory decreases with deterioration due to reduced capacity.
- In the deterioration case, the optimal policy leads to a lower O&M cost by frequently replacing or salvaging deteriorating assets at the expense of lost demands. When the budget is kept at a constant value while demand increases, the optimal policy replaces assets more frequently because the model aims to reduce O&M cost under high demand while paying an increased penalty of losing some of the demands.
- As the δ-value increases, the objective function value decreases under technological change due to the increased capacity, while the costs increase in the deterioration case. The optimal solution also implies that the number of new asset purchases shows a decreasing (increasing) trend under technological change (deterioration) as we increase the δ-values. We also observe that the style and type of the new assets purchased are specific to the case and the δ-value considered.

- Technological advances motivate replacements in order to take advantage of new technology, and thus assets are replaced more frequently compared to no technological change and no deterioration cases. This result is compatible with the conclusions of Kusaka and Suzuki (1988) and Büyüktahtakın and Hartman (2015), who claim that continuous technological change shortens the optimal service life of an asset under certain conditions. In our case study, with the purchase of new technology, increased capacity leads to a higher cost advantage compared to the O&M cost reduction over the older assets, which motivates the introduction of a new technology, as shown by Hritonenko and Yatsenko (2008). It is also worth mentioning that while previous asset-replacement literature commonly assumes that technological improvement will reduce the optimal service life of an operating asset (e.g., Büyüktahtakın and Hartman, 2015; Kusaka and Suzuki, 1988; Rogers and Hartman, 2005), recent studies have shown that depending on the technological change rate and its relation to purchase and O&M costs, the optimal service life of an asset equipment can increase, decrease, or remain constant under technological change (Hritonenko and Yatsenko, 2008; Mardin and Arai, 2012). Our results imply that given the case study cost structure, technological change increases the replacement frequency, while the replacement age shows a decreasing trend when only technological improvement is larger than a certain threshold.
- According to the MST-PRES analysis, the healthcare industry will gain from investing in new MRI and eMRI units that have increased technology, because technology reduces penalties and costs by allowing a longer utilization of assets with increased capacity.
- The Pareto optimal solution analysis helps to assist healthcare managers in identifying objective function weights in order to make better decisions regarding penalties and costs, thus defining optimal replacement strategies.

We provide a general MIP model for the multiple style and type parallel asset replacement under technological change and deterioration. While our model is general, some results presented here such as optimal costs and penalties, depend on assumptions made on the case study data. For example, if one assumes that purchase price increases significantly under technological advances, then technological change may not lead to reduced total costs, as in the case of small increments in the purchase price. Therefore, future research can consider the application of the proposed model to different cases where cost structure as well as timing and intensity of technological change varies significantly.

For future research, additional specifications, such as warranty and upgrades, could be incorporated into the model. A stochastic process with uncertainty regarding demand or other parameters could also be considered. The model presented in Chapter 3 can be applied to other asset management problems, such as fleet and aircraft management, in addition to the healthcare industry, in order to obtain insights for various management scenarios.

6.3 A Review of Mathematical Modeling and Data Analyses of Ebola Epidemics

Epidemiological models play a central role by enabling policymakers to determine control intervention strategies in order to minimize the catastrophic impacts of an epidemic and eventually stop the outbreak. In Chapter 4 of this dissertation, we review literature from the standpoint of mathematical modeling to summarize the efforts developed to understand the spread of Ebola and suggest appropriate control interventions in the most affected nations in West Africa. We also provide compact economic cost data due to Ebola as well as epidemiological parameters defining the disease transmission and their values from the literature for both the past Ebola epidemic and also the 2014 epidemic in order to provide useful insights for future planning.

Various studies employ specific infectious disease models including SIR and other variants based on partitioning the population into several compartments where various type of compartments are considered to incorporate distinct stages of the disease. For example, to account for the exposed period in SIR-related models for the EVD, many epidemiologists have modified the SIR basic model to derive the SEIR model. Other studies involving the EVD also include classes such as death or funeral, and thus leading to the susceptible-exposed-infected-recovered-dead (SEIRD) or susceptible-exposed-infected-recovered-funeral (SEIRF) compartmental models. We summarize various type of Ebola epidemic compartmental models, their analyses, objectives, and considered control intervention strategies previously in Table 4.1.

Mathematical models require sufficient infectious disease data that could be used to estimate model parameters. Often epidemic data is quite dependent on the timing and conditions of data collection. Therefore, researchers are faced with issues that involve fitting models to data sets, which consequently affect the analysis of the data. For example, in the case of the 2014 Ebola outbreak, several researchers proposed a range of epidemic models to predict the growth of the disease and number of cumulative cases. However, inconsistency in the data and under-reported cases have led to unrealistic conclusions about the ongoing epidemic (Feldmann and Geisbert, 2011; Nishiura and Chowell, 2014). Despite data issues, mathematical models that utilize the best data available and perform sensitivity analysis on data values can provide useful insights about a disease, its spread, and control strategies.

We provide compact EVD biological data that exists in the literature. Further, we survey many studies on Ebola transition rates from one compartmental stage of the disease to the next, while we further expand our work to present a comprehensive review of the parameter estimation for past and present Ebola outbreaks. Remarkably, studies show that transmission of Ebola is either due to person-to-person interaction in communities, contact during burial rituals of Ebola-related deceased individuals, and contact in ETC facilities.

We also discuss economic impact and implications of Ebola outbreaks, especially the 2014 Ebola crisis in West Africa. In particular, we investigate low and high estimates of the cost of treating EVD patients, and the economic costs in terms of lost productivity and household income. With this information, several cost analysis can be developed for future control of Ebola in West Africa. Our review on Ebola models and data help us to understand patterns in the several outbreaks and major medical resource requirements for controlling the epidemic.

Future research should consider a comprehensive review of the aftermath of the epidemic and therefore discuss how the most affected nations could cope with current productivity and economic losses, and rebuild their broken infrastructures including healthcare systems. Despite existing models on Ebola control, there is still a need for new models that capture the behavior of individuals and the EVD characteristics in order to identify the disease early on and explore new control interventions in addition to evaluating existing ones. Furthermore, there is a research need for developing cost-structured mathematical models that take into account a full description of the treatment cost of infected individuals and optimize the allocation of medical resources such as treatment facilities to minimize the spread of the disease.

6.4 A Mixed-Integer Optimization Approach for Controlling Spread and Dynamics of the 2014 Ebola Epidemic

The management of outbreak of infectious diseases should not only consider the modeling of the disease but also take into account other important issues such as logistics, migration, and infection control strategies. In Chapter 5, we propose an optimization model by considering three forms of control interventions (budget for ETC, early safe burial, and recovery) to study spatial spread and control of the 2014 Ebola epidemic in Guinea, Liberia, and Sierra Leone. We also study the problem of effective allocation of ETC facilities among six model regions in Guinea, Liberia, and Sierra Leone to confront spread of Ebola outbreak.The proposed model also accounts for migration of susceptible and infectious individuals to evaluate movement of individuals between model regions in Guinea, Liberia, and Sierra Leone. To address these epidemic challenges in West Africa, our SITR-FB epidemic model solution aims at minimizing a cumulative number of cases and deaths under a restricted budget over a sixty-period horizon (from June 16, 2014 to August 15, 2015).

We draw interesting conclusions from our computational analysis as we consider a case study of the 2014 Ebola outbreak in Guinea, Liberia, and Sierra Leone from several sources including the WHO and other Ebola literature to illustrate the performance of the optimization model.We further develop up to five scenarios of the case study in terms of their starting dates (June 16, June 30, July, July 30, August 29, and September 29) in 2014 thus providing different situations of the outbreak dynamics in terms of the cumulative number of cases and deaths to explain the impact of control intervention and its timing. For these scenarios, we also show the allocation of 50- and 100-bed ETC facilities among the six distinct model regions with control interventions. Other important results studied in this chapter worth mentioning include geographic representation of systematic growth of Ebola outbreak. Numerical results show that immediate implementation and early timing of control interventions such as safe burial and available infrastructure (healthcare system) during an epidemic of this magnitude improves confidence in the citizens and reduces the number of infections significantly. However, delay in control interventions results in an outbreak situation that becomes difficult to contain and possibly get out of control as experienced in the 2014 Ebola epidemic (see, e.g., Ivorra et al., 2014; Meltzer et al., 2014; Nishiura and Chowell, 2014). Meanwhile, the early intervention in the 2003 severe acute respiratory syndrome (SARS) outbreak quickly contained the outbreak (Bloom, 2003; Riley et al., 2003).

In the absence of control intervention, our numerical results show that the SITR-FB Ebola epidemic model solution (cumulative number of cases and deaths) closely follows the actual outbreak data reported from the WHO. Similarly, the epidemic optimization solution is shown to grow exponentially, with numbers from Sierra Leone reaching three times the combined cases and deaths in Guinea and Liberia (WHO, 2015). While our epidemic model is specific to the 2014 EVD West Africa, results in general indicate that the epidemic-logistic model solution can be used to predict future outbreaks of the disease and it can also be used to study possible impact of the virus on the West African continent. All results from the case study consistently show that early stage introduction of control intervention reduces the number of infections and fatalities by nearly 99%, while absence of control intervention exponentially increases both the infections and fatalities.

We also perform several sensitivity analysis with control and non-control intervention strategies to determine effects of key epidemiological parameters on transmission dynamics of Ebola. We observe that EVD transition rates such as transmission rates, recovery rate, and burial rate are key parameters that impact the objective function values (number of infections and fatalities) and hence form the most sensitive model parameters. On the other hand, funeral rates have much less effect on the objective function compared to the others. Thus, the introduction of control interventions such as immediate isolation and treatment of cases, and safe burial of Ebola-related deaths could significantly reduce the number of secondary infections.

Our study also considers the geographic distribution of the disease in all six distinct model regions in Guinea, Liberia, and Sierra Leone to assess spatial pattern of the disease and the area of high concentration of Ebola. Numerical analysis in this section helps to determine other demographic factors that impact the spread of the disease including other environmental factors. As an example, the movement of individuals during an outbreak of an infectious disease contributes to the severity and as such becomes difficult to contain.

Finally, we analyze cost components (variable treatment, fixed, and safe burial costs) for all six model regions where control interventions start on June 30, July 30, August 29, and September 29 in Guinea, Liberia, and Sierra Leone. This analysis of cost components and distribution of treatment centers to the three most-affected nations depends on the severity and extent of infection and is illustrated graphically over the planning horizon. Our results reveal that variable treatment cost forms the major cost driver of the optimal budget, while fixed and burial costs are significantly less compared to variable treatment cost. Therefore the proposed model can be used as follows:

- A decision-making tool for resource allocation during the course of an epidemic outbreak including Ebola.
- To study transmission dynamics of other epidemic diseases such as cholera, chickenpox, and tuberculosis with slight variations.

Future research could consider a stochastic process with uncertainty regrading sensitive parameters such as community interaction and funeral transmission rates. The SITR-FB epidemiology disease model can be extended by adding a compartment class E, which represents exposed individuals.

REFERENCES

REFERENCES

Aksüt, Z. H. Valid inequalities for the problem of optimizing a nonseparable piecewise linear function on 0–1 variables. Master's thesis, Bilkent University, Ankara, Turkey, 2011.

Alexanderian, A., Gobbert, M. K., Fister, K. R., Gaff, H., Lenhart, S., and Schaefer, E. An age-structured model for the spread of epidemic cholera: Analysis and simulation. *Nonlinear Analysis: Real World Applications*, 12(6):3483–3498, 2011.

Allen, L. J. Some discrete-time SI, SIR, and SIS epidemic models. *Mathematical Biosciences*, 124(1):83–105, 1994.

Allen, L. J. and Burgin, A. M. Comparison of deterministic and stochastic SIS and SIR models in discrete time. *Mathematical Biosciences*, 163(1):1–33, 2000.

Allen, L. J., Brauer, F., Van den Driessche, P., and Wu, J. *Mathematical epidemiology*. Springer, 2008.

Althaus, C. L. Estimating the reproduction number of Ebola virus (EBOV) during the 2014 outbreak in West Africa. *Public Library of Science*, 6, 2014.

Althaus, C. L., Low, N., Musa, E. O., Shuaib, F., and Gsteiger, S. Ebola virus disease outbreak in Nigeria: Transmission dynamics and rapid control. *Epidemics*, 11:80–84, 2015.

Amenaghawon, O. C. et al. Mathematical modelling of the transmission dynamics of Ebola virus. *Applied and Computational Mathematics*, 4(4):313–320, 2015.

Anderson, R. M. *The population dynamics of infectious diseases: Theory and applications*. Springer, 2013.

Anderson, R. M. and May, R. M. Population biology of infectious diseases: Part I. *Nature*, 280:361–367, 1979.

Anderson, R. M., May, R. M., and Anderson, B. *Infectious diseases of humans: Dynamics and control*, volume 28. Wiley Online Library, 1992.

Appleget, J. A. *Knapsack cuts and explicit-constraint branching for solving integer programs*. PhD thesis, Naval Postgraduate School, Monterey, California, 1997.

Area, I., Batarfi, H., Losada, J., Nieto, J. J., Shammakh, W., and Torres, Á. On a fractional order Ebola epidemic model. *Advances in Difference Equations*, 2015(1):1–12, 2015.

Arie, S. et al. Only the military can get the Ebola epidemic under control: Médecins Sans Frontiéres head. *BMJ*, 349:g6151, 2014.

Armstrong, D. MRI and CT centers offer doctors way to profit on scans. *The Wall Street Journal*, 1, 2005.

Arreola, R., McDuffy, D., Mejia, M., and Oliver, A. The Ebola virus: Factors affecting the dynamics of the disease. http://dspace.library.cornell.edu/bitstream/1813/32110/1/BU-1519-M.pdf, 1999. Accessed September 12, 2014.

Astacio, J., Briere, D., Guillén, M., Martínez, J., Rodŕiguez, F., and Valenzuela-Campos, N. Mathematical models to study the outbreaks of Ebola. http://mtbi.asu.edu/research/archive/paper/mathematical-models-study-outbreaks-ebola, 1996. Accessed September 22, 2014.

Atamtürk, A. and Muñoz, J. C. A study of the lot–sizing polytope. *Mathematical Programming*, 99(3):443–465, 2004.

Bailey, N. T. et al. *The mathematical theory of infectious diseases and its applications*. Charles Griffin & Company Ltd., 1975.

Baize, S., Pannetier, D., Oestereich, L., Rieger, T., Koivogui, L., Magassouba, N., Soropogui, B., Sow, M. S., Keïta, S., De Clerck, H., et al. Emergence of Zaire Ebola virus disease in Guinea. *New England Journal of Medicine*, 371(15):1418–1425, 2014.

Balas, E. Recognizing facet defining inequalities. *Axta Mathematica Vietnamica*, 22(1):7–28, 1997.

Balas, E. Facets of the knapsack polytope. *Mathematical Programming*, 8(1):146–164, 1975.

Balas, E. and Zemel, E. An algorithm for large zero–one knapsack problems. *Operations Research*, 28(5):1130–1154, 1980.

Balev, S., Yanev, N., Fréville, A., and Andonov, R. A dynamic programming based reduction procedure for the multidimensional 0–1 knapsack problem. *European Journal of Operational Research*, 186(1):63–76, 2008.

Barbarossa, M. V., Dénes, A., Kiss, G., Nakata, Y., Röst, G., and Vizi, Z. Transmission dynamics and final epidemic size of Ebola virus disease outbreaks with varying interventions. *PLOS ONE*, 10(7), 2015.

Baron, R. C., McCormick, J. B., and Zubeir, O. A. Ebola virus disease in southern Sudan: Hospital dissemination and intrafamilial spread. *Bulletin of the World Health Organization*, 61(6):997, 1983.

Barry, M. H. Magnetic resonance imaging needs assessment. http://novascotia.ca, 2004. Accessed December 18, 2013.

Bartsch, S. M., Gorham, K., and Lee, B. Y. The cost of an Ebola case. *Pathogens and Global Health*, 109(1):4–9, 2015.

Bashar, S., Percy, M., and Singhai, R. Predicting the 2014 Ebola outbreak in West Africa using network analysis. http://web.stanford.edu/class/cs224w/projects/cs224w-45-final.pdf, 2015. Accessed August 10, 2015.

Bausch, D. G. and Schwarz, L. Outbreak of Ebola virus disease in Guinea: Where ecology meets economy. *Public Library of Science*, 8(7), 2014.

Bean, J. C., Lohmann, J. R., and Smith, R. L. Equipment replacement under technological change. *Naval Research Logistics*, 41(1):117–128, 1994.

Bellman, R. On the theory of dynamic programming. *Proceedings of the National Academy of Sciences of the United States of America*, 38(8):716, 1952.

Bellman, R. Equipment replacement policy. *Journal of the Society for Industrial & Applied Mathematics*, 3(3):133–136, 1955.

Bellman, R. E. and Dreyfus, S. E. *Applied dynamic programming*, volume 7962. Princeton University Press, 1966.

Bennington, G. and Lubore, S. Resource allocation for transportation. *Naval Research Logistics Quarterly*, 17(4):471–484, 1970.

Bernoulli, D. Essai d'une nouvelle analyse de la mortalité causée par la petite vérole et des avantages de l'inoculation pour la prévenir. *Histoire de l'Académie Royale Science avec Mém. des Mathématiques et Physiques*, pages 1–45, 1760.

Beyer, C. A. *Exact synchronized simultaneous uplifting over arbitrary initial inequalities for the knapsack polytope*. PhD thesis, Kansas State University, Manhattan, Kansas, 2011.

Bjørnstad, O. N., Finkenstädt, B. F., and Grenfell, B. T. Dynamics of measles epidemics: Estimating scaling of transmission rates using a time series SIR model. *Ecological Monographs*, 72(2):169–184, 2002.

Bloom, B. R. Lessons from SARS. *Science*, 300(5620):701–701, 2003.

Bogoch, I. I., Creatore, M. I., Cetron, M. S., Brownstein, J. S., Pesik, N., Miniota, J., Tam, T., Hu, W., Nicolucci, A., Ahmed, S., et al. Assessment of the potential for international dissemination of Ebola virus via commercial air travel during the 2014 West African outbreak. *The Lancet*, 385(9962):29–35, 2015.

Boyer, V., El Baz, D., and Elkihel, M. Solution of multidimensional knapsack problems via cooperation of dynamic programming and branch and bound. *European Journal of Industrial Engineering*, 4(4):434–449, 2010.

Breman, J., Piot, P., Johnson, K., White, M., Mbuyi, M., Sureau, P., Heymann, D., Van Nieuwenhove, S., McCormick, J., Ruppol, J., et al. The epidemiology of Ebola hemorrhagic fever in Zaire, 1976. *Ebola Virus Haemorrhagic Fever*, pages 103–124, 1978.

Breman, J. G. and Johnson, K. M. Ebola then and now. *New England Journal of Medicine*, 371(18):1663–1666, 2014.

Brown, C. S. and Cropley, I. M. Ebola virus disease: Where are we now and where do we go? *Postgraduate Medical Journal*, 90(1069):610–612, 2014.

Brown, G. G., Dell, R. F., and Newman, A. M. Optimizing military capital planning. *Interfaces*, 34(6):415–425, 2004.

Büyüktahtakın, I. E. and Hartman, J. C. A mixed-integer programming approach to the parallel replacement problem under technological change. Forthcoming in *International Journal of Production Research*, 2015.

Büyüktahtakin, İ. E., Feng, Z., Olsson, A. D., Frisvold, G., and Szidarovszky, F. Invasive species control optimization as a dynamic spatial process: An application to buffelgrass (Pennisetum ciliare) in Arizona. *Invasive Plant Science and Management*, 7(1):132–146, 2014.

Büyüktahtakın, I. E., Smith, C. J., Hartman, J. C., and Luo, S. Parallel asset replacement problem under economies of scale with multiple challengers. *The Engineering Economist*, 59 (4):237–258, 2014.

Camacho, A., Kucharski, A., Funk, S., Breman, J., Piot, P., and Edmunds, W. Potential for large outbreaks of Ebola virus disease. *Epidemics*, 9:70–78, 2014.

Capasso, V. and Serio, G. A generalization of the Kermack-McKendrick deterministic epidemic model. *Mathematical Biosciences*, 42(1):43–61, 1978.

CDC. Ebola hemorrhagic fever: Table showing known cases and outbreaks, in chronological order. http://www.cdc.gov/ncidod/dvrd/spb/mnpages/dispages/ebotabl.htm, 2003. Accessed September 29, 2014.

Cergnul, J. J. Using cost in strategic decision making. The 2013 AFWA Conference. http://www.afwa.org, 2013. Accessed January 24, 2014.

Chan, M. Ebola virus disease in West Africa – No early end to the outbreak. *New England Journal of Medicine*, 371(13):1183–1185, 2014.

Chan, T. M. Optimal output-sensitive convex hull algorithms in two and three dimensions. *Discrete & Computational Geometry*, 16(4):361–368, 1996.

Chatterji, A. K. Spawned with a silver spoon? Entrepreneurial performance and innovation in the medical device industry. *Strategic Management Journal*, 30(2):185–206, 2009.

Chen, D.-S., Batson, R. G., and Dang, Y. *Applied integer programming: Modeling and solution*. John Wiley & Sons, 2011.

Chen, M. and Feldman, R. M. Optimal replacement policies with minimal repair and age-dependent costs. *European Journal of Operational Research*, 98(1):75–84, 1997.

Chen, T., Leung, R. K.-K., Liu, R., Chen, F., Zhang, X., Zhao, J., and Chen, S. Risk of imported Ebola virus disease in China. *Travel Medicine and Infectious Disease*, 12(6): 650–658, 2014.

Chen, Z.-L. Solution algorithms for the parallel replacement problem under economy of scale. *Naval Research Logistics*, 45(3):279–295, 1998.

Chowell, G. and Nishiura, H. Transmission dynamics and control of Ebola virus disease (EVD): A review. *BMC Medicine*, 12(1):196, 2014.

Chowell, G., Hengartner, N. W., Castillo-Chavez, C., Fenimore, P. W., and Hyman, J. The basic reproductive number of Ebola and the effects of public health measures: The cases of Congo and Uganda. *Journal of Theoretical Biology*, 229(1):119–126, 2004.

Chowell, G., Simonsen, L., Viboud, C., and Kuang, Y. Is West Africa approaching a catastrophic phase or is the 2014 Ebola epidemic slowing down? Different models yield different answers for Liberia. *PLOS Currents*, 6, 2014.

Christer, A. and Scarf, P. A robust replacement model with applications to medical equipment. *The Journal of the Operational Research Society*, 45(3):261–275, 1994.

Cobuloglu, H. I. and Büyüktahtakın, İ. E. Food vs. biofuel: An optimization approach to the spatio-temporal analysis of land-use competition and environmental impacts. *Applied Energy*, 140:418–434, 2015.

Coburn, B., Wagner, B., and Blower, S. Modeling influenza epidemics and pandemics: Insights into the future of swine flu (H1N1). *BioMed Central Ltd*, 7:30–30, 2008.

Coffman, E. G., Jr, Garey, M. R., and Johnson, D. S. An application of bin–packing to multiprocessor scheduling. *SIAM Journal on Computing*, 7(1):1–17, 1978.

Cohen, S. Extremity magnetic resonance imaging in rheumatoid arthritis: Report of the American College of Rheumatology Extremity Magnetic Resonance Imaging Task Force. *Arthritis & Rheumatism*, 54(4):1034–1047, 2006.

Cohen, T. Validating medical equipment repair and maintenance metrics: A progress report. *Biomedical Instrumentation & Technology–Association for the Advancement of Medical Instrumentation*, 31(1):23, 1997.

Cooper, L. and Cooper, M. W. *Introduction to dynamic programming.* Franklin Book Company, Incorporated, 1981.

Cox, J. and Abeku, T. A. Early warning systems for malaria in Africa: From blueprint to practice. *Trends in Parasitology*, 23(6):243–246, 2007.

Dantzig, G. B. Discrete-variable extremum problems. *Operations Research*, 5(2):266–288, 1957.

Das, T. and Savachkin, A. A large scale simulation model for assessment of societal risk and development of dynamic mitigation strategies. *Institute of Industrial Engineers Transactions*, 40(9):893–905, 2008.

Denardo, E. *Dynamic programming: Models and applications.* Prentice Hall Inc., 1982.

Derman, C. Optimal replacement and maintenance under Markovian deterioration with probability bounds on failure. *Management Science*, 9(3):478–481, 1963.

Diekmann, O., Dietz, K., and Heesterbeek, J. The basic reproduction ratio for sexually transmitted diseases: Part 1: Theoretical considerations. *Mathematical Biosciences*, 107(2): 325–339, 1991.

Diekmann, O., Heesterbeek, H., and Britton, T. *Mathematical tools for understanding infectious disease dynamics*. Princeton University Press, 2012.

Duyn, J. H. The future of ultra-high field MRI and fMRI for study of the human brain. *Neuroimage*, 62(2):1241–1248, 2012.

Dyer, M., Riha, W., and Walker, J. A hybrid dynamic programming/branch-and-bound algorithm for the multiple–choice knapsack problem. *Journal of Computational and Applied Mathematics*, 58(1):43–54, 1995.

Eichner, M., Dowell, S. F., and Firese, N. Incubation period of Ebola hemorrhagic virus subtype Zaire. *Osong public health and research perspectives*, 2(1):3–7, 2011.

Eisenberg, M. C., Eisenberg, J. N., D'Silva, J. P., Wells, E. V., Cherng, S., Kao, Y.-H., and Meza, R. Modeling surveillance and interventions in the 2014 Ebola epidemic. *arXiv preprint arXiv:1501.05555*, 2015.

Eubank, S. Network based models of infectious disease spread. *Japanese Journal of Infectious Diseases*, 58(6):9–13, 2005.

Eubank, S., Guclu, H., Kumar, V. A., Marathe, M. V., Srinivasan, A., Toroczkai, Z., and Wang, N. Modelling disease outbreaks in realistic urban social networks. *Nature*, 429(6988): 180–184, 2004.

Evans, A. S. and Kaslow, R. A. *Viral infections of humans: Epidemiology and control*. Springer Science & Business Media, 1997.

Evans, R. J. and Mammadov, M. Dynamics of Ebola epidemics in West Africa 2014. `http://f1000research.com/articles/3-319/v2`, 2014. Accessed October 15, 2015.

Fan, V. and Glassman, A. Local. *Finance & Development*, 51(4):800, 2014.

Farnham, P. G. Defining and measuring the costs of the HIV epidemic to business firms. *Public Health Reports*, 109(3):311, 1994.

Fasina, F., Shittu, A., Lazarus, D., Tomori, O., Simonsen, L., Viboud, C., and Chowell, G. Transmission dynamics and control of Ebola virus disease outbreak in Nigeria, July to September 2014. *European Surveillance*, 19(40):20920, 2014.

Fauci, A. S. Ebola – Underscoring the global disparities in health care resources. *New England Journal of Medicine*, 371(12):1084–1086, 2014.

Feldmann, H. and Geisbert, T. W. Ebola haemorrhagic fever. *The Lancet*, 377(9768):849–862, 2011.

Fisman, D., Khoo, E., and Tuite, A. Early epidemic dynamics of the West African 2014 Ebola outbreak: Estimates derived with a simple two-parameter model. *Public Libaray of Science*, 2014.

Fletcher, J., Clark, M., Sutton, F., Wellings, R., and Garas, K. The cost of MRI: Changes in costs 1989–1996. *British Journal of Radiology*, 72(857):432–437, 1999.

Fowler, R. A., Fletcher, T., Fischer, W. A., Lamontagne, F., Jacob, S., Brett-Major, D., Lawler, J. V., Jacquerioz, F. A., Houlihan, C., and O'Dempsey, T. Caring for critically ill patients with Ebola virus disease. Perspectives from West Africa. *American Journal of Respiratory and Critical Care Medicine*, 190(7):733–737, 2014.

Fraser, C., Riley, S., Anderson, R. M., and Ferguson, N. M. Factors that make an infectious disease outbreak controllable. *Proceedings of the National Academy of Sciences of the United States of America*, 101(16):6146–6151, 2004.

Freeman, J. SEIR with pulse control measures: A model for the 2014 West Africa Ebola epidemic . `https://pdf.yt/d/xEH603r0SJ5XTMaz`, 2014. Accessed June 06, 2015.

Frieden, T. R., Damon, I., Bell, B. P., Kenyon, T., and Nichol, S. Ebola 2014–New challenges, new global response and responsibility. *New England Journal of Medicine*, 2014.

Frieze, A. M. Shortest path algorithms for knapsack type problems. *Mathematical Programming*, 11(1):150–157, 1976.

Funk, S., Gilad, E., Watkins, C., and Jansen, V. A. The spread of awareness and its impact on epidemic outbreaks. *Proceedings of the National Academy of Sciences*, 106(16):6872–6877, 2009.

Gani, J. Modelling epidemic diseases. *Australian & New Zealand Journal of Statistics*, 52(3): 321–329, 2010.

Gavish, B. and Pirkul, H. Efficient algorithms for solving multiconstraint zero–one knapsack problems to optimality. *Mathematical Programming*, 31(1):78–105, 1985.

Gay, D. M. and Kernighan, B. Ampl: A modeling language for mathematical programming. *Duxbury Press/Brooks/Cole*, 2, 2002.

Geisbert, T. W., Hensley, L. E., Larsen, T., Young, H. A., Reed, D. S., Geisbert, J. B., Scott, D. P., Kagan, E., Jahrling, P. B., and Davis, K. J. Pathogenesis of Ebola hemorrhagic fever in cynomolgus macaques: Evidence that dendritic cells are early and sustained targets of infection. *The American Journal of Pathology*, 163(6):2347–2370, 2003.

GeoHive. Global population statistics. `http://www.geohive.com/cntry/`, 2014. Accessed April 15, 2015.

Georges, A.-J., Leroy, E. M., Renaut, A. A., Benissan, C. T., Nabias, R. J., Ngoc, M. T., Obiang, P. I., Lepage, J., Bertherat, E. J., Bénoni, D. D., et al. Ebola hemorrhagic fever outbreaks in Gabon, 1994–1997: Epidemiologic and health control issues. *Journal of Infectious Diseases*, 179(Supplement 1):S65–S75, 1999.

Germann, T. C., Kadau, K., Longini, I. M., and Macken, C. A. Mitigation strategies for pandemic influenza in the United States. *Proceedings of the National Academy of Sciences*, 103(15):5935–5940, 2006.

Gilmore, P. and Gomory, R. The theory and computation of knapsack functions. *Operations Research*, 14(6):1045–1074, 1966.

Glover, F. and Kochenberger, G. A. Critical event tabu search for multidimensional knapsack problems. In *Meta-heuristics*, pages 407–427. Springer, 1996.

Gomes, M. F., y Piontti, A. P., Rossi, L., Chao, D., Longini, I., Halloran, M. E., and Vespignani, A. Assessing the international spreading risk associated with the 2014 West African Ebola outbreak. *Public Library of Science*, 6, 2014.

Gostin, L. O. The future of the World Health Organization: Lessons learned from Ebola. *Milbank Quarterly*, 93(3):475–479, 2015.

Goufo, E. D. and Maritz, R. A note on Ebola outbreak and human migration dynamic. *Journal of Human Ecology*, 51(3):257–263, 2015.

Green, A. WHO and partners launch Ebola response plan. *The Lancet*, 384(9942):481, 2014.

Grenfell, B. and Harwood, J. Meta-population dynamics of infectious diseases. *Trends in Ecology & Evolution*, 12(10):395–399, 1997.

Griggs, M. B. What happens after someone survives Ebola? `http://www.popsci.com/article/science/what-happens-after-someone-survives-ebola`, 2014. Accessed March 03, 2015.

Grigorieva, E. and Khailov, E. Analytical study of optimal control intervention strategies for Ebola epidemic model. In *2015 Proceedings of the Conference on Control and its Applications*, pages 392–399. SIAM, 2015a.

Grigorieva, E. V. and Khailov, E. N. Optimal intervention strategies for a SEIR control model of Ebola epidemics. *Mathematics*, 3(4):961–983, 2015b.

Haas, C. N. On the quarantine period for Ebola virus. *PLOS Currents*, 6, 2014.

Hartman, J. C. The parallel replacement problem with demand and capital budgeting constraints. *Naval Research Logistics*, 47(1):40–56, 2000.

Hartman, J. C. Multiple asset replacement analysis under variable utilization and stochastic demand: The two asset case. *European Journal of Operational Research*, 159(1):145–165, 2004.

Hartman, J. C., Büyüktahtakin, İ. E., and Smith, J. C. Dynamic programming-based inequalities for the capacitated lot-sizing problem. *IIE Transactions*, 42(12):915–930, 2010.

Heffernan, J., Smith, R., and Wahl, L. Perspectives on the basic reproductive ratio. *Journal of the Royal Society Interface*, 2(4):281–293, 2005.

Hethcote, H. W. The mathematics of infectious diseases. *SIAM*, 42(4):599–653, 2000.

Hewlett, B. and Hewlett, B. *Ebola, culture and politics: The anthropology of an emerging disease*. Cengage Learning, 2007.

Hewlett, B. S. and Amola, R. P. Cultural contexts of Ebola in northern Uganda. *Emerging Infectious Diseases*, 9(10):1242, 2003.

Heymann, D., Weisfeld, J., Webb, P., Johnson, K., Cairns, T., and Berquist, H. Ebola hemorrhagic fever: Tandala, Zaire, 1977–1978. *Journal of Infectious Diseases*, 142(3):372–376, 1980.

Hill, M. M. Magnetic resonance imaging at HSDA. `http://tennessee.gov`, 2011. Accessed March, 18 2014.

Hillier, F. S. *Introduction to operations research*. Tata McGraw-Hill Education, 1995.

Hodge, M. *Managing high value capital equipment in the NHS in England: Fifty-third report of session 2010-12 report, together with formal minutes, oral and written evidence*. The Stationery Office, 2011.

Hodge Jr, J., Barraza, L., Measer, G., and Agrawal, A. Global emergency legal responses to the 2014 ebola outbreak: Public health and the law. *The Journal of the American Society of Law*, 42(4):595, 2014.

Hoenen, T., Groseth, A., Falzarano, D., and Feldmann, H. Ebola virus: Unravelling pathogenesis to combat a deadly disease. *Trends in Molecular Medicine*, 12(5):206–215, 2006.

Hooker, J. N. and Osorio, M. A. Mixed logical-linear programming. *Discrete Applied Mathematics*, 96:395–442, 1999.

Hopp, W. J. and Nair, S. K. Timing replacement decisions under discontinuous technological change. *Naval Research Logistics*, 38(2):203–220, 1991.

Horowitz, E. and Sahni, S. Computing partitions with applications to the knapsack problem. *Journal of the ACM*, 21(2):277–292, 1974.

Hotta, L. K. Bayesian melding estimation of a stochastic SEIR model. *Mathematical Population Studies*, 17(2):101–111, 2010.

Howard, R. A. *Dynamic programming and Markov processes*. Technology Press of MIT, 1960.

Hritonenko, N. and Yatsenko, Y. The dynamics of asset lifetime under technological change. *Operations Research Letters*, 36(5):565–568, 2008.

Hu, K., Bianco, S., Edlund, S., and James, K. The impact of human behavioral in 2014 West Africa Ebola outbreak. In *Proceedings of 8th International Conference, SBP 2015 on Social Computing, Behavioral-Cultural Modeling and Prediction*, pages 75–85. Springer, 2015.

Hunt, A. G. Exponential growth in Ebola outbreak since May 14, 2014. *Complexity*, 20(2): 8–11, 2014.

Hwang, E. S. Preparedness for prevention of Ebola virus disease. *Journal of Korean Medical Science*, 29(9):1185–1185, 2014.

Iannelli, M. and Pugliese, A. Mathematical modeling of epidemics. In *An Introduction to Mathematical Population Dynamics*, pages 209–264. Springer, 2014.

Ibarra, O. H. and Kim, C. E. Fast approximation algorithms for the knapsack and sum of subset problems. *Journal of the ACM*, 22(4):463–468, 1975.

Iglehart, J. K. The new era of medical imaging–progress and pitfalls. *New England Journal of Medicine*, 354(26):2822, 2006.

ILOG, I. CPLEX optimization studio. `http://www-03.ibm.com/software/products/en/ibmilogcpleoptistud`, 2014. Accessed October 18, 2014.

Ippolito, G., Puro, V., and Piselli, P. Ebola in West Africa: Who pays for what in the outbreak? *The New Microbiologica*, 38(1):1–3, 2015.

Isham, V. and Medley, G. *Models for infectious human diseases: Their structure and relation to data*, volume 6. Cambridge University Press, 1996.

Ivorra, B., Ngom, D., and Ramos del Olmo, Á. M. Be-CoDiS: A mathematical model to predict the risk of human diseases spread between countries. Validation and application to the 2014 Ebola Virus Disease epidemic. `http://eprints.ucm.es/28809/`, 2014. Accessed October 15, 2015.

Jacquez, J. A. Compartmental analysis in biology and medicine. *Applied Mathematics and Computation*, 10:12, 1972.

Jeroslow, R. and Lowe, J. Modelling with integer variables. In *Mathematical Programming at Oberwolfach II*, pages 167–184. Springer, 1984.

Joffe, H. and Haarhoff, G. Representations of far-flung illnesses: The case of Ebola in Britain. *Social Science & Medicine*, 54(6):955–969, 2002.

Jones, K. E., Patel, N. G., Levy, M. A., Storeygard, A., Balk, D., Gittleman, J. L., and Daszak, P. Global trends in emerging infectious diseases. *Nature*, 451(7181):990–993, 2008.

Jones, P. C., Zydiak, J. L., and Hopp, W. J. Parallel machine replacement. *Naval Research Logistics*, 38(3):351–365, 1991.

Kalra, S., Kelkar, D., Galwankar, S. C., Papadimos, T. J., Stawicki, S. P., Arquilla, B., Hoey, B. A., Sharpe, R. P., Sabol, D., and Jahre, J. A. The emergence of Ebola as a global health security threat: From lessons learned to coordinated multilateral containment efforts. *Journal of global infectious diseases*, 6(4):164, 2014.

Kara, D. C. *Production of a viable product in MRI using MgB2*. PhD thesis, Case Western Reserve University, Cleveland, Ohio, 2014.

Karabakal, N., Lohmann, J. R., and Bean, J. C. Parallel replacement under capital rationing constraints. *Management Science*, 40(3):305–319, 1994.

Katoh, N. and Ibaraki, T. Resource allocation problems. *Handbook of combinatorial optimization*, 2:159–260, 1998.

Keeling, M. J. and Eames, K. T. Networks and epidemic models. *Journal of the Royal Society Interface*, 2(4):295–307, 2005.

Keles, P. and Hartman, J. C. Case study: Bus fleet replacement. *The Engineering Economist*, 49(3):253–278, 2004.

Kellerer, H. and Pferschy, U. Improved dynamic programming in connection with an FPTAS for the knapsack problem. *Journal of Combinatorial Optimization*, 8(1):5–11, 2004.

Kellerer, H., Pferschy, U., and Pisinger, D. *Knapsack problems*. Springer, 2004.

Kermack, W. and McKendrick, A. Contributions to the mathematical theory of epidemics II. The problem of endemicity. *Royal Society of London Proceedings Series A*, 138:55–83, 1932.

Khan, A., Naveed, M., Dur-e Ahmad, M., and Imran, M. Estimating the basic reproductive ratio for the Ebola outbreak in Liberia and Sierra Leone. *Infectious Diseases of Poverty*, 4 (1):13, 2015.

Kindhauser, M. K. *Communicable diseases 2002. Global defence against the infectious disease threat*. WHO, 2003.

Kiskowski, M. A. A three-scale network model for the early growth dynamics of 2014 West Africa Ebola epidemic. *PLOS Currents*, 6, 2014.

Klenk, H.-D. and Becker, S. Ebola virus vaccines–preparing for the unexpected. *Science*, 349 (6249):693–694, 2015.

Kolesar, P. J. A branch and bound algorithm for the knapsack problem. *Management Science*, 13(9):723–735, 1967.

Kucharski, A. J., Camacho, A., Checchi, F., Waldman, R. J., Grais, R. F., Cabrol, J.-C., Briand, S., Baguelin, M., Flasche, S., Funk, S., et al. Evaluation of the benefits and risks of introducing Ebola community care centers, Sierra Leone. *Emerging Infectious Diseases*, 21, 2015.

Kusaka, Y. and Suzuki, H. Equipment replacement with consideration of technological advances-determination of replacement times by control limit policy. *Journal of the Operations Research Society of Japan*, 31(3):389–412, 1988.

Lamunu, M., Lutwama, J., Kamugisha, J., Opio, A., Nambooze, J., Ndayimirije, N., and Okware, S. Containing a haemorrhagic fever epidemic: The Ebola experience in Uganda (october 2000–january 2001). *International Journal of Infectious Diseases*, 8(1):27–37, 2004.

Lancaster, H. O. *Expectations of life: A study in the demography, statistics, and history of world mortality.* Springer Science & Business Media, 2012.

Lawler, E. L. Fast approximation algorithms for knapsack problems. *Mathematics of Operations Research*, 4(4):339–356, 1979.

Legrand, J., Grais, R., Boelle, P., Valleron, A., and Flahault, A. Understanding the dynamics of Ebola epidemics. *Epidemiology and Infection*, 135(04):610–621, 2007.

Lekone, P. E. and Finkenstädt, B. F. Statistical inference in a stochastic epidemic SEIR model with control intervention: Ebola as a case study. *Biometrics*, 62(4):1170–1177, 2006.

Leslie, J. Newcastle disease: Outbreak losses and control policy costs. *The Veterinary Record*, 146(21):603–606, 2000.

Lexa, F. J., Mehta, T., and Seidmann, A. Managerial accounting applications in radiology. *Journal of the American College of Radiology*, 2(3):262–270, 2005.

Li, M. Y. and Muldowney, J. S. Global stability for the SEIR model in epidemiology. *Mathematical Biosciences*, 125(2):155–164, 1995.

Li, Z., Teng, Z., Feng, X., Li, Y., and Zhang, H. Dynamical analysis of an SEIT epidemic model with application to Ebola virus transmission in Guinea. *Computational and Mathematical Methods in Medicine*, 2015, 2015.

Liu, B., Wang, X., Liu, C., and Gao, Q. A k-means based model towards Ebola virus prorogation prediction. *International Journal of Science and Engineering Applications*, 4(3): 95–99, 2015.

Longini, I. M. The generalized discrete-time epidemic model with immunity: A synthesis. *Mathematical Biosciences*, 82(1):19–41, 1986.

Longini, I. M., Clark, W. S., Byers, R. H., Ward, J. W., Darrow, W. W., Lemp, G. F., and Hethcote, H. W. Statistical analysis of the stages of HIV infection using a Markov model. *Statistics in Medicine*, 8(7):831–843, 1989.

Lopez, A. D., Mathers, C. D., Ezzati, M., Jamison, D. T., and Murray, C. J. Global and regional burden of disease and risk factors, 2001: Systematic analysis of population health data. *The Lancet*, 367(9524):1747–1757, 2006.

Lorie, J. H. and Savage, L. J. Three problems in rationing capital. *The Journal of Business*, 28(4):229–239, 1955.

Mamo, D. K. and Koya, P. R. Mathematical modeling and simulation study of SEIR disease and data fitting of Ebola epidemic spreading in West Africa. *Journal of Multidisciplinary Engineering Science and Technology*, 2:3159–0040, 2015.

Mardin, F. and Arai, T. Capital equipment replacement under technological change. *The Engineering Economist*, 57(2):119–129, 2012.

Martello, S. and Toth, P. An upper bound for the zero–one knapsack problem and a branch and bound algorithm. *European Journal of Operational Research*, 1(3):169–175, 1977.

Martello, S. and Toth, P. *Knapsack problems: Algorithms and computer implementations*. John Wiley & Sons, Inc., 1990.

Meltzer, M. I., Atkins, C. Y., Santibanez, S., Knust, B., Petersen, B. W., Ervin, E. D., Nichol, S. T., Damon, I. K., and Washington, M. L. Estimating the future number of cases in the Ebola epidemic: Liberia and Sierra Leone, 2014–2015. *Morbidity and Mortality Weekly Response Surveillance Summaries*, 63(Supplement 3):1–14, 2014.

Mishra, B. et al. The threat of Ebola: An update. *Indian Journal of Medical Microbiology*, 32(4):364, 2014.

Muyembe-Tamfum, J., Mulangu, S., Masumu, J., Kayembe, J., Kemp, A., and Paweska, J. T. Ebola virus outbreaks in Africa: Past and present. *Onderstepoort Journal of Veterinary Research*, 79(2):06–13, 2012.

Muyembe-Tamfum, J., Kipasa, M., Kiyungu, C., and Colebunders, R. Ebola outbreak in Kikwit, Democratic Republic of the Congo: Discovery and control measures. *Journal of Infectious Diseases*, 179(Supplement 1):S259–S262, 1999.

Nåsell, I. Extinction and quasi-stationarity in the verhulst logistic model. *Journal of Theoretical Biology*, 211(1):11–27, 2001.

Ndanguza, D., Tchuenche, J., and Haario, H. Statistical data analysis of the 1995 Ebola outbreak in the Democratic Republic of Congo. *Afrika Matematika*, 24(1):55–68, 2013.

Nemhauser, G. L. *Introduction to dynamic programming*. Wiley New York, 1966.

Nemhauser, G. L. and Ullmann, Z. Discrete dynamic programming and capital allocation. *Management Science*, 15(9):494–505, 1969.

Nishiura, H. and Chowell, G. Early transmission dynamics of Ebola virus disease (EVD), West Africa, March to August 2014. *European Surveillance*, 19:36, 2014.

Nyampong, S. A. Communicating the Ebola crisis in West Africa. *Developing Country Studies*, 5(8):90–95, 2015.

Obilade, T. T. The political economy of the Ebola virus disease (EVD); Taking individual and community ownership in the prevention and control of EVD. *Healthcare*, 3(1):36–49, 2015.

Oguz, O. Cutting plane algorithms for 0–1 programming based on cardinality cuts. *European Journal of Operational Research*, 205(2):273–279, 2010.

Okware, S., Omaswa, F., Zaramba, S., Opio, A., Lutwama, J., Kamugisha, J., Rwaguma, E., Kagwa, P., and Lamunu, M. An outbreak of Ebola in Uganda. *Tropical Medicine & International Health*, 7(12):1068–1075, 2002.

Omonzejele, P. F. Ethical challenges posed by the Ebola virus epidemic in West Africa. *Journal of Bioethical Inquiry*, 11(4):417–420, 2014.

Oswald, W. B. *Antibody responses to a related series of highly glycosylated Ebola virus proteins*. ProQuest, 2007.

Padberg, M. W. Technical note- a note on zero–one programming. *Operations Research*, 23 (4):833–837, 1975.

Pandey, A., Atkins, K. E., Medlock, J., Wenzel, N., Townsend, J. P., Childs, J. E., Nyenswah, T. G., Ndeffo-Mbah, M. L., and Galvani, A. P. Strategies for containing Ebola in West Africa. *Science*, 346(6212):991–995, 2014.

Peh, W. C. Dedicated extremity 1.5 T MRI: The future of ankle imaging. `http://mskrad.hamad.qa`, 2013. Accessed March 16, 2014.

Peker Cansizoglu, A. *Solving the multi-dimensional 0–1 knapsack problem using depth-k canonical cuts*. PhD thesis, North Carolina State University, Raleigh, North Carolina, 2011.

Pferschy, U. Dynamic programming revisited: Improving knapsack algorithms. *Computing*, 63(4):419–430, 1999.

Philips, M. and Markham, Á. Ebola: A failure of international collective action. *The Lancet*, 384(9949):1181, 2014.

Pisinger, D. *Algorithms for knapsack problems*. PhD thesis, DIKU, University of Copenhagen, Copenhagen, Denmark, 1995a.

Pisinger, D. An expanding-core algorithm for the exact 0–1 knapsack problem. *European Journal of Operational Research*, 87(1):175–187, 1995b.

Pisinger, D. Budgeting with bounded multiple-choice constraints. *European Journal of Operational Research*, 129(3):471–480, 2001.

Powell, W. B. *Approximate dynamic programming: Solving the curses of dimensionality*, volume 703. John Wiley & Sons, 2007.

Rachah, A. and Torres, D. F. Mathematical modelling, simulation, and optimal control of the 2014 Ebola outbreak in West Africa. *Discrete Dynamics in Nature and Society*, 501:1–9, 2015.

Rajagopalan, S. Capacity expansion and equipment replacement: A unified approach. *Operations Research*, 46(6):846–857, 1998.

Reaves, E. J., Mabande, L. G., Thoroughman, D. A., Arwady, M. A., and Montgomery, J. M. Control of Ebola virus disease-Firestone District, Liberia, 2014. *Morbidity and Mortality Weekly Report*, 63(42):959–965, 2014.

Regnier, E., Sharp, G., and Tovey, C. Replacement under ongoing technological progress. *IIE Transactions*, 36(6):497–508, 2004.

Riley, S., Fraser, C., Donnelly, C. A., Ghani, A. C., Abu-Raddad, L. J., Hedley, A. J., Leung, G. M., Ho, L.-M., Lam, T.-H., and Thach, T. Q. Transmission dynamics of the etiological agent of SARS in Hong Kong: Impact of public health interventions. *Science*, 300(5627): 1961–1966, 2003.

Rivers, C. M., Lofgren, E. T., Marathe, M., Eubank, S., and Lewis, B. L. Modeling the impact of interventions on an epidemic of Ebola in Sierra Leone and Liberia. *PLOS Currents*, 6, 2014.

Rizkalla, C., Blanco-Silva, F., and Gruver, S. Modeling the impact of Ebola and bushmeat hunting on western lowland gorillas. *EcoHealth*, 4(2):151–155, 2007.

Rogers, J. L. and Hartman, J. C. Equipment replacement under continuous and discontinuous technological change. *IMA Journal of Management Mathematics*, 16(1):23–36, 2005.

Ross, R. *The prevention of malaria.* Dutton, 1910.

Rothman, K. J. *Epidemiology: An introduction.* Oxford University Press, 2012.

Ryan, J. Can a post–crisis country survive in the time of Ebola? *Harvard International Review*, 36(2):25, 2014.

Sahni, S. Approximate algorithms for the 0/1 knapsack problem. *Journal of the ACM*, 22(1): 115–124, 1975.

Salkin, H. M. *Integer programming.* Addison-Wesley Reading, MA, 1975.

Salkin, H. M., Mathur, K., and Haas, R. *Foundations of integer programming.* North-Holland New York, 1989.

Sanchez, A. *Ebola viruses.* Wiley Online Library, 2001.

Sashi Bhusan, D., Bagaban, B., and Tripathy, J. Some results on facets for linear inequality in 0–1 variables. *Iranian Jornal of Optimization*, 2(2):334–349, 2010.

Sashi Bhusan, D., Bagaban, B., and Tripathy, J. Some results on facets for linear inequality in 0-1 variables. *Iranian Journal of Optimization*, 2(2):334–339, 2011.

Sattenspiel, L. and Dietz, K. A structured epidemic model incorporating geographic mobility among regions. *Mathematical Biosciences*, 128(1):71–91, 1995.

Seitz, N. and Ellison, M. *Capital budgeting and long–term financing decisions*. Harcourt Brace College Publishers, 1995.

Shih, W. A branch and bound method for the multiconstraint zero–one knapsack problem. *Journal of the Operational Research Society*, pages 369–378, 1979.

Shohet, I. M. and Lavy, S. Healthcare facilities management: State of the art review. *Facilities*, 22(7/8):210–220, 2004.

Shuaib, F., Gunnala, R., Musa, E. O., Mahoney, F. J., Oguntimehin, O., Nguku, P. M., Nyanti, S. B., Knight, N., Gwarzo, N. S., Idigbe, O., et al. Ebola virus disease outbreak in Nigeria, July–September 2014. *Morbidity and Mortality Weekly Response Suveillance Summaries*, 63:1–6, 2014.

Siettos, C., Anastassopoulou, C., Russo, L., Grigoras, C., and Mylonakis, E. Modeling the 2014 Ebola virus epidemic–Agent-based simulations, temporal analysis and future predictions for Liberia and Sierra Leone. *PLOS Currents*, 1, 2015.

Smailhodzic, A. Adapting the standard SIR disease model in order to track and predict the spreading of the Ebola virus using twitter data. Master's thesis, Western Kentucky University, Bowling Green, Kentucky, 2015.

Smith, R. The geographic spread of infectious diseases. *Lancet Infectious Diseases*, 10(3):153, 2010.

Snow, J. *On the mode of communication of cholera*. John Churchill, 1855.

Sobol, W. T. Recent advances in MRI technology: Implications for image quality and patient safety. *Saudi Journal of Ophthalmology*, 26(4):393–399, 2012.

Songwe, V. Fighting Ebola: A strategy for action. `http://www.brookings.com`, 2015. Accessed January 12, 2015.

Stadler, T., Kühnert, D., Rasmussen, D. A., and du Plessis, L. Insights into the early epidemic spread of Ebola in Sierra Leone provided by viral sequence data. *PLOS Currents*, 6, 2014.

Taha, H. A. *Integer programming: Theory, applications, and computations*, volume 975. Academic Press New York, 1975.

Tao, G., Abban, B. K., Gift, T. L., Chen, G., and Irwin, K. L. Applying a mixed-integer program to model re-screening women who test positive for C. trachomatis infection. *Healthcare Management Science*, 7(2):135–144, 2004.

Team. Ebola virus disease in West Africa–The first 9 months of the epidemic and forward projections. *New England Journal of Medicine*, 371(16):1481–95, 2014.

Toth, P. Dynamic programming algorithms for the zero–one knapsack problem. *Computing*, 25(1):29–45, 1980.

Towers, S., Patterson-Lomba, O., and Castillo-Chavez, C. Temporal variations in the effective reproduction number of the 2014 West Africa Ebola outbreak. *Public Library of Science*, 6, 2014.

Tri Juliansyah, M. S., Dipo, A., and Edy, S. Epidemic model for Ebola disease. In *Proceedings of the Second International Conference on Advances in Applied Science and Environmental Technology*, pages 16–20, 2015.

UN. Backgrounder for ECOSOC special session on Ebola. http://www.un.org, 2014. Accessed November 15, 2014.

Valesquez, A., Ugarte Montoya, R., and De La Pena, K. Magnetic resonance imaging. http://web.eng.fiu.edu, 2012. Accessed December 18, 2013.

Vander Veen, D. J. and Jordan, W. C. Analyzing trade-offs between machine investment and utilization. *Management Science*, 35(10):1215–1226, 1989.

Waaler, H., Geser, A., and Andersen, S. The use of mathematical models in the study of the epidemiology of tuberculosis. *American Journal of Public Health and the Nations Health*, 52 (6):1002–1013, 1962.

Waddington, C. Ebola in West Africa: The long term impact of the 2014 outbreak–Economic, social and political repercussions are likely long after the disease is controlled: West Africa-Issue in focus. *Africa Conflict Monitor*, pages 54–58, 2014.

Wagner, H. M. Principles of operations research: With applications to managerial decisions. *AMC*, 10:12, 1969.

WBG. Update on the economic impact of the 2014 Ebola epidemic in Liberia, Sierra Leone, and Guinea. http://www.worldbank.org, 2014. Accessed December 25, 2014.

Webb, G., Browne, C., Huo, X., Seydi, O., Seydi, M., and Magal, P. A model of the 2014 Ebola epidemic in West Africa with contact tracing. *Public Library of Science*, 7, 2014.

Weingartner, H. M. and Ness, D. N. Methods for the solution of the multidimensional 0/1 knapsack problem. *Operations Research*, 15(1):83–103, 1967.

Weitz, J. S. and Dushoff, J. Modeling post-death transmission of Ebola: Challenges for inference and opportunities for control. *Scientific Reports*, 5, 2015.

WHO. World health report. http://www.who.int/whr/1996/media_centre/press_release/en/, 1996. Accessed October 28, 2015.

WHO. Ebola hemorrhagic fever. http://www.who.int/inf-fs/en/fact103.html, 2003. Accessed September 29, 2014.

WHO. Ebola virus disease. http://www.who.int/mediacentre/factsheets/fs103/en/, 2014a. Accessed June 11, 2015.

WHO. Ebola response roadmap situation reports. http://apps.who.int/ebola/en/current-situation/ebola-situation-report, 2014b. Accessed December 10, 2014.

WHO. Ebola response roadmap situation reports. http://www.who.int/csr/resources/publications/ebola/response-roadmap/en/, 2014c. Accessed September 28, 2014.

WHO. Ebola response roadmap situation report. http://www.who.int/csr/disease/ebola/situation-reports/archive/en/, 2015. Accessed August 20, 2015.

Wilkinson, A. and Leach, M. Briefing: Ebola- Myths, realities, and structural violence. *African Affairs*, pages 1–13, 2014.

Wilson, C. The long battle to find a cure for Ebola. *New Scientist*, 223(2981):7, 2014.

Wolsey, L. A. Faces for a linear inequality in 0–1 variables. *Mathematical Programming*, 8(1): 165–178, 1975.

Wolsey, L. A. *Integer programming.* Wiley-Interscience, 1998. ISBN 0-471-28366-5.

Wolsey, L. A. and Nemhauser, G. L. *Integer and combinatorial optimization.* John Wiley & Sons, 2014.

Yarus, Z. Mathematical look at the Ebola Virus. http://home2.fvcc.edu, 2012. Accessed September 22, 2014.

Yatsenko, Y. and Hritonenko, N. Properties of optimal service life under technological change. *International Journal of Production Economics*, 114(1):230–238, 2008.

Yatsenko, Y. and Hritonenko, N. Technological breakthroughs and asset replacement. *The Engineering Economist*, 54(2):81–100, 2009.

Yazdanpanah, Y., Arribas, J. R., and Malvy, D. Treatment of Ebola virus disease. *Intensive Care Medicine*, 41(1):115–117, 2015.

Yoakam, D., Nelson, W., Springsteen, B., and Williams, C. Radiology technology and technologist. http://www.aaarad.org, 2013. Accessed December 13, 2013.

Zaman, G., Kang, Y. H., and Jung, I. H. Optimal treatment of an SIR epidemic model with time delay. *BioSystems*, 98(1):43–50, 2009.

Zaric, G. S. and Brandeau, M. L. Resource allocation for epidemic control over short time horizons. *Mathematical Biosciences*, 171(1):33–58, 2001.

Zemel, E. Lifting the facets of zero–one polytopes. *Mathematical Programming*, 15(1):268–277, 1978.

Zhou, L. and Fan, M. Dynamics of an SIR epidemic model with limited medical resources revisited. *Nonlinear Analysis: Real World Applications*, 13(1):312–324, 2012.